Preprint
UCRL-ID-139093-PT-1

Saturation of Impurity-Rich Phases in a Cerium-Substituted Pyrochlore-Rich Titanate Ceramic: Part 1. Experimental Results

F. J. Ryerson, B. Ebbinghaus, O. Kirkorian, R. VanKonynenburg

U.S. Department of Energy

Lawrence Livermore National Laboratory

May 25, 2000

This work was performed under the auspices of the U. S. Department of Energy by the University of California, Lawrence Livermore National Laboratory under Contract No. W-7405-Eng-48.

Saturation of impurity-rich phases in a cerium-substituted pyrochlore-rich titanate ceramic: Part 1. Experimental Results *

by

F.J. Ryerson[1], Bartley Ebbinghaus[2], Oscar Kirkorian[2], Richard VanKonynenburg[2],

1. Earth and Environmental Sciences

Lawrence Livermore National Laboratory

Livermore, CA 94550

2. Chemistry and Material Sciences

Lawrence Livermore National Laboratory

Livermore, CA 94550

*This work was performed under the auspices of the U.S. Department of Energy by University of California Lawrence Livermore National Laboratory under contract No. W-7405-Eng-48

Abstract. The saturation of impurity-rich accessory phases in a Ce-analog baseline ceramic formulation for the immobilization of excess plutonium has been tested by synthesizing an impurity-rich baseline compositions at 1300°C 1350°C and 1400°C in air. Impurity oxides are added at the 10 wt% level. The resulting phases assemblages are typically rich in pyrochlore, Hf-zirconolite (hafnolite), brannerite and rutile, but in many instances also contain an accessory mineral enriched in the impurity oxide. The concentration of that oxide in coexisting pyrochlore sets the saturation limit for solid solution of the component in question. In most cases, the accessory phase does not contain significant amounts of Ce, Gd or U. Exceptions are the stabilization of a Ca-lanthanide phosphate and a phosphate glass when P_2O_5 is added to the formulation. P_2O_5 addition is also very effective in reducing the modal amount of pyrochlore in the form relative to brannerite. Addition of the sodium-aluminosilicate, $NaAlSiO_4$, also results in the formation of a grain boundary melt at run conditions, but the fate of this phase on cooling is not well determined. At temperatures above 1300°C, addition of 10 wt% Fe_2O_3 also leads to melting. Substitution of cations of different valences can also be associated with model-dependent changes in the oxidation state of uranium via charge transfer reactions. A set of simple components is suggested for the description of pyrochlores in both impurity-free and impurity-rich formulations.

1. Introduction

A primary goal of the Plutonium Immobilization Project is to determine the phase equilibria for the baseline ceramic formulation (Ebbinghaus *et al.* 1999) as a function of potential processing conditions and variations in chemistry. These variables will effect the partitioning of the various elements among the phases which constitute the wasteform, and may also lead to the formation of additional phases which may or may not include either plutonium or neutron absorbers. In a companion document, we considered the effect of changing oxidation state on the phase equilibria of cerium- and thorium-substituted analogs with and without alumina (Ryerson and Ebbinghaus, 2000). Here we assess the effects of potential wastestream impurities on the phase assemblage in a Ce-substituted analog.

The baseline formulation (Table 1) is designed to produce a pyrochlore of composition $(Ca_{0.89}Gd_{0.22}Hf_{0.23}U_{0.44}Pu_{0.22})Ti_2O_7$, and rutile of composition $(Hf_{0.2}Ti_{0.8})O_2$. The target phase assemblage comprises 95 wt% pyrochlore and 5 wt% rutile. While plutonium is the element of major interest, the formulation also contains hafnium, gadolinium and uranium to act as both neutron absorbers in the wasteform itself, or in possible dissolution products (Ebbinghaus *et al,* 1999). When synthesized under relatively oxidizing conditions (air or argon) in the temperature range 1300-1400°C both the Pu-bearing and Ce-analog materials have been shown to crystallize a hafnium-rich analog of zirconolite, $CaHfTi_2O_7$ (referred to here as "hafnolite"), and brannerite, (nominally, UTi_2O_6) in addition to pyrochlore and rutile. The appearance of these phases may be attributed to variations in the oxidation states of cerium, plutonium and uranium, as well as to the presence of additional impurity elements that may stabilize these phases.

Fortunately, both zirconolite/hafnolite and brannerite are known to be chemically durable, and their appearance in the wasteform may not have deleterious effects upon it ability to immobilize plutonium (cf., Bourcier *et al.*, 1999). However, potential waste streams can contain a broad array of chemical constituents, and the ability of a pyrochlore-brannerite-hafnolite-rutile assemblage to incorporate other elements without the formation of additional phases (subsequently referred to as "accessory phases") depends upon the solubilities of such elements in pyrochlore, brannerite, hafnolite, and rutile. These solubility limits can be determined by measuring the amount of a particular element in each of the primary phases when they coexist with an accessory phase in which the impurity element can be considered as essential structural constituent. For instance, the solubility of nickel oxide in pyrochlore in a NiO-rich composition is fixed when pyrochlore coexists $NiTiO_3$. Here we have imposed the saturation of a number of such accessory phases on a Ce-analog of the baseline composition by adding ~10 wt% of the impurity oxide to the composition (Table 1).

Table 1. "As-made" starting compositions

	M1	M2	M3	M4	M5	M6	M7	M8	M9	M10	M11	M12	M13
Na_2O	0.00	0.00	0.00	0.00	0.00	0.00	0.00	0.00	0.00	0.00	0.00	0.00	0.00
CaO	10.48	9.34	9.32	9.33	10.33	9.32	9.32	9.93	19.36	9.30	9.30	9.51	13.12
TiO_2	36.90	33.59	33.60	33.65	37.45	33.57	33.55	35.77	33.58	33.63	33.46	34.25	34.17
HfO_2	11.20	10.06	10.10	9.95	11.10	10.06	10.02	10.73	10.07	10.01	9.94	10.20	10.20
Gd_2O_3	8.33	7.44	7.46	7.47	8.28	7.45	7.52	7.93	7.48	7.47	7.44	7.61	7.60
UO_2	24.85	22.12	22.23	22.19	24.61	22.17	22.24	23.63	22.14	22.19	22.11	22.63	22.62
CeO_2	8.23	7.41	7.37	7.39	8.21	7.37	7.35	0.00	7.38	7.37	7.36	7.54	7.50
P_2O_5	0.00	10.05	0.00	0.00	0.00	0.00	0.00	0.00	0.00	0.00	0.00	0.00	0.00
CaF_2	0.00	0.00	9.92	0.00	0.00	0.00	0.00	0.00	0.00	0.00	0.00	0.00	0.00
Fe_2O_3	0.00	0.00	0.00	10.02	0.00	0.00	0.00	0.00	0.00	0.00	4.54	0.00	0.00
MgO	0.00	0.00	0.00	0.00	0.00	10.05	0.00	0.00	0.00	0.00	0.00	2.88	0.00
Al_2O_3	0.00	0.00	0.00	0.00	0.00	0.00	10.00	0.00	0.00	0.00	5.86	5.38	4.79
SiO_2	0.00	0.00	0.00	0.00	0.00	0.00	0.00	0.00	0.00	10.01	0.00	0.00	0.00
NiO	0.00	0.00	0.00	0.00	0.00	0.00	0.00	0.00	0.00	0.00	0.00	0.00	0.00
Ga_2O_3	0.00	0.00	0.00	0.00	0.00	0.00	0.00	0.00	0.00	0.00	0.00	0.00	0.00
Cr_2O_3	0.00	0.00	0.00	0.00	0.00	0.00	0.00	0.00	0.00	0.00	0.00	0.00	0.00
MnO_2	0.00	0.00	0.00	0.00	0.00	0.00	0.00	0.00	0.00	0.00	0.00	0.00	0.00
CuO	0.00	0.00	0.00	0.00	0.00	0.00	0.00	0.00	0.00	0.00	0.00	0.00	0.00
ZnO	0.00	0.00	0.00	0.00	0.00	0.00	0.00	0.00	0.00	0.00	0.00	0.00	0.00
MoO_3	0.00	0.00	0.00	0.00	0.00	0.00	0.00	0.00	0.00	0.00	0.00	0.00	0.00
WO_3	0.00	0.00	0.00	0.00	0.00	0.00	0.00	0.00	0.00	0.00	0.00	0.00	0.00
$Nb2O_5$	0.00	0.00	0.00	0.00	0.00	0.00	0.00	0.00	0.00	0.00	0.00	0.00	0.00
ThO_2	0.00	0.00	0.00	0.00	0.00	0.00	0.00	12.02	0.00	0.00	0.00	0.00	0.00
Total	100.00	100.00	100.00	100.00	100.00	100.00	100.00	100.00	100.00	100.00	100.00	100.00	100.00

Table 1 (cont.). "As-made" starting compositions

	M14	M15	M16	M17	M18	M19	M20	M21	M22	P229	P232	P243
Na_2O	0.00	2.31	4.50	0.00	0.00	0.00	0.00	0.00	0.00	0.00	0.00	0.00
CaO	9.66	9.39	8.46	9.35	9.32	9.32	9.32	9.31	9.34	11.56	10.85	10.65
TiO_2	34.34	33.96	30.40	33.52	33.54	33.55	33.56	33.63	33.54	32.49	30.51	29.94
HfO_2	10.18	10.12	9.10	10.01	10.02	10.11	10.01	10.08	10.03	9.65	9.07	8.90
Gd_2O_3	15.61	7.51	6.76	7.48	7.43	7.46	7.45	7.44	7.44	7.24	6.80	6.68
UO_2	22.68	22.33	20.11	22.22	22.19	22.24	22.23	22.22	22.23	21.57	20.26	27.89
CeO_2	7.53	7.45	6.68	7.36	7.37	7.36	7.36	7.35	7.37	6.88	6.46	6.34
P_2O_5	0.00	0.00	0.00	0.00	0.00	0.00	0.00	0.00	0.00	0.00	0.00	0.00
CaF_2	0.00	0.00	0.00	0.00	0.00	0.00	0.00	0.00	0.00	0.00	0.00	0.00
Fe_2O_3	0.00	0.00	0.00	0.00	0.00	0.00	0.00	0.00	0.00	0.00	0.00	0.00
MgO	0.00	0.00	0.00	0.00	0.00	0.00	0.00	0.00	0.00	0.00	0.00	0.00
Al_2O_3	0.00	2.61	5.31	0.00	0.00	0.00	0.00	0.00	0.00	0.00	0.00	0.00
SiO_2	0.00	4.32	8.68	0.00	0.00	0.00	0.00	0.00	0.00	0.00	0.00	0.00
NiO	0.00	0.00	0.00	10.05	0.00	0.00	0.00	0.00	0.00	0.00	0.00	0.00
Ga_2O_3	0.00	0.00	0.00	0.00	0.00	9.97	0.00	0.00	0.00	0.00	0.00	0.00
Cr_2O_3	0.00	0.00	0.00	0.00	10.13	0.00	0.00	0.00	0.00	0.00	0.00	0.00
MnO_2	0.00	0.00	0.00	0.00	0.00	0.00	10.08	0.00	0.00	0.00	0.00	0.00
CuO	0.00	0.00	0.00	0.00	0.00	0.00	0.00	9.99	0.00	0.00	0.00	0.00
ZnO	0.00	0.00	0.00	0.00	0.00	0.00	0.00	0.00	10.05	0.00	0.00	0.00
MoO_3	0.00	0.00	0.00	0.00	0.00	0.00	0.00	0.00	0.00	10.61	0.00	0.00
WO_3	0.00	0.00	0.00	0.00	0.00	0.00	0.00	0.00	0.00	0.00	16.05	0.00
$Nb2O_5$	0.00	0.00	0.00	0.00	0.00	0.00	0.00	0.00	0.00	0.00	0.00	9.61
ThO_2	0.00	0.00	0.00	0.00	0.00	0.00	0.00	0.00	0.00	0.00	0.00	0.00
Total	100.00	100.00	100.00	100.00	100.00	100.00	100.00	100.00	100.00	100.00	100.00	100.00

2. Starting materials and experimental methods

The goal of this investigation was to assess the effects of impurities in the waste stream on the phase equilibria of the baseline composition. This allows us to make relatively small batches, 1-2 g, of starting materials from mixtures of hydroxides, nitrates, hydrated-nitrates, carbonates, ammoniates and oxides (Appendix A). As many of the starting materials were extremely hygroscopic, we determined the useful oxide yield of each reagent by loss on ignition. Starting materials were ground by hand under ethanol in an alumina mortar and pestle. The resulting slurry was dried under a heat lamp producing a paste; due to the hygroscopic nature of the starting materials, a fully dry powder was never obtained at this stage of the preparation procedure. The paste was then transferred to a Pt crucible and calcined in air at 1000°C for at least 3 hours. This calcine was then reground by hand under ethanol in an alumina mortar and pestle prior to the addition of a polyvinyl alcohol solution to act as a binder. The calcine-polyvinyl alcohol slurry was dried under a heat lamp and then ground dry in an alumina mortar and pestle to obtain a free-flowing powder. Individual samples were hand-pressed in a stainless steel die and piston to produce disks approximately 2 mm thick, with an outside diameter of <5 mm, weighing ~50 mg.

A bottom-loading Deltech furnace was used to anneal samples equilibrated in air. Samples were loaded in open Pt crucibles that were then placed on the lower platen of the furnace and hydraulically lifted into the furnace that was already at run temperature. Temperature was monitored using a Pt-Rh thermocouple placed within 5 mm of the sample. Samples reached run conditions within 2-4 minutes after insertion, and run duration was always in excess of 24 hours. Runs were quenched by lowering the platen and removing the crucibles that then cooled in air, reaching room temperature in less than five minutes.

3. Sample characterization

The sintered disks were mounted in epoxy and then polished with alumina grits prior to final polishing with colloidal silica. The polished mounts were then carbon coated for SEM and electron probe analysis. Compositional analysis was performed on a JEOL-733 electron probe using wavelength dispersive analysis. The probe was operated at an accelerating voltage of 15 KV with a beam current (measured in a Faraday cup embedded in the standard holder) of 5-100 na; lower currents were used on beam sensitive materials such as silica glass. X-ray intensities were reduced to oxide concentrations using the ZAF method as revised by Armstrong *et al.* (1995). The standards used in these analyses are given in Appendix B. Two notable x-ray interferences were observed. The $Ce_{L\beta 1}$ line interferes with the Gd $_{L\alpha 1}$ requiring the use of the Gd $_{L\beta 1}$ line, and in the Th-bearing samples, the $Th_{M\beta 1}$ interferes with the $U_{M\alpha 1\text{-}1}$ requiring use of the $U_{M\beta 1}$ line.

4. Results

In many of the experiments presented here, the addition of 10 wt% of a waste stream impurity oxide resulted in the formation of an accessory phase coupled with limited solution of the impurity element in the pyrochlore-brannerite-hafnolite-rutile phase assemblage (Table 2). We have divided the elements into two groups depending upon whether there is "appreciable" dissolution of the impurity element in pyrochlore. Weight fractions of phases in runs performed at 1350°C were determined by linear regression of the average phase compositions and the "as-made" bulk compositions of the samples (Table 3).

Table 2. Run Results

Run #	Starting Composition	Variation	T (C)	Phases
1/1	M1	Hf-Ce-U	1300	pyr, brn, rut
1/2	M1	Hf-Ce-U	1400	pyr, brn, rut
1/3	M1	Hf-Ce-U	1350	pyr, rut
2/1	M2	Hf-Ce-U + P	1300	brn, rut, CLP, P-glass
2/2	M2	Hf-Ce-U + P	1400	brn, rut, P-glass
2/3	M2	Hf-Ce-U + P	1350	brn, rut, CLP, P-glass
3/1	M3	Hf-Ce-U + CaF_2	1300	pyr, pv, hfn
3/2	M3	Hf-Ce-U + CaF_2	1400	pyr, pv
3/3	M3	Hf-Ce-U + CaF_2	1350	pyr, pv
4/1	M4	Hf-Ce-U + Fe_2O_3	1300	pyr, brn, hfn, ilm
4/2	M4	Hf-Ce-U + Fe_2O_3	1400	melted
4/3	M4	Hf-Ce-U + Fe_2O_3	1350	melted
5/1	M5	Hf-Ce-U	1300	pyr, brn, rut
5/2	M5	Hf-Ce-U	1400	pyr, brn, rut
5/3	M5	Hf-Ce-U	1350	pyr, brn, rut
6/1	M6	Hf-Ce-U + MgO	1300	pyr, hfn, pv, MgTi-1
6/2	M6	Hf-Ce-U + MgO	1400	pyr, pv, MgTi-1, MgTi-2
6/3	M6	Hf-Ce-U + MgO	1350	pyr, pv, MgTi-1, MgTi-2
7/1	M7	Hf-Ce-U + Al_2O_3	1300	pyr, brn, hfn, cor, rut
7/2	M7	Hf-Ce-U + Al_2O_3	1400	pyr, brn, hfn, psd
7/3	M7	Hf-Ce-U + Al_2O_3	1350	pyr, brn, hfn, psb
8/1	M8	Hf-Th-U	1300	pyr, brn, rut
8/2	M8	Hf-Th-U	1400	pyr, brn, rut
8/3	M8	Hf-Th-U	1350	pyr, brn, rut
9/1	M9	Hf-Ce-U + CaO	1300	pyr, pv
9/2	M9	Hf-Ce-U + CaO	1400	pyr, pv
9/3	M9	Hf-Ce-U + CaO	1350	pyr, pv
10/1	M10	Hf-Ce-U +10% SiO_2	1300	brn, rut, glass
10/2	M10	Hf-Ce-U +10% SiO_2	1350	brn, hfO_2, glass
11/2	M11	Hf-Ce-U +10% $FeAl_2O_4$	1300	py, hfn, psd
11/1	M11	Hf-Ce-U +10% $FeAl_2O_4$	1350	py, hfn, psd
11/3	M11	Hf-Ce-U +10% $FeAl_2O_4$	1400	melted

All runs performed in air.

Py=pyrochlore, brn=brannerite, ru=rutile, hfn=hafnolite, pv=perovskite, CLP=calcium-lanthanide phosphate, P-glass=phosphorus-rich glass, MgTi-1=$MgTiO_3$, MgTi-2=Mg_2TiO_4, psb=psuedobrookite, cor=corundum, CTA=calcium-lanthanide titanium aluminate, Ga="galonite", croxy=Cr_xO_y, Ni-Ti=$NiTiO_3$, Ca-Mo=calcium molybdate, Ca-W=calcium tungstate

Table 2 (cont.). Run Results

Run #	Starting Composition	Variation	T (C)	Phases
12/2	M12	Hf-Ce-U +10% $MgAl_2O_4$	1300	py, hfn, psb
12/1	M12	Hf-Ce-U +10% $MgAl_2O_4$	1350	py, psb
12/3	M12	Hf-Ce-U +10% $MgAl_2O_4$	1400	melted
13/2	M13	Hf-Ce-U +10% $CaAl_2O_4$	1300	py, hfn, CTA, cor, rut
13/1	M13	Hf-Ce-U +10% $CaAl_2O_4$	1350	py, hfn,CTA
13/3	M13	Hf-Ce-U +10% $CaAl_2O_4$	1400	py, hfn,CTA
14/2	M14	Hf-Ce-U +10% Gd_2O_3	1300	py, brn, rut
14/1	M14	Hf-Ce-U +10% Gd_2O_3	1350	py, brn, rut
14/3	M14	Hf-Ce-U +10% Gd_2O_3	1400	py, brn, rut
15/2	M15	Hf-Ce-U +10% $NaAlSiO_4$	1300	py, hfn, rut, glass
15/1	M15	Hf-Ce-U +10% NaAlSiO	1350	py, hfn, glass
16/2	M16	Hf-Ce-U +20% NaAlSiO	1300	py, hfn, qlass
16/1	M16	Hf-Ce-U +20% NaAlSiO	1350	py, hfn, qlass
17/2	M17	Hf-Ce-U +10% NiO	1300	py, hfn, Ni-Pv
17/1	M17	Hf-Ce-U +10% NiO	1350	py, hfn, Ni-Pv
17/3	M17	Hf-Ce-U +10% NiO	1400	melted
18/2	M18	Hf-Ce-U +10% Cr_2O_3	1300	py, hfn, rut, crxoy
18/1	M18	Hf-Ce-U +10% Cr_2O_3	1350	py, hfn, rut, crxoy
18/3	M18	Hf-Ce-U +10% Cr_2O_3	1400	py, hfn, rut, crxoy
19/2	M19	Hf-Ce-U +10% Ga_2O_3	1300	py, hfn, Ga
19/1	M19	Hf-Ce-U +10% Ga_2O_3	1350	py, hfn, Ga
20/2	M20	Hf-Ce-U +10% MnO_2	1300	py, pv
20/1	M20	Hf-Ce-U +10% MnO_2	1350	py, pv
20/3	M20	Hf-Ce-U +10% MnO_2	1400	py, pv
21/2	M21	Hf-Ce-U +10% CuO	1300	py, rut
21/1	M21	Hf-Ce-U +10% CuO	1350	py, rut
22/2	M22	Hf-Ce-U +10% ZnO	1300	py, hfn
22/1	M22	Hf-Ce-U +10% ZnO	1350	py, rut
P229	P229	Hf-Ce-U +10% MoO_3	1350	py, brn, Ca-Mo
P232	P232	Hf-Ce-U +10% WO_3	1350	py, brn, rut, Ca-W
P243	P243	Hf-Ce-U +10% Nb_2O_5	1350	py, brn, rut

All runs performed in air.

Py=pyrochlore, brn=brannerite, ru=rutile, hfn=hafnolite, pv=perovskite, CLP=calcium-lanthanide phosphate, P-glass=phosphorus-rich glass, MgTi-1=$MgTiO_3$, MgTi-2=Mg_2TiO_4, psb=psuedobrookite, cor=corundum, CTA=calcium-lanthanide titanium aluminate, Ga="galonite", croxy=Cr_xO_y, Ni-Ti=$NiTiO_3$, Ca-Mo=calcium molybdate, Ca-W=calcium tungstate

Table 3. Phase fractions based on linear regression of bulk and phase compositions

	1/3	±	2/3	±	3/3	±	4/1	±	5/3	±	6/3	±	7/3	±	8/3	±
Py	1.049	0.074	0.659	0.037	0.918	0.059	0.418	0.079	0.79	0.035	0.813	0.028	0.522	0.207	0.733	0.036
Brn	0	0	0	0	0	0	0.066	0.043	0.187	0.031	0	0	0.187	0.156	0.282	0.034
Hfn	0	0	0	0	0	0	0.41	0.117	0	0	0	0	0.142	0.091	0	0
Ru	0.021	0.041	0.105	0.026	0	0	0	0	0.052	0.01	0	0	0	0	-0.004	0.013
Pv	0	0	0	0	0.09	0.044	0	0	0	0	-0.012	0.029	0	0	0	0
CTA	0	0	0	0	0	0	0	0	0	0	0	0	0	0	0	0
$MgTiO_3$	0	0	0	0	0	0	0	0	0	0	0.07	0.046	0	0	0	0
$MgTi_2O_4$	0	0	0	0	0	0	0	0	0	0	0.155	0.053	0	0	0	0
$NiTiO_3$	0	0	0	0	0	0	0	0	0	0	0	0	0	0	0	0
Galonite	0	0	0	0	0	0	0	0	0	0	0	0	0	0	0	0
Psb	0	0	0	0	0	0	0	0	0	0	0	0	0.129	0.039	0	0
Fe-psb	0	0	0	0	0	0	0	0	0	0	0	0	0	0	0	0
Mg-psb	0	0	0	0	0	0	0	0	0	0	0	0	0	0	0	0
Ilmenite	0	0	0	0	0	0	0.085	0.034	0	0	0	0	0	0	0	0
CLP	0	0	0.106	0.072	0	0	0	0	0	0	0	0	0	0	0	0
P-glass	0	0	0.135	0.082	0	0	0	0	0	0	0	0	0	0	0	0
Si-glass	0	0	0	0	0	0	0	0	0	0	0	0	0	0	0	0
Ca-Mo	0	0	0	0	0	0	0	0	0	0	0	0	0	0	0	0
Ca-W	0	0	0	0	0	0	0	0	0	0	0	0	0	0	0	0
Hf-Ti	0	0	0	0	0	0	0	0	0	0	0	0	0	0	0	0

Table 3 (cont.). Phase fractions based on linear regression of bulk and phase compositions

	9/3	±	10/1	±	11/1	±	12/1	±	13/1	±	15/1	±	16/1	±	17/1	±
Py	0.797	0.07	0	0	0.651	0.096	0.886	0.069	0.84	0.079	0.791	0.063	0.556	0.078	0.85	0.076
Brn	0	0	0.376	0.055	0	0	0	0	0	0	0	0	0	0	0	0
Hfn	0	0	0	0	0.157	0.115	0	0	0.1	0.077	-0.002	0.047	-0.043	0.055	0.01	0.077
Ru	0	0	-0.048	0.029	0	0	0	0	0	0	0	0	0	0	0	0
Pv	0.231	0.049	0	0	0	0	0	0	0	0	0	0	0	0	0	0
CTA	0	0	0	0	0	0	0	0	0.056	0.033	0	0	0	0	0	0
$MgTiO_3$	0	0	0	0	0	0	0	0	0	0	0	0	0	0	0	0
$MgTi_2O_4$	0	0	0	0	0	0	0	0	0	0	0	0	0	0	0	0
$NiTiO_3$	0	0	0	0	0	0	0	0	0	0	0	0	0	0	0.155	0.033
Galonite	0	0	0	0	0	0	0	0	0	0	0	0	0	0	0	0
Psb	0	0	0	0	0	0	0	0	0	0	0	0	0	0	0	0
Fe-psb	0	0	0	0	0.195	0.033	0	0	0	0	0	0	0	0	0	0
Mg-psb	0	0	0	0	0	0	0.094	0.048	0	0	0	0	0	0	0	0
Ilmenite	0	0	0	0	0	0	0	0	0	0	0	0	0	0	0	0
CLP	0	0	0	0	0	0	0	0	0	0	0	0	0	0	0	0
P-glass	0	0	0	0	0	0	0	0	0	0	0	0	0	0	0	0
Si-glass	0	0	0.696	0.068	0	0	0	0	0	0	0.199	0.052	0.476	0.068	0	0
Ca-Mo	0	0	0	0	0	0	0	0	0	0	0	0	0	0	0	0
Ca-W	0	0	0	0	0	0	0	0	0	0	0	0	0	0	0	0
Hf-Ti	0	0	0	0	0	0	0	0	0	0	0	0	0	0	0	0

Table 3 (cont.). Phase fractions based on linear regression of bulk and phase compositions

	18/1	±	19/1	±	20/1	±	21/1	±	22/1	±	P229		P232		P243	
Py	0.777	0.044	0.611	0.086	1.075	0.029	1.002	0.069	1.003	0.073	0.576	0.069	0.781	0.094	0.667	0.152
Brn	0	0	0	0	0	0	0	0	0	0	0.359	0.056	0.17	0.073	0.479	0.156
Hfn	0.018	0.039	0.277	0.115	0	0	0	0	0	0	0	0	0	0	0	0
Ru	0.143	0.03	0	0	0	0	0.043	0.04	0.034	0.041	0	0	0	0	0	0
Pv	0	0	0	0	-0.024	0.021	0	0	0	0	0	0	0.047	0.018	-0.057	0.065
CTA	0	0	0	0	0	0	0	0	0	0	0	0	0	0	0	0
$MgTiO_3$	0	0	0	0	0	0	0	0	0	0	0	0	0	0	0	0
$MgTi_2O_4$	0	0	0	0	0	0	0	0	0	0	0	0	0	0	0	0
$NiTiO_3$	0	0	0	0	0	0	0	0	0	0	0	0	0	0	0	0
Galonite	0	0	0.1	0.073	0	0	0	0	0	0	0	0	0	0	0	0
Psb	0	0	0	0	0	0	0	0	0	0	0	0	0	0	0	0
Fe-psb	0	0	0	0	0	0	0	0	0	0	0	0	0	0	0	0
Mg-psb	0	0	0	0	0	0	0	0	0	0	0	0	0	0	0	0
Ilmenite	0	0	0	0	0	0	0	0	0	0	0	0	0	0	0	0
CLP	0	0	0	0	0	0	0	0	0	0	0	0	0	0	0	0
P-glass	0	0	0	0	0	0	0	0	0	0	0	0	0	0	0	0
Si-glass	0	0	0	0	0	0	0	0	0	0	0	0	0	0	0	0
Ca-Mo	0	0	0	0	0	0	0	0	0	0	0.137	0.012	0	0	0	0
Ca-W	0	0	0	0	0	0	0	0	0	0	0	0	0.061	0.021	0	0
Hf-Ti	0	0	0	0	0	0	0	0	0	0	0	0	0	0	0.02	0.049

4.1 Insoluble Impurities

4.1.1 The baseline assemblage

Two Ce-analog baseline mixtures were synthesized in order to compare the resulting phase assemblage as a function of starting materials (Plate 1). The first, M1, was made from a combination of nitrates, ammoniates and oxides, while the second, M5, was made strictly from oxides and carbonates. Runs were performed in air at 1300°C, 1350°C and 1400°C and produce the assemblage pyrochlore+rutile±brannerite (Table 3). Brannerite was found in all of the runs synthesized from oxides, and in all but the 1350°C run from the M1 compositions. Its absence in run "1/3" may simply be the result of small variations in bulk chemistry, kinetics, or difficulties associated in detecting phases with low modal abundance

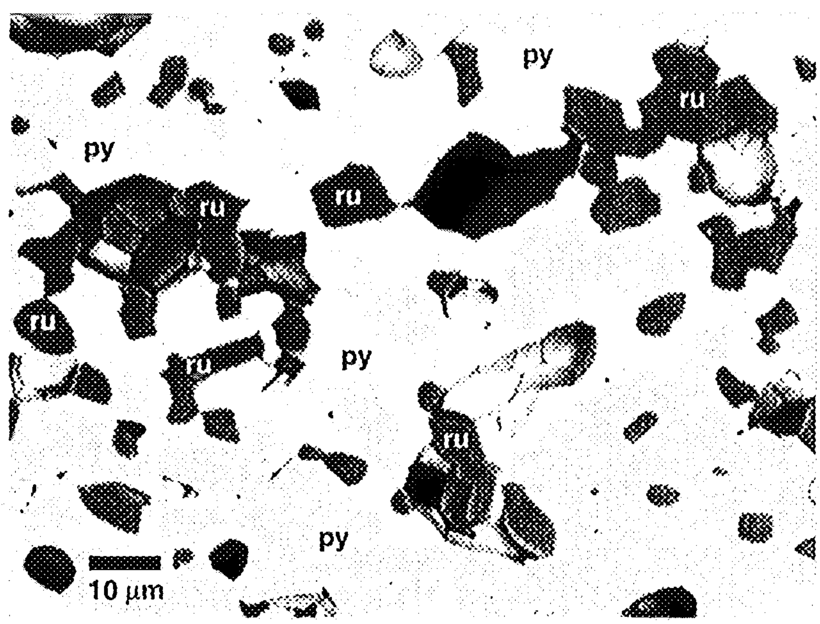

Plate 1a. Backscattered electron image of Ce-analog baseline formulation sintered at 1350°C in air (1/3). Phase assemblage includes pyrochlore (py) and rutile (ru).

The compositions of the individual phases do not show significant variation as a function of either starting material or run temperature (Tables C1 and C2). The typical pyrochlore composition (see sample 1/3, Table C1) is $Ca_{1.02}Ce_{0.25}Gd_{0.23}Hf_{0.16}U_{0.35})(Ti_{1.93}Hf_{0.06}Al_{0.02})O_{6.74}$, in which Ce replaces Pu, is somewhat different from that in the nominal baseline formulation, $(Ca_{0.89}Gd_{0.22}Hf_{0.23}U_{0.44}Pu_{0.22})Ti_2O_7$. The observed Ce/Gd ratio in pyrochlore, 1.02, is equal, within error, to that in the bulk composition, 1.04, and is consistent with the modal predominance of this phase. The observed analog pyrochlore composition is higher in calcium than that used in the target formulation, however. Mass balance, therefore requires the presence of a phase with lower calcium content, explaining the common occurrence of brannerite. The observed pyrochlore is also slightly lower in titanium and uranium than that of the baseline model.

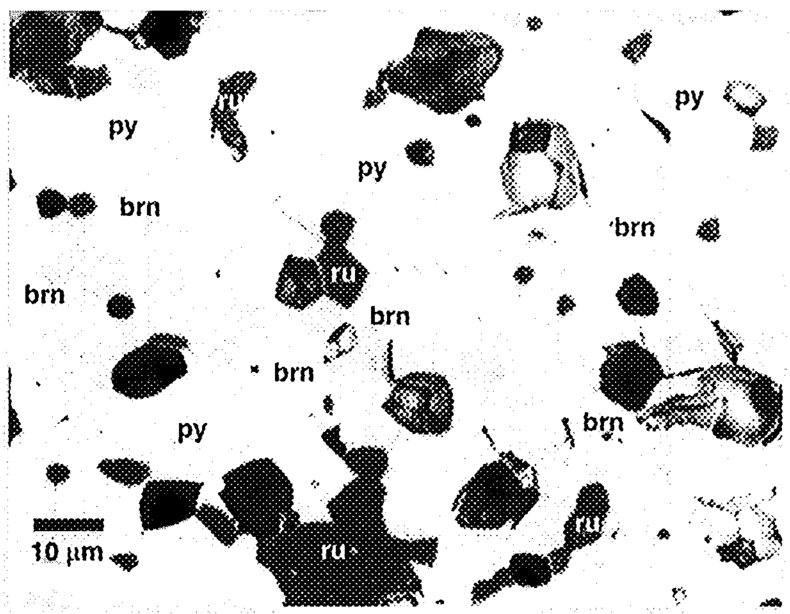

Plate 1b. Backscattered electron image of Ce-analog baseline formulation sintered at 1350°C in air (5/3). Phase assemblage includes pyrochlore (py), brannerite (brn) and rutile (ru). Materials synthesized from oxide and carbonates only.

Brannerite displays little run-to-run variation in chemistry, and has an average composition of $(Ca_{0.11}Ce_{0.22}Gd_{0.15}Hf_{0.12}U_{0.43})Ti_{1.95}O_{5.7}$; the Ti-site is essentially full. The average rutile composition, $(U_{0.01}Hf_{0.09}Ti_{0.9})O_2$, is somewhat depleted in hafnium relative to the target composition used in the formulation, $(Hf_{0.2}Ti_{0.8})O_2$. The disparity can be resolved by minor variation in the modal abundance and also by the presence of brannerite in most runs.

Using the average phase compositions given above, and the "as-made" composition of M1, the modal phase proportions determined by linear regression are 75±8 wt% pyrochlore, 24±7 wt% brannerite and 2±1 wt% rutile. These proportions are substantially different from the target concentrations, reflecting the disparity between target and observed phase compositions.

Both pyrochlore and brannerite are oxygen deficient for stoichiometries based upon Ce^{+3} and U^{+4}. For instance, if uranium and cerium are assumed to be present as +4 and +3 cations, respectively, then the average pyrochlore has only 6.7 oxygens per 4 cations, rather than the ideal 7 oxygen per formula unit (pfu). These disparities can be resolved if some combination of U and Ce are present in a higher oxidation state. Unfortunately, a unique valence distribution cannot be determined from chemical analysis alone.

Fortner *et al.* (1999) have determined the valence of Ce and U in a ceramic formulation similar to that presented here by XANES and EXAFS spectroscopy. They find that cerium exists in a mixed oxidation state ($Ce^{+4}/\sum Ce$ ~0.33) and that uranium is present largely as the pentavalent species (personal communication, 1999). It is likely, however, that addition of other components will perturb the valence states of these cations even at constant external conditions. By assuming a fixed $Ce^{+4}/\sum Ce$ ratio, we calculate the "average valence" of uranium based on the ideal 4/7 and 3/6 stoichiometries of pyrochlore/hafnolite and brannerite, respectively. As various combinations of valence states can satisfy the ideal stoichiometry, the result obtained is not unique, nor does it resolve the distribution of uranium among U^{+4}, U^{+5} and U^{+6}.

If we assume that $Ce^{+4}/\sum Ce$ ~0.33, we obtain average valence for uranium (expressed as x in UO_x) of 2.62±0.08 (2δ), which is equivalent to $U^{+5.24}$, for our experiments on the impurity-free baseline composition (Tables 4 and 5). The agreement between this calculation and the spectroscopic determinations of Fortner *et al.* (1999), suggests, that while our calculation cannot provide a unique valence determination, it does, however, allow simple comparison between different materials, and can act as monitor of the effects of minor element addition.

4.1.2 The baseline assemblage with 10 wt% Al_2O_3

The addition of Al_2O_3 to the baseline formulation stabilizes hafnolite and an Al-rich accessory mineral (Table 2). At 1300°C the Al-rich phase is corundum in equilibrium with rutile. At higher temperatures, these phases react to form Al-psuedobrookite, Al_2TiO_5. The individual phases are 5-10 μm in diameter with brannerite and Al-psuedobrookite being

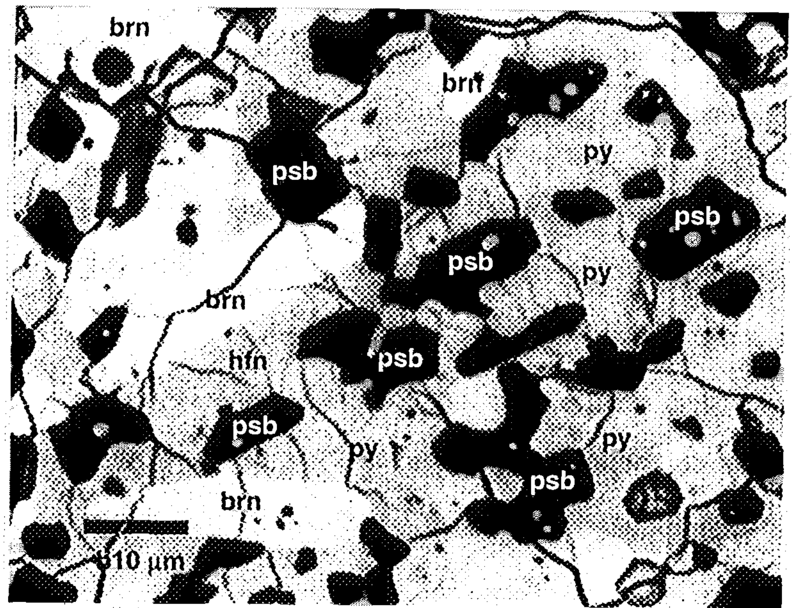

Plate 2. Baseline formulation with 10 wt% Al_2O_3 added. Sintered at 1350°C in air (7/3). Phase assemblage includes pyrochlore (py), brannerite (brn), hafnolite (hfn) and rutile (ru).

somewhat elongate (Plate 2). The phases fractions for the 1350°C run are given in Table 3, and indicate that pyrochlore remains the most abundant phase (~52 wt%). Both corundum and Al-psuedobrookite are essentially free of constituents other than Al_2O_3 and TiO_2 (Table C3). Hafnolite contains ~4 wt% Al_2O_3 and has the structural formula $(Ca_{0.78}Gd_{0.18})$(Al-

$_{0.09}Ce_{0.10}Hf_{0.68}U_{0.15})(Ti_{1.75}Al_{0.25})O_{6.92}$ at 1350°C. The close approach to 7 oxygens per 4 cations is consistent with uranium and cerium being in the +4 and +3 oxidation states, respectively.

The compositions of pyrochlore and brannerite (Table 6) are virtually identical to those in the baseline formulation, and contain insignificant amounts of Al_2O_3. Pyrochlore contains only ~0.4 wt% Al_2O_3 and brannerite ~1.4 wt%. The structural formula for pyrochlore at 1350°C is $(Ca_{1.05}Ce_{0.26}Gd_{0.21}Hf_{0.09}U_{0.38})(Ti_{1.91}Hf_{0.06}Al_{0.03})O_{6.7}$ and that of brannerite is $Ca_{0.08}Ce_{0.24}Gd_{0.13}Hf_{0.09}U_{0.46}Ti_{1.90}Al_{0.11}O_{5.68}$, and as is the case with the impurity-free baseline sample they are oxygen deficient which is mostly likely indicative of uranium in an oxidation state greater than +4. If $Ce^{+4}/\Sigma Ce=0.33$, the average uranium valence, UO_x, is close to x=2.7 and is within error of the value obtained for the impurity-free baseline formulation, consistent with the overall similarity in phase composition and the low concentrations of Al_2O_3 in brannerite and pyrochlore.

The low concentrations of Al_2O_3 in pyrochlore and brannerite indicate that even small amounts of Al_2O_3 in the waste stream will result in either the formation or hafnolite on an Al-rich accessory phase. For instance, if the desired phase assemblage was formulated to produce a pyrochlore-rutile assemblage, molar ratio above 0.08 moles Al_2O_3/mole of PuO_2 would result in the stabilization of Al-psuedobrookite at 1350°C. However, the Al-rich accessory phases do not alter the ratio of Pu to neutron absorbers in pyrochlore or brannerite, and they contain no plutonium. As such, its presence will have negligible effect on the wasteform performance.

4.1.3 The baseline assemblage with 10 wt% Fe_2O_3

For materials synthesized at 1300°C the addition of 10 wt% Fe_2O_3 yields results similar to those observed for the Al_2O_3. Iron stabilizes hafnolite, and a Fe-rich accessory phase, ilmenite (Table 2). With the exception of a small amount of HfO_2, ilmenite contains only iron and titanium. However, pyrochlore and brannerite do contain significant iron and are somewhat different in composition from those in the baseline composition (Table C4). Pyrochlore has the structural formula $(Ca_{1.09}Ce_{0.25}Gd_{0.14}Fe_{0.07}U_{0.45})(Ti_{1.85}Hf_{0.07}Al_{0.04}Fe_{0.07})O_{6.43}$ and contains ~2.4 wt% FeO. Brannerite, $(Ca_{0.11}Ce_{0.24}Gd_{0.10}Hf_{0.04}U_{0.49})(Ti_{1.84}Al_{0.01}Fe_{0.17})O_{5.39}$ and contains ~3 wt% FeO. Of the primary phases hafnolite contains the highest concentration of iron at ~11 wt%. The concentration of iron in hafnolite, $(Ca_{0.62}Ce_{0.17}Gd_{0.17}U_{0.05})(Fe_{0.56}Hf_{0.32}U_{0.12})(Ti_{1.90}Al_{0.03}Fe_{0.07})O_{5.94}$, alters the nominal phase proportions such that the weight fractions of both pyrochlore and hafnolite are ~40 wt% of the sample (Table 3). The presence of iron also appears to alter the partitioning of neutron absorbing elements relative to that in the impurity-free Ce-analog, as the Ce/Gd ratio in the pyrochlore in this run is 1.7 while that in the baseline composition is ~1.

When calculated as Ce^{+3}, U^{+4} and Fe^{+2}, pyrochlore, hafnolite and brannerite are quite oxygen deficient, 6.5 oxygens/4 cations and 5.9 oxygens per 4 cations, respectively, and the deficiency correlates with iron concentration. However, if Fe is cast as Fe^{+3} values of UO_x close to those of the baseline formulation and Al_2O_3-doped run products are obtained, suggesting that the iron is present primarily as Fe^{+3} in these materials. This is not the case for the ilmentie-hematite phase ($FeTiO_3$-Fe_2O_3) in which the $Fe^{+3}/\Sigma Fe = 0.41$. the substitution of Fe^{+3} for quadravalent cations may enhance the solubility of lanthanides in pyrochlore via $Ca^{+2} + U^{+4} = 2\ Gd^{+3}$.

Stewart *et al.* (1999) added Fe along with a suite of other divalent cations (Mg, Co, Ni, Cu, Zn, ~16 wt% total) to the baseline formulation. Instead of ilmenite, they observed an ulvöspinel-rich spinel solid solution (M_2TiO_4, where M is a divalent cation). The difference between the two sets of experiments can be explained by the ability of Fe to exist as Fe^{+2} and/or Fe^{+3} rather than to be wholly divalent. As such, Fe^{+3} stabilizes the ilmenite solid solution by increasing the activity of Fe_2O_3, while divalent cations favor ulvöspinel. Ilmenite is also stabilized by the higher Ti/Fe ratio of our materials.

A more serious concern with respect to the addition of Fe is that samples synthesized at 1350°C and 1400°C both melted and could not be recovered for analysis. The presence of a eutectic in the pyrochlore-brannerite-hafnolite-ilmenite field at these temperatures limits the compositional range for successful synthesis. If the composition of pyrochlore is taken as a limit on the Fe content, then the limiting ratio of Fe could be as low as 0.56 moles for FeO/mole of PuO_2. Perhaps a more realistic estimate can be obtained by eliminating ilmenite from the assemblage and combining pyrochlore, hafnolite and brannerite in a 0.4:0.4:0.2 weight ratio yielding an composition with a ratio of moles FeO per mole of PuO_2 equal to 1.6. An absolute upper limit is given by the composition of hafnolite in which the moles for FeO/mole of PuO_2 is 3.74.

4.1.4 The baseline assemblage with 10 wt% MgO

The assemblages resulting from the addition of MgO vary with synthesis temperature (Table 2). At 1300°C pyrochlore, hafnolite, perovskite and $MgTiO_3$ coexist. At 1350°C hafnolite disappears and is replaced by Mg_2TiO_4 (Plate 3). Finally at 1400°C perovskite is no longer part of the assemblage. However, regression analysis indicates that only pyrochlore, which is always greater than 80 wt% of the sample (Table 3) and the Mg-titanates are present in non-negligible amounts. In addition to Mg and Ti, the Mg-titanates contain only HfO_2 in detectable amounts.

The average pyrochlore formula from the 1350°C run is $(Ca_{1.01}Ce_{0.26}Gd_{0.24}U_{0.46})(Ti_{1.51}Hf_{0.30}Mg_{0.22})O_{6.53}$ (Table C5). The Ca content is similar to that in previous experiments, and since pyrochlore is the only modally significant lanthanide-bearing phase, the Ce/Gd ratio approximates that of the starting material. The Hf concentration of pyrochlore is somewhat higher than that of materials containing either brannerite or hafnolite.

The Ti content of both pyrochlore and hafnolite are significantly lower than that in the impurity-free or Al-doped runs (Table C1, C2, C3 and C5). If, due to its small cationic

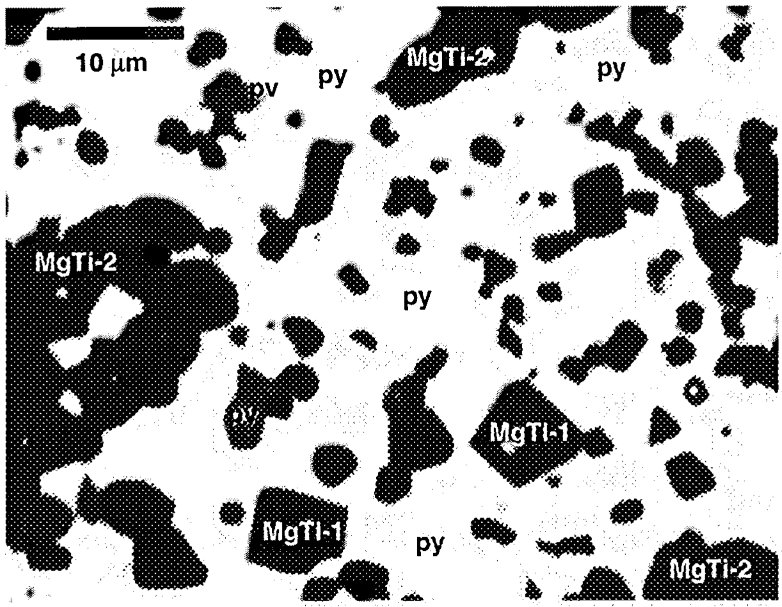

Plate 3. Backscattered electon image of baseline formulation with 10 wt% MgO added. Sintered at 1350°C in air (6/3). Phase assemblage includes pyrochlore (py), perovskite (pv) and two magnesium titanates, $MgTiO_3$ (MgTi-1) and Mg_2TiO_4 (MgTi-2).

radius, Mg^{+2} substitutes for Ti on the Ti-site, then the Ti-site will be charge deficient. One way to maintain charge compensation is to oxidize either U and/or Ce on the A-site. This appears to be the case. For $Ce^{+4}/\Sigma Ce=0.33$, the average uranium valence of pyrochlore is ~$UO_{2.9}$ as opposed to $UO_{2.6}$ in the impurity-free baseline formulation run products. A similar calculation for the hafnolite yields $UO_{2.7}$ at 1300°C (Table C5). Another product of the low Ti content is that the A-site is now free of Hf that resides only on the Ti-site. This could effect the partitioning of hafnium and explain the elevated hafnium concentration levels in the pyrochlores produced here. The addition of MgO may also effect the partitioning of uranium by coupled substitutions such as,

$$Mg^{+2} + U^{+6} = 2Ti^{+4}$$

Indeed, the hafnolite in the 1300°C run contains 22.7 wt% UO_2, about 3 times more than in the hafnolites from the Al-doped run products.

Stewart *et al.* (1999) added Mg along with a suite of other divalent cations (Mg, Co, Ni, Cu, Zn, ~16 wt% total) to a Ce-analog formulation and observed an ulvöspinel spinel solid solution, M_2TiO_4, where M is a divalent cation. The Mg_2TiO_4 observed here is equivalent to that phase. As the Mg-titanates contain no significant nuclides and the pyrochlore composition is not substantially altered by the presence of Mg, it appears that MgO may be accommodated in unlimited concentrations. The major effects are the stabilization of hafnolite and the Mg-titanates and to a lesser extent perovskite. Incorporation of MgO in these phases may also effect the valence states of U, Ce and, by extension, Pu.

4.1.5 The baseline assemblage with 10 wt% NiO

The addition of NiO results in a phase assemblage that is largely pyrochlore and $NiTiO_3$ with minor hafnolite at 1300°C and 1350°C (Table 2, 3 and C6, Plate 4). The $NiTiO_3$ is the major repository of Ni and also contains ~4 wt% HfO_2, but no other neutron

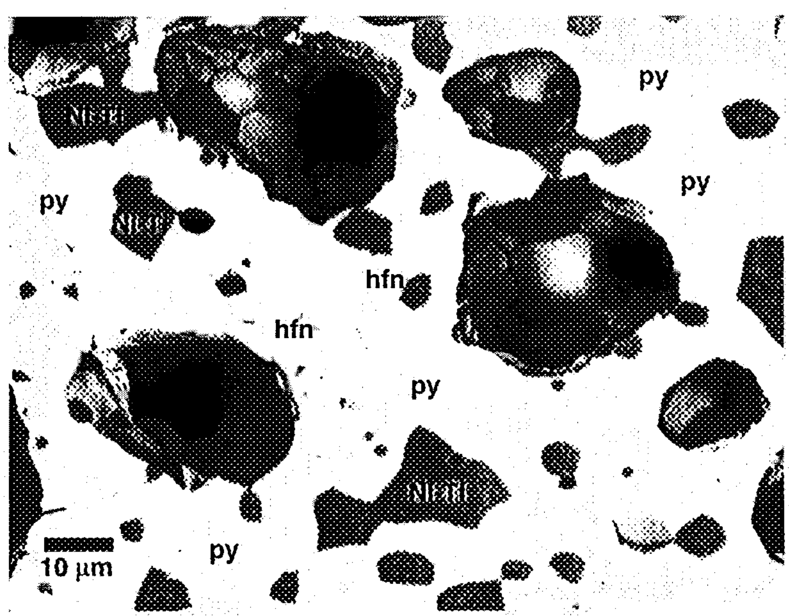

Plate 4. Baseline formulation with 10 wt% NiO added. Sintered at 1350°C in air (17/1). Phase assemblage includes pyrochlore (py), hafnolite (hfn), and Ni-titanate (Ni-Ti).

absorbers or cerium. Hafnolite also contains NiO (~6 wt%), but is modally insignificant (Table 3). The pyrochlore formula (1350°C) resembles that in previous runs and is given by the formula, $(Ca_{1.00}Ni_{0.13}Ce_{0.24}Gd_{0.23}Hf_{0.01}U_{0.39})(Ti_{1.79}Hf_{0.21})O_{6.63}$. As there are no other lanthanide-bearing phases present, the Gd/Ce ratio is that of the starting material. Nickel addition may also effect valence states as it increases the divalent cations content of the A-site in pyrochlore and the B-site in hafnolite. The UO_x values at 1350°C, assuming $Ce^{+4}/\Sigma Ce=0.33$ are x=2.85 and x=2.7, respectively, for pyrochlore and hafnolite. Oxidation of uranium or cerium maintains charge balance. As such, the only real effect of adding Ni to the sample is to produce radionuclide and neutron absorber-free $NiTiO_3$, and therefore does not limit the composition of the wasteform.

4.1.6 The baseline assemblage with 10 wt% CuO

The results from experiments at 1300°C and 1350°C in which CuO was added are equivocal, as it appears to have almost completely volatilized, producing the baseline assemblage pyrochlore plus rutile (Table 2, 3 and C7). Minor amounts of CuO are

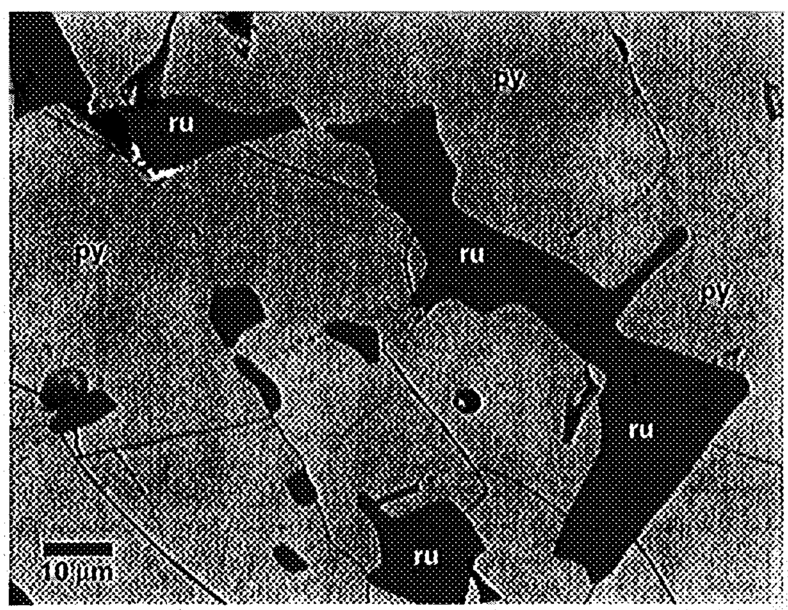

Plate 5. Baseline formulation with 10 wt% CuO added. Sintered at 1350°C in air (21/1). Phase assemblage includes pyrochlore (py) and rutile (ru).

detectable in pyrochlore at the 1-2 wt% level, but are close to detection limits in rutile (Table C7). One noticeable feature of the CuO-bearing runs is the relatively large grain size (Plate 5); pyrochlore grains are in excess of 30 μm in diameter relative to 10 μm or less in most other runs. This suggests that CuO may have acted as a flux during sintering of these materials. In fact, a run at 1400°C melted. Given the intended processing range of 1300-1350°C it is likely that CuO will not limit the composition of the wasteform as it will be lost to volatilization. However, caution should be exercised for production sized material where rapid sintering of the outer portions of a puck could inhibit volatile loss from the interior, enhancing the potential for melting. Otherwise, the pyrochlore and rutile compositions and the values of UO_x required for stoichiometry, x=2.68, are virtually indistinguishable from the baseline formulation run products (Tables C1 and C7)

4.1.7 The baseline assemblage with 10 wt% ZnO

The results of ZnO-bearing runs are quite similar to those from the Cu-bearing experiments (Table 2, 3 and C8). The Zn-bearing runs have grain sizes near 30 μm, similar to those in the Cu-bearing runs (Plate 6), suggesting that ZnO may also act as a flux during sintering. At 1350°C the assemblage is pyrochlore plus rutile. The concentration of ZnO in both phases is close to the detection limit. However, at 1300°C the assemblage is pyrochlore plus hafnolite. Pyrochlore contains ~2 wt% ZnO and hafnolite greater than 7 wt%. Clearly, Zn stabilizes hafnolite at the expense of rutile. It is also clear that the volatilization of Zn increases between 1300°C and 1350°C.

Using the normal structural assignments, zinc enters the A-site in pyrochlore and the B-site in hafnolite. Like Ni and Mg addition, the zinc increases the number of divalent cations on these sites requiring charge excess on adjacent sites, or in a system of fixed composition, increases in cation valence. The later is the case here, as the average uranium valence for the 1300°C Zn-bearing runs, $UO_{2.87}$ and $UO_{2.85}$ in pyrochlore and hafnolite, respectively, are higher than those of the 1350°C runs where Zn has been volatilized.

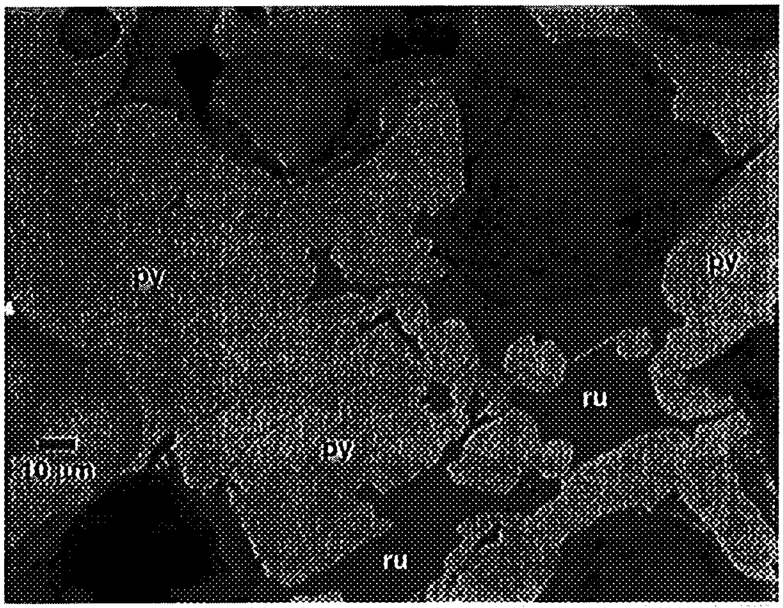

Plate 6. Backscattered electron image of baseline formulation with 10 wt% ZnO added. Sintered at 1350°C in air (2/3). Phase assemblage includes pyrochlore (py) and rutile (ru).

The 1350°C run does not contain a Zn-rich accessory phase, and as such pyrochlore and hafnolite are not buffered with respect to Zn-concentration. This is also the case in the experiments of Stewart *et al.* (1999) where Zn was added with a suite of other divalent cations (Mg, Co, Ni, Cu and Zn, ~16 wt% total) which resulted in a pyrochlore, hafnolite, perovskite, ulvöspinel assemblage. Ulvöspinel was the high Zn-phase and the concentration of Zn in hafnolite was 0.11 Zn per 4 cations as opposed to 0.39 Zn per 4 cations. Hence, it appears that zinc addition has little effect on the phase assemblage, other than to stabilize hafnolite when added alone, or hafnolite and spinel when added with an excess of other divalent cations.

4.1.8 The baseline assemblage with 10 wt% Cr_2O_3

The addition of Cr_2O_3 stabilizes hafnolite and is also strongly incorporated in rutile (Table 2, 3 and C9, Plate 7). Also present is a poorly characterized sub-mircon size Cr-rich phase; due to the inability to obtain quantitative analyses of this phase, it was not included in the regression in Table 3, it is however a minor constituent based upon SEM characterization (Plate 7). Regression analysis indicates that hafnolite is present only at the wt% level. This is reflected in the pyrochlore composition in which the Ce/Gd ratio is that of the starting material as it is the only lanthanide-bearing phase in the assemblage.

Along with chromium, the rutiles in these experiments also contain significant uranium. For instance, the structural formula for the rutile from the 1350°C run is $U_{0.04}Cr_{0.11}Hf_{.07}Ti_{0.77}O_{1.94}$. Uranium incorporation can be accomplished by substitutions such as,

$$U^{+5} + Cr^{+3} \Leftrightarrow 2\ Ti^{+4}$$

$$U^{+6} + 2Cr^{+3} \Leftrightarrow 3\ Ti^{+4}$$

The change in rutile chemistry is also reflected in that of pyrochlore composition which has ~1.75 Ti per 4 cations here as opposed to ~1.9 Ti per 4 cations in rutile-saturated impurity-free run products. The incorporation of additional species in rutile decreases the

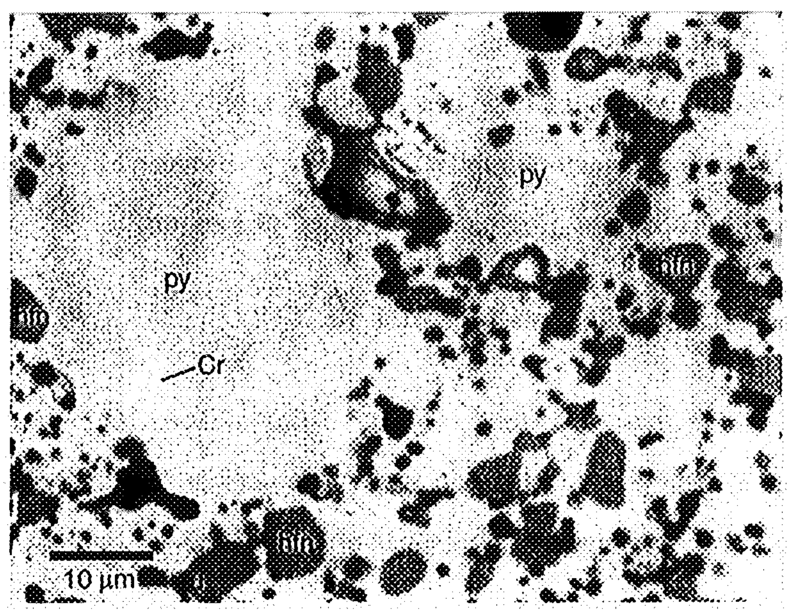

Plate 7. Backscattered electron image of baseline formulation with 10 wt% Cr_2O_3 added. Sintered at 1350°C in air (18/1). Phase assemblage includes pyrochlore (py) and hafnolite (hfn), rutile (ru) and CrxOy (Cr).

activity of TiO_2 in the rutile solid solution and, hence, the entire assemblage, resulting in lower TiO_2 contents in the coexisting phases. The reduction of Ti on the Ti-site also results in a charge deficit (Table C9) which can be compensated by oxidation of uranium and cerium. This is reflected in uranium valences of ~$UO_{2.9}$ in pyrochlores from Cr-doped runs relative to $UO_{2.62}$ in the impurity-free baseline run products.

Stewart *et al.* (1999) added Cr_2O_3 along with Al, Mn, Fe, and Ga to a Pu-bearing baseline formulation and obtained a pyrochlore-hafnolite-magnetoplumbite-loveringite assemblage in air at 1350°C. Chromium partitioned into hafnolite relative to pyrochlore, but was most strongly enriched in magnetoplumbite and loveringite. Formation of these phases requires additional components be present (iron and gallium in particular). The absence of such elements here explains the presence of Cr-oxide. Cr-oxide buffers the Cr_2O_3 activity at values greater than those imposed by magnetoplumbite and loveringite. This is refelected in higher chromium contents in the hafnolites from our experiments, 0.34 Cr per 4 cations versus 0.14 Cr per 4 cations in the run products of Stewart *et al.* (1999). So, while the addition of Cr_2O_3 alone does not significantly alter the composition of pyrochlore or result in the formation of radionuclide-bearing accessory phases, the presence of other trivalent cations can stabilize more complex Cr-bearing phases. Fortunately, neither the magnetoplumbite nor loveringite produced by Stewart *et al.* (1999) for such compositions contain significant plutonium or uranium.

4.1.9 The baseline assemblage with 10 wt% $FeAl_2O_4$

Ryerson (1984) has described Synroc formulations for US Defense waste immobilization in which zirconolite and perovskite coexist with mixed transition metal aluminate spinels. To evaluate the potential effects of spinel saturation on the current formulation aluminate components were added to the baseline composition.

At 1300°C and 1350°C the addition of 10 wt% $FeAl_2O_4$ yields the assemblage pyrochlore, hafnolite and Fe-psuedobrookite (Table 2, 3 and C10). Pyrochlore contains 1-

1.5 wt% FeO with trace Al_2O_3. The average structural formula is $(Ca_{1.02}Fe_{0.05}Ce_{0.25}Gd_{0.24}Hf_{0.06}U_{0.38})(Ti_{1.85}Hf_{0.07}Al_{0.03}Fe_{0.05})O_{6.63}$, maintaining the Ce/Gd ratio (~1) of the starting materials. Hafnolite, with the structural formula $(Ca_{0.60}Ce_{0.14}Gd_{0.24}U_{0.02})(Al_{0.13}Fe_{0.31}Hf_{0.47}U_{0.10})(Al_{0.16}Ti_{1.84})O_{6.76}$, is stabilized through incorporation of both Fe and Al at the ~3.5 wt% and the ~5 wt% levels, respectively (Table 13). This is not unexpected since both Fe and Al alone stabilize hafnolite. Both pyrochlore and hafnolite have less than 7 oxygens per 4 cations when calculated on the basis of Fe^{+2}, Ce^{+3} and U^{+4}.

If we assume Fe^{+3}, $Ce^{+4}/\sum Ce=0.33$, ideal stoichiometries for pyrochlore and hafnolite are obtained for $UO_{2.7}$ and $UO_{2.51}$, respectively at 1350°C. These values are indistinguishable from those obtained in the Al- and Fe-doped runs suggesting that the Fe valence in all runs is Fe^{+3}.

Stewart *et al.* (1999) have added Fe and Al together with Cr, Mn and Ga to both Ce-analog and Pu-bearing formulations. In air and Ar at 1350°C loveringite was the saturating accessory phase enriched in both Fe and Al. The chemically more complex loveringite,

$$(Ca_{2.1}Gd_{0.35}Hf_{0.73}U_{0.45}Ce_{0.45})(Al_{3.02}Cr_{1.67}Mn_{0.81}Fe_{1.74}Ga_{4.16}Ti_{7.5})O_{23}$$

is clearly stabilized by the presence of Ga, Cr, Mn, etc. In the absence of additional di- and trivalent cations we observe Fe-Al psuedobrookite $(Al_{1.6}Fe_{0.4})TiO_5$ which is free of Ce, Gd and U. In more complex compositions the effect of Fe-Al additions will depend upon the other cations present and the chemical durability of phases like loveringite.

4.1.10 The baseline assemblage with 10 wt% $MgAl_2O_4$

At 1300°C and 1350°C the addition of 10 wt% $MgAl_2O_4$ yields assemblages containing pyrochlore and Mg-psuedobrookite (Table 2, 3 and C11, Plate 8). Hafnolite is also found in the 1300°C experiment and contains ~1.5 wt% MgO. Pyrochlore contains less than 1 wt% MgO, and has the structural formula

$(Ca_{0.98}Ce_{0.25}Gd_{0.22}U_{0.37})(Ti_{1.90}Hf_{0.16}Al_{0.03}Mg_{0.09})O_{6.68}$ with the nominal Ce/Gd ratio of the starting material.

Mg-psuedobrookite, $Mg_{0.5}Al_{1.0}Ti_{1.5}O_5$, like the Fe-psuedobrookite from the previous section has virtually no Ce or Gd, but does contain HfO_2 at the ~3 wt% level. Mg-Al psuedobrookite clearly buffers the Mg content of pyrochlore at a lower value than Mg_2TiO_4 or $MgTiO_3$ in the MgO-doped runs. As such, the Ti-site has ~1.9 Ti per 4 cations requiring little Mg on the Ti-site, which precludes a charge deficiency on this site. This is reflected in lower UO_x values, x=2.76.

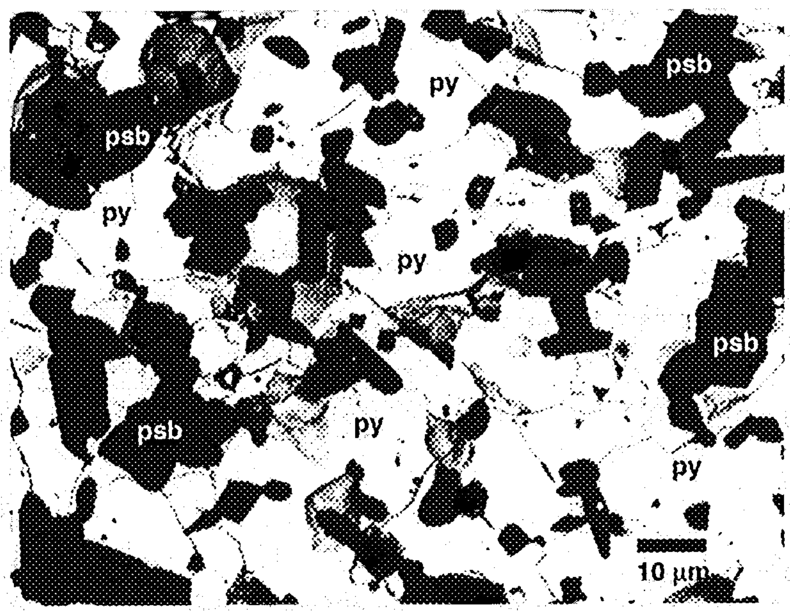

Plate 8. Backscattered electron image of baseline formulation with 10 wt% $MgAl_2O_4$ added. Sintered at 1350°C in air (12/1). Phase assemblage includes pyrochlore (py) and psuedobrookite (psb)

4.1.11 The baseline assemblage with 10 wt% $CaAl_2O_4$

As is the case with the addition of Al_2O_3 alone, the addition of $CaAl_2O_4$ to the baseline formulation leads to the stabilization of hafnolite and a number of aluminate phases (Table 2, 3, C12, Plate 9). Pyrochlore is present in all runs and has the structural formula (1350°C) $(Ca_{1.13}Ce_{0.22}Gd_{0.18}Hf_{0.11}U_{0.36})(Al_{0.03}Hf_{0.03}Ti_{1.95})O_{6.6}$. Hafnolite is also present in runs conducted at both 1300°C and 1350°C and contains ~3.5 wt% Al_2O_3. Brannerite does not appear in any of these runs, which may be a result of the increased Ca concentration.

The elevated Ca activity is apparent in the pyrochlore chemistry which has greater than 1 Ca per 4 cations in these materials. Like the addition of other divalent cations, addition of Ca to the A-site in pyrochlore requires oxidation of uranium or cerium to maintain stoichiometry, reflected here as $UO_{2.85}$ assuming $Ce^{+4}/\Sigma Ce=0.33$.

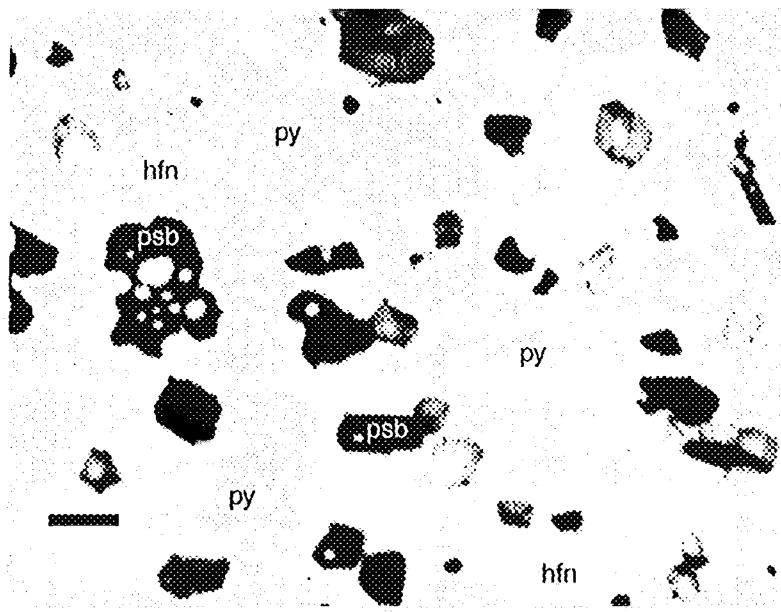

Plate 9. Backscattered electron image of baseline formulation with 10 wt% $CaAl_2O_4$ added. Sintered at 1350°C in air (13/1). Phase assemblage includes pyrochlore (py) and hafnolite (hfn) and psuedobrookite (psb).

The aluminate assemblage varies with temperature (Table 2). At 1300°C corundum and rutile coexist with a calcium-lanthanide aluminotitanate. At 1350°C the calcium-lanthanide aluminotitanate (CTA) is the only Al-rich phase present. The nominal CTA stoichiometry is 12 cations/19 oxygens, $(Ca_{0.76}Ce_{2.35}Gd_{0.04})(Al_{8.2}Ti_{2.75})O_{19}$ (in the 1350°C experiment) and is similar to the magnetoplumbite structure analogs found in wasteforms formulated for US Defense wastes (Ryerson, 1984, Morgan *et al.*, 1981). Unlike many of the titanate phases encountered here, CTA appears to preferentially incorporate the light lanthanide elements, and contains little gadolinium (< 1 wt%). CTA also contains no uranium. If cerium is an adequate analog for plutonium in this phase, then these results indicate that a Pu-bearing phase with virtually no neutron absorbers will be produced by the addition of calcium and aluminum together. In this connection, Stewart *et al.* (1999) found no detectable Pu in magnetoplumbite in a Pu-bearing formulation with enriched levels of Al, Cr, Mn, Fe and Ga synthesized in air at 1350°C. The compositions required to eliminate CTA from the wasteform can be estimated using the compositions of pyrochlore and hafnolite from our 1350°C run. For instance a CTA-free material with 10 wt% hafnolite and 90% pyrochlore would have an Al_2O_3/PuO_2 ratio of 0.13; 20% hafnolite and 80% pyrochlore yields Al_2O_3/PuO_2=0.21.

4.1.12 The baseline assemblage with 10 wt% MoO_3

A single experiment conducted in air at 1350°C to which 10wt% MoO_3 was added (Table 2, 3, C13) resulted in the assemblage pyrochlore-brannerite and the Ca-molybdate, powellite. The Ca-molybdate is nominally $CaMoO_4$ which contains ~1 wt% each CeO_2 and Gd_2O_3 and insignificant uranium. Molybdenum is also slightly soluble in pyrochlore and contains 1.73 wt% and has the structural formula, $Ca_{1.06}Ce_{0.21}Gd_{0.26}Hf_{0.12}U_{0.36}(Ti_{1.81}Hf_{0.13}Mo_{0.06})O_{6.76}$. The number of Ti cations/4 total cations, 1.81, is lower than that in the baseline assemblage, ~1.9, and is likely due to the incorporation of Mo on the Ti-site. Substitution of Mo^{+6} for Ti results in excess charge on the Ti-site. This can be balanced by reduction in the valence of Ce and U on the A-site. As such the valence of uranium here is $UO_{2.57}$. Brannerite contains negligible molybdenum.

The composition of a $CaMoO_4$-free assemblage is fixed by the solubility of Mo in pyrochlore. The molar ratio MoO_4/CeO_2 in this pyrochlore is 0.27; at higher Mo contents, a molybdate is likely to form. However, since the phase contains little of the plutonium-analog element, Ce, it is unlikely to degrade the durability of the waste form.

4.1.13 The baseline assemblage with 10 wt% WO_3

The addition of 10 wt% WO_3 to the baseline assemblage has an effect similar to that of MoO_3, resulting in the stabilization of scheelite, $CaWO_4$, coexisting with rutile, brannerite and pyrochlore at 1350°C in air (Table 2, 3, C14). However, unlike molybdenum, tungsten has significant solubility in pyrochlore which contains 14.37 wt% WO_3. Stewart *et al.* (1999) observed a similar preference of pyrochlore for tungsten relative to molybdenum in experiments where pyrochlore coexisted with a powellite-scheelite solid solution. The pyrochlore structural formula is $(Ca_{1.08}Ce_{0.19}Gd_{0.22}Hf_{0.15}U_{0.36})(Ti_{1.68}Hf_{0.02}W_{0.31})O_{7.02}$. Unlike many of the pyrochlores discussed above, the Ti content of this pyrochlore is well below that of the baseline, and the number of oxygens/4 cations is close to the ideal stoichiometry of 7. The low Ti content is due to the incorporation of W on the Ti-site. The ideal stoichiometry is obtained by casting uranium as U^{+4} and Ce as Ce^{+3}. The apparent reduction of uranium and cerium is the result of the excess charge on the Ti-site resulting from the exchange of W^{+6} for Ti^{+4}. This is balanced by a charge deficit on the B-site which can be achieved by reduction of uranium. The presence of rutile in this sample compared to its absence in the Mo-doped runs is also a product of tungsten occupying the Ti-site in pyrochlore. This produces excess Ti which stabilizes rutile. Brannerite also incorporates some tungsten (Table C14).

The high concentrations of tungsten in pyrochlore allow very loose limits to be placed on the amount of tungsten that can be safely incorporated in the ceramic. A WO_3/CeO_2 ratio of 1.68 would yield a $CaWO_3$-free ceramic containing only pyrochlore.

4.1.14 The baseline assemblage with 10 wt% P_2O_5

Phosphorus, a potential glass-former, was added to the baseline formulation at the 10 wt% level and sintered at 1300°C, 1350°C and 1400°C (Table 2, 3, C15; Plate 10). P_2O_5 has a profound effect on the wasteform mineralogy at these concentration levels, eliminating the characteristic phase, pyrochlore, from the assemblage. Instead, the assemblage found in these compositions is brannerite - rutile - Ca-lanthanide-phosphate (CLP) ± phosphate glass. The phosphate glass clearly penetrates the grain edge junctions of the coexisting solid phases at each temperature. Ca-lanthanide-phosphate, CLP, has the nominal formula $Ca_{6.2}Ce_{0.4}Gd_{0.4}Ti_{0.2}P_{4.8}O_{20}$. CLP is missing from the assemblage at 1400°C, indicating that the CLP liquidus lies between 1350°C and 1400°C.

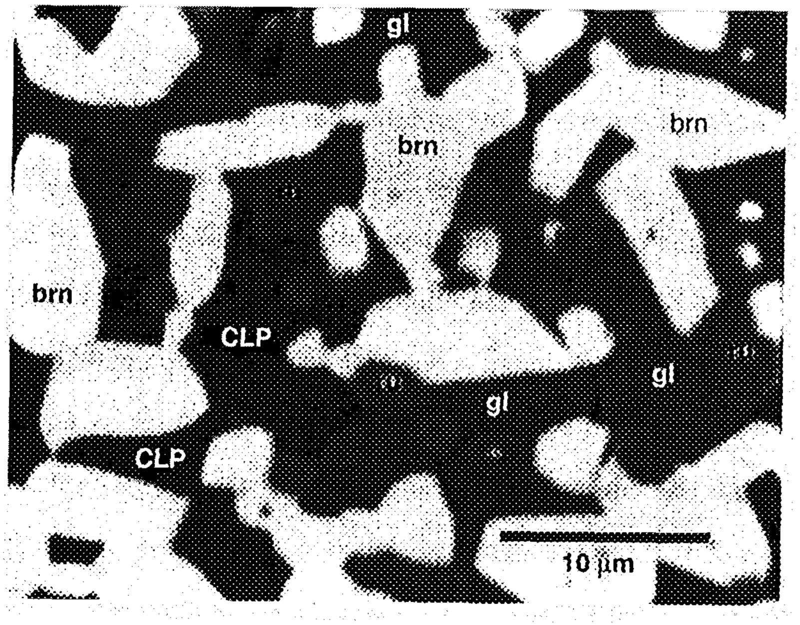

Plate 10. Backscattered electron image of baseline formulation with 10 wt% P_2O_5 added. Sintered at 1350°C in air (2/3). Phase assemblage includes brannerite (brn) and a calcium-lanthanide phosphate (CLP), rutile (ru) and phosphaste glass (gl).

In the absence of pyrochlore, the phosphorus-bearing phases become the major hosts for the Pu-analog element, cerium. The phosphate glass contains 16-18wt% Ce_2O_3 compared with ~7 wt% in brannerite and CLP. Both phosphorus-bearing phases have Ce/Gd ratios close to unity, but are essentially devoid of uranium and hafnium which are largely concentrated in brannerite.

The effect of P_2O_5 addition can be represented by its reaction with the endmember pyrochlore components, $CaUTi_2O_7$ and $Ln_2Ti_2O_7$ (where Ln is a lanthanide),

$$6CaUTi_2O_7 + 1/2\ Ln_2Ti_2O_7 + 2.5\ P_2O_5 \Leftrightarrow Ca_6Ln_1P_5O_{20} + 6UTi_2O_6 + TiO_2$$

$$(Py) + (Py) + (P_2O_5) \Leftrightarrow (CLP) + (brn) + (rut)$$

in which P_2O_5 reacts with pyrochlore to form CLP and additional brannerite. The reaction demonstrates that each mole of P_2O_5 consumes more than twice as many moles of pyrochlore. In these experiments the amount of P_2O_5 added was sufficient to consume all of the pyrochlore present. Smaller P_2O_5 additions would result in a pyrochlore-brannerite-rutile-CLP±P-glass assemblage. However, the due to the absence of pyrochlore in these runs, we are unable to determine the P_2O_5 concentration in pyrochlore when it coexist s with a phosphorus-rich accessory mineral. However, P_2O_5 in phosphorus-rich-accessory mineral-saturated brannerite is below detection. Assuming that pyrochlore concentrates similar quantities of P_2O_5, yields the conservative approximation that any addition of P_2O_5 will result in the stabilization of a phosphorus-rich accessory mineral. This is supported by the work of Stewart *et al.* (1999) who were unable to detect P_2O_5 in pyrochlore, hafnolite and brannerite coexisiting with a silicate that contained 3 wt% P_2O_5.

4.1.15 The baseline assemblage with 10 wt% SiO_2

The addition of SiO_2 at the 10 wt% level also results also results in a pyrochlore-free assemblage at 1300°C and 1350°C (Table 2, 3, C16). Here the absence of pyrochlore is explained by its dissolution in a compositionally unusual high-TiO_2 silicate glass. The glass contains only 15 wt% SiO_2 and 32 wt% TiO_2. In addition the glass is high in lanthanides, hafnium and uranium (Table C16). The conesiting brannerite is slightly higher in HfO_2 than the baseline run products, but otherwise very similar. Neither brannerite nor rutile contain detectable SiO_2.

4.1.16 The baseline assemblage with 10 and 20 wt% $NaAlSiO_4$

Sodium is a difficult element to immoblize in a titanate assemblage, typically requiring the addition of pentavlent cations such as niobium to allow coupled substitution such as,

$$Na + Nb \Leftrightarrow Ca + Ti$$

which promote sodium incorporation in titanate minerals (cf, Vance *et al.*, 1991). The alternative is to add silica and alumina to fix sodium as an alkali alumino-silicate mineral and/or glass, as proposed for the immobilization of Savannah River wastes in a Synroc assemblage (Ryerson, 1984). The component phases of Synroc are not stable in assemblages with high silica activity, (e.g., in equilibrium with quartz, cf, Nesbitt *et al*, 1981). Since, nepheline, $NaAlSiO_4$ is also unstable in assemblages with high silica activities, it is a reasonable component to use in simulating the effects of alkali alumino-silicate additions to this Pu-disposition ceramic. Here, in an attempt to generate sufficient quenched melt to analyze with the electron probe, we have prepared starting materials with 10 and 20 wt% $NaAlSiO_4$ (Table 2, 3, C17 and C18).

Samples containing 10 wt% $NaAlSiO_4$ result in pyrochlore-rutile-melt assemblages at 1300°C and 1350°C (Plate 11). These samples also contain small (~1 $\times$ 10 μm) laths of hafnolite (Plate 12). The hafnolite is euhedral and in spite of its size relative to the coexisting pyrochlore and rutile appears to be a part of the stable phase assemblage. Dendritic quench crystals are also obvious in some parts of the sample (Plate 12). With the addition of 20 wt% $NaAlSiO_4$, rutile is no longer present, and the quenched assemblage consists of pyrochlore and hafnolite. These phases coexist with quenched melt containing abundant dendritic quench crystals (Plate 12).

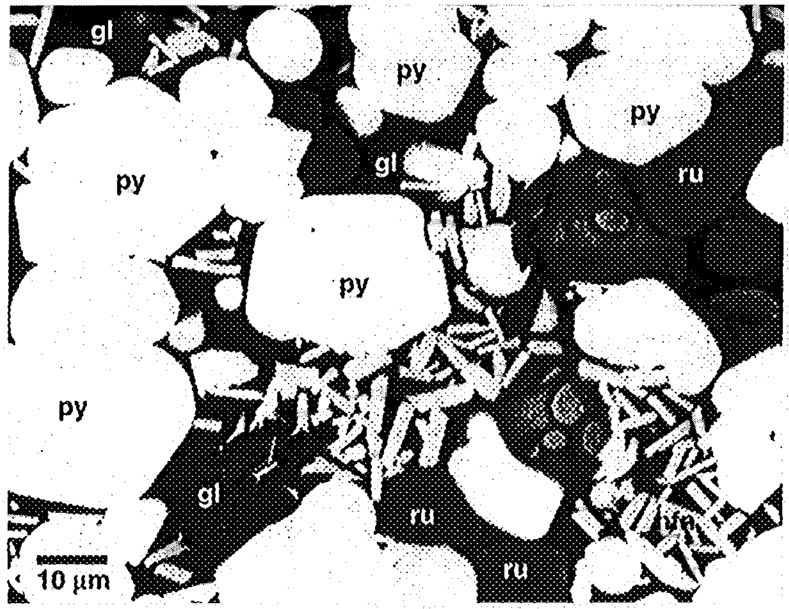

Plate 11. Backscattered electron image of baseline formulation plus 10wt% $NaAlSiO_4$ sintered at 1350°C in air (15/1). Phase assemblage contains pyrochlore (py), hafnolite (hfn, as small laths) rutile (ru) and silicate glass (gl).

The pyrochlore composition is relatively consistent among these 4 experiments, although different from that in the baseline assemblage, as it contains ~1 wt% Na_2O. The nominal structural formula for these pyrochlores is $Na_{0.14}Ca_{0.89}Ce_{0.25}Gd_{0.24}Hf_{0.1}U_{0.38}(Ti_{1.87}Hf_{0.12})O_{6.65}$ compared to that in the baseline material, $Ca_{1.04}Ce_{0.23}Gd_{0.23}Hf_{0.21}U_{0.39}(Ti_{1.89}Al_{.01})O_{6.7}$. Based upon the decreased calcium content of the Na-bearing pyrochlore, it appears that sodium replaces calcium in the structure. Given the similarity in the other cation concentrations, the exact substitution is difficult to determine. It is possible that Na is accommodated through a change in the oxidation state of either cerium or uranium,

$$Na^{+} + U^{+5} \Leftrightarrow Ca^{+2} + U^{+4}$$

or

$$Na^{+} + Ce^{+4} \Leftrightarrow Ca^{+2} + Ce^{+3}$$

Values of UO_x are all more oxidized than $UO_{2.8}$ which is consistent with these reactions (Table C17 and C18). None of the pyrochlores contains detectable SiO_2, and the Ce/Gd ratios are all close to unity, the same as the ratio in the starting material.

The hafnolites contain ~2.5-3.0 wt% Al_2O_3. This is slightly lower than the Al_2O_3 concentrations in hafnolites from the experiments in which they coexist with corundum or Al-psuedobrookite (section 4.1.2). Like the other hafnolites observed, the lanthanides are fractionated with a Ce/Gd ratio of ~0.5.

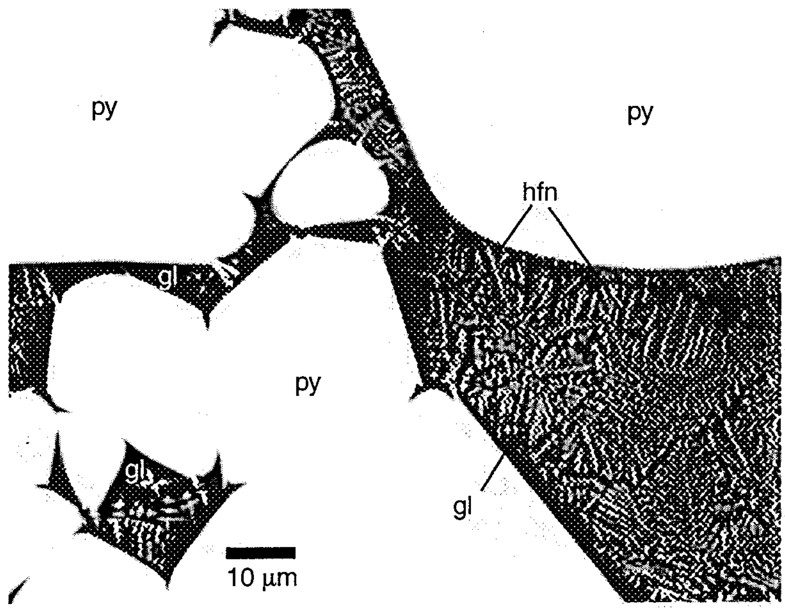

Plate 12. Backscattered electron image of baseline formulation plus 20 wt% $NaAlSiO_4$ sintered at 1350°C in air (16/1). Phase assemblage contains pyrochlore (py), hafnolite (hfn, as small quench crystals), and silicate glass (gl).

Analysis of the glass phase is complicated by the presence of quench material (Plate 12). This is especially true for the samples containing 20 wt% $NaAlSiO_4$ (Plate 12). Nevertheless, by focussing analyses on regions with low concentrations of quench crystals, clear trends in melt composition as a function of temperature are revealed. The glass composition at 1350°C is rather unusual, containing only 15 wt% SiO_2 and 43 wt% TiO_2 (Table C18). The 1350°C glass also contains significant amounts of Ce, Gd, Hf and U. Relative to the 1350°C glass composition, that of the 1300°C run is higher in Na, Al, and

Si, but lower in Ti, Ce, Gd, Hf and U. The Ce/Gd ratio is >2 in the glass, reflecting the strong factionation of the lanthanides by hafnolite. Partition coefficients between pyrochlore and melt, $D^{py/melt}$ (= wt% in pyrochlore/wt% in melt) are less than unity for Na, Al and Si, and greater than unity for Ce, Gd, Hf and U (Ti is complicated by the appearance of rutile which buffers its concentration in the melt). The compositional trends with temperature are exactly what one would predict from simple mineral-melt fractionation – depletion of pyrochlore-compatible elements and the enrichment of pyrochlore-incompatible elements. Most importantly, the trend indicates that the silicate melt will become increasingly depleted in radionuclide and neutron absorbers during slow cooling and continued crystallization of the melt. Analysis of the melt compositions from the 20 wt% $NaAlSiO_4$ runs leads to identical conclusions.

Much like the silicate melt bearing materials described in section 4.1.15 (10 wt% SiO_2 added to the baseline formulation), the titanate phase assemblage is incapable of accommodating more than trace levels of silica, and at least in these "quench experiments" we have not observed silicate mineral phases such as titanite, $CaTiSiO_5$, that could conceivably coexist with Ti-rich mineral assemblages. Given the proposed processing conditions (Ebbinghaus *et al.,* 1999), any silica in the wasteform will result in the presence of a silicate melt during sintering. The compositional evolution of this melt during cooling observed here suggests that the eventual glass phase may be low in radionuclides and neutron absorbers, however, and may not have a deleterious effect on the chemical durability of the form. Time-temperature-transformation studies of the melt composition and crystallization are needed to validate and quantify these effects.

Interestingly, in the absence of silica, this titanate assemblage can accommodate sodium without the addition of pentavalent cations such as niobium or tantalum. This is facilitated by charge-transfer reactions involving uranium and cerium (and presumably Pu in the full radioactive equivalent of the Ce-analogs). Using the pyrochlore composition from run 15-1, the molar Na_2O/PuO_2 limit precluding the formation of an accessory phase is 0.29.

4.1.17 The baseline assemblage with added calcium

CaO is a major component of the wasteform. However, the activity of CaO is not buffered by a specific phase as is the case for TiO_2, which is fixed by the presence of rutile in the baseline assemblage. While addition of TiO_2 will result in more modal rutile, variations in CaO concentration will qualitatively change the phase assemblage (Table 2, 3). This is clearly the case in experiments where 10 wt% CaO was added to the baseline and results in the phase assemblage pyrochlore and perovskite (Plate 13) at 1300°C, 1350°C and 1400°C. Neither rutile nor brannerite is observed in any of the runs.

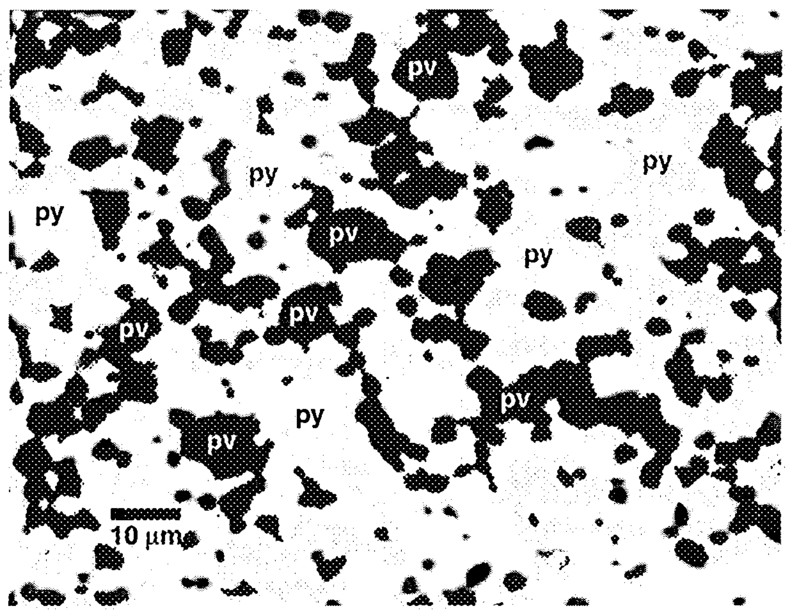

Plate 13a. Backscattered electron image of baseline formulation plus 10 wt% CaO sintered at 1350°C in air (3/3). Phase assemblage contains pyrochlore (py), perovskite (pv).

The qualitative changes observed in the phase assemblage due to variations in the activity of CaO are also reflected in quantitative changes in the pyrochlore chemistry (Table C19). For instance, the structural formula for the pyrochlore in the 1350°C run on the CaO-doped material is $Ca_{1.21}Ce_{0.20}Gd_{0.19}U_{0.43}(Ti_{1.58}Hf_{0.39}Al_{.01})O_{6.59}$ compared to

$Ca_{1.04}Gd_{0.23}Hf_{0.11}U_{0.39}Ce_{0.23}(Ti_{1.89}Hf_{0.10}Al_{.01})O_{6.7}$ in the undoped baseline material at the same temperature. The number of Ca per 4 total cations exceeds the more typical value of ~1 in most other runs. As the overall structural formula for pyrochlore, $A_2Ti_2O_7$, possesses 2 equivalent A-sites there is no structural constraint precluding more than one Ca per formula unit. Rather, in these high variance assemblages, the typical single Ca per formula unit reflects the bulk composition rather than a limit imposed by phase equilibria or crystal chemistry. The Ce/Gd molar ratio in pyrochlore remains close to unity in all runs, despite the change in the Ca-content. The high Ca content is also reflected in uranium valences greater that $UO_{2.87}$ (Table C19).

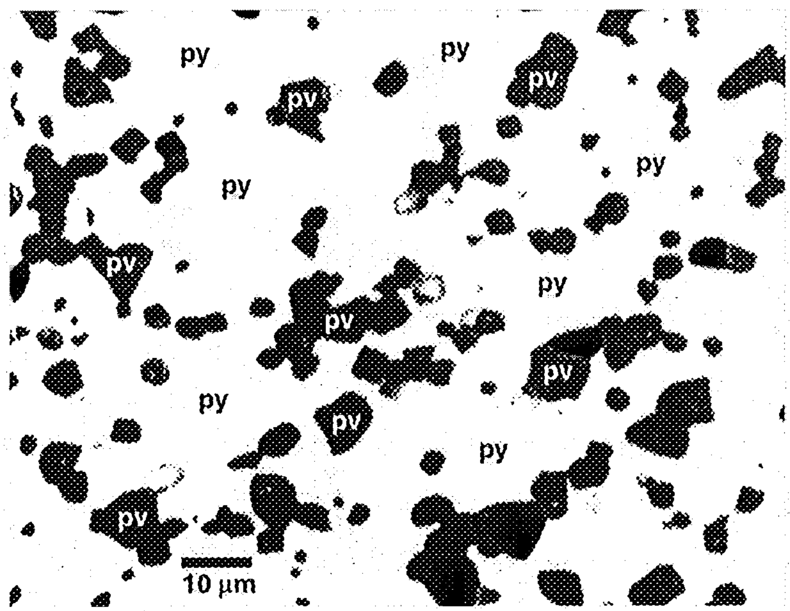

Plate 13b. Backscattered electron image of baseline formulation plus 10 wt% CaF_2 sintered at 1350°C in air (3/3). Phase assemblage contains pyrochlore (py), perovskite (pv).

Perovskite has somewhat lower lanthanide concentrations than the coexisting pyrochlore and is virtually free of uranium (Table C19). At 1350°C the nominal perovskite formula is $(Ca_{0.87}Ce_{0.06}Gd_{0.05}Hf_{0.01})Ti_{1.01}O_{3.08}$. The excess oxygen (calculated for Ce^{+3}) may indicate the presence of minor cation vacancies in these perovskites.

Calcium was also added to the baseline formulation as CaF_2 (10 wt%) in an attempt to saturate the assemblage in fluorite. Microprobe analysis failed to detect any fluorine-bearing phase however, indicating that fluorine was lost due to volatilization at high temperature (Table C20). The primary phase assemblage in the CaF_2-doped experiments is pyrochlore and perovskite, and is similar to those observed in CaO-doped runs (Table 2). The only exception is the presence of hafnolite in the 1300°C (3/1, Table C20). In addition, CaF_2 appears to have enhanced densification and grain growth relative to CaO (Plate 13), presumably resulting from rapid grain boundary transport due to the escaping molten or vapor phase.

The chemistry of pyrochlore in the CaF_2-doped materials differs somewhat from those in the CaO-doped samples. For instance, the structural formula for the pyrochlore produced in the 1350°C CaF_2-doped experiment is $Ca_{1.17}(Ce_{0.19}Gd_{0.17}Hf_{0.11}U_{0.38})(Ti_{1.83}Hf_{0.16})O_{6.65}$. The Ca concentration is again greater than 1 as a result of increased CaO-activity. However, the Hf/Ti ratio of this pyrochlore is lower than that in the CaO-doped samples. As the compositions of the perovskites in both materials is essentially the same (Table C19 and C20), the variation in the Hf/Ti ratio can only result in a change in bulk composition. However, the "as-made" compositions have the same Hf/Ti ratio (Table 1). The presence of hafnolite in some runs may resolve this paradox, if hafnolite nucleation was somehow enhanced by the presence of a fluorine-rich volatile phase early in the experiment. If this early hafnolite failed to re-equilibrate, it would effectively decrease the Hf/Ti ratio in the remainder of the sample. Comparison of the structural formulas for the CaO- and CaF_2-doped runs demonstrates that the variation in this Hf/Ti ratio is accommodated on the Ti-site, with the concentration of Hf on the A-site remaining constant. This observation may be valuable in predicting the change in pyrochlore chemistry with variations in Hf/Ti.

4.1.18 The baseline assemblage with 10 wt% MnO_2

The addition of MnO_2 to the baseline formulation also results in the stabilization of perovskite at the expense of brannerite and rutile (Tables 2 and C21, Plate 14). Unlike the addition of CaO in which CaO is concentrated in and thereby stabilizes perovskite, manganese is actually partitioned into pyrochlore (Table C21). At 1350°C the pyrochlore stoichiometry is $(Ca_{0.72}Gd_{0.19}Ce_{0.19}Mn_{0.46}Hf_{0.12}U_{0.34})(Ti_{1.87}Hf_{0.12}Al_{0.01})O_{6.62}$. Notably, the Ti-site occupancy is ~2 cations/4 total cations which essentially precludes the incorporation of Mn on that site. Unlike all of the previous samples discussed, however, the Ca concentration on the A-site is much less than 1, equaling 0.72 Ca per 4 total cations. Similarly, the concentrations of Ce and Gd are lower in these pyrochlores than in the baseline formulation processed under identical conditions; 0.19 vs 0.25 Ce per 4 cations

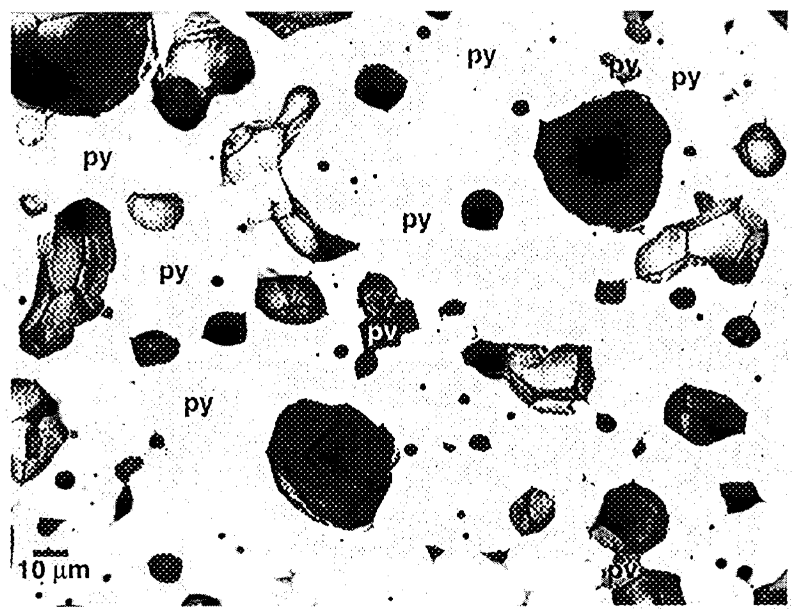

Plate 14. Backscattered electron image of a baseline formulation plus 10 wt% MnO_2, sintered at 1350 C in air (20/1). Assemblage includes pyrochlore (py) and perovskite (pv).

and 0.19 vs 0.23 Gd/4 cations for the Mn-doped and baseline formulations, respectively (Tables 4, 5 and C21). The decreased Ca and lanthanide concentrations are balanced by the incorporation of manganese. Clearly, the strong affinity of manganese for pyrochlore releases Ca and lanthanides to the matrix that in turn stabilize perovskite. The Ce/Gd molar ratio of the Mn-doped pyrochlore is not significantly different from those of the baseline. The uranium content is also similar.

When calculated on the basis of $Ce^{+4}/\Sigma Ce=0.33$ and Mn^{+2}, the average uranium valence is greater than UO_3. This requires that all uranium be hexavalent or $Ce^{+4}/\Sigma Ce$ greater than 0.33. Alternatively, Mn could be present in a higher valence state that would allow more typical values of UO_x and $Ce^{+4}/\Sigma Ce$.

The perovskites in the Mn-doped runs are very similar to those observed in the CaO-doped experiments (section 4.1.17 and Table C19 and C20). The T-site is essentially filled by Ti, with small amounts of Hf and Al, and uranium is barely detectable. The Ce/Gd molar ratio is slightly less than one. The only significant difference in the perovskites from the Mn-doped runs is the decreased Ca content that is compensated by the presence of manganese.

Like the pyrochlores described for other formulations, those in the Mn-doped runs are oxygen deficient for stoichiometries calculated on the basis of Ce^{+3}, U^{+4} Mn^{+2} and no cation vacancies. Unfortunately, given the number of possible combinations of valence states that could be used to reconcile the non-stoichiometry, no unique solution can be obtained based upon the observed chemistry alone. For instance, at 1350°C conversion of all the uranium to U^{+6} and cerium and manganese as +3 and +2, respectively yields close-to-ideal stoichiometry, 6.90 O/4 cations. Other combinations including U^{+4}, U^{+5}, Ce^{+4} and Mn^{+3} would yield equivalent results. The uncertainty in valence states propagates into similar uncertainties regarding pyrochlore components and the reactions that describe phase changes due to manganese addition. Possible reactions include the following in which rutile and pyrochlore components are consumed and perovskite and Mn-bearing pyrochlores are produced,

$$Gd_2Ti_2O_7 + 2MnO + 3\,TiO_2 \Leftrightarrow Mn_2Ti_2O_7 + 3Gd_{2/3}\square_{1/3}TiO_3 + 1/2\,O_2 \qquad 18.1$$

$$Ce_2Ti_2O_7 + 2MnO + 3\,TiO_2 \Leftrightarrow Mn_2Ti_2O_7 + 3Ce_{2/3}\square_{1/3}TiO_3 + 1/2\,O_2 \qquad 18.2$$

where □ represents a vacancy. Reactions 18.1 and 18.2 illustrate the consumption of trivalent lanthanide pyrochlore to produce non-stoichiometric lanthanide perovskite and a trivalent manganese pyrochlore, and involve no change in valence. Oxygen is involved due to the non-stoichiometry of the perovskite components.

$$CaCe^{+4}Ti_2O_7 + TiO_2 + MnO \Leftrightarrow Mn^{+2}Ce^{+4}Ti_2O_7 + CaTiO_3 \qquad 18.3$$

Reaction 18.3 illustrates the consumption of a Ca-quadravalent Ce pyrochlore to produce and Mn-Ce pyrochlore and a stoichiometric Ca-Ti perovskite molecule. Reactions 18.1, 18.2 and 18.3 are consistent with the reduction in Ca and lanthanides in pyrochlore and with the stabilization of perovskite resulting from MnO addition.

Other endmember reactions involve changes in the valence of uranium with addition of manganese. For instance, reaction 18.4 illustrates the consumption of a pentavalent uranium-bearing pyrochlore component, $(Ca_{1.33}U_{0.66}^{+5})Ti_2O_7$, to produce a quadravalent uranium-bearing pyrochlore and perovskite.

$$(Ca_{1.33}U_{0.66}^{+5})Ti_2O_7 + 0.66\,MnO + 0.66\,TiO_2 \Leftrightarrow$$

$$0.66\,(MnU^{+4})Ti_2O_7 + 1.33\,CaTiO_3 + 0.167\,O_2 \qquad 18.4$$

This reaction also mimics the relatively small change in uranium concentration of pyrochlore with Mn addition and the decrease in calcium. As in the previous reactions, rutile is consumed and perovskite created. The release of a calcium-rich component in the reactions above, also explains the absence of brannerite in these samples, as calcium reacts with brannerite to form additional pyrochlore.

Since there is no Mn-rich accessory phase in these assemblages, the impurity limit for manganese will be an issue of desired loading levels as opposed to accessory phase formation.

4.1.19 The baseline assemblage with 10 wt% Gd_2O_3

The addition of 10 wt% Gd_2O_3 to the baseline formulation changes the Ce/Gd molar ratio of the mixture from ~1 to ~0.5, but has no effect on the nature of the baseline phase assemblage (Tables 2 and C22, Plate 15). Experiments at 1300°C and 1350°C both yield the assemblage pyrochlore – brannerite - rutile. When cast in the lowest potential valence state, the pyrochlore formula from the 1350°C run is $(Ca_{0.93}Ce_{0.19}Gd_{0.42}Hf_{0.22}U_{0.33})(Ti_{1.91}Hf_{0.22})O_{6.76}$ which is typically oxygen deficient. This composition yields the ideal 4/7 stoichiometry if $Ce^{+4}/\sum Ce=0.33$ and the average uranium

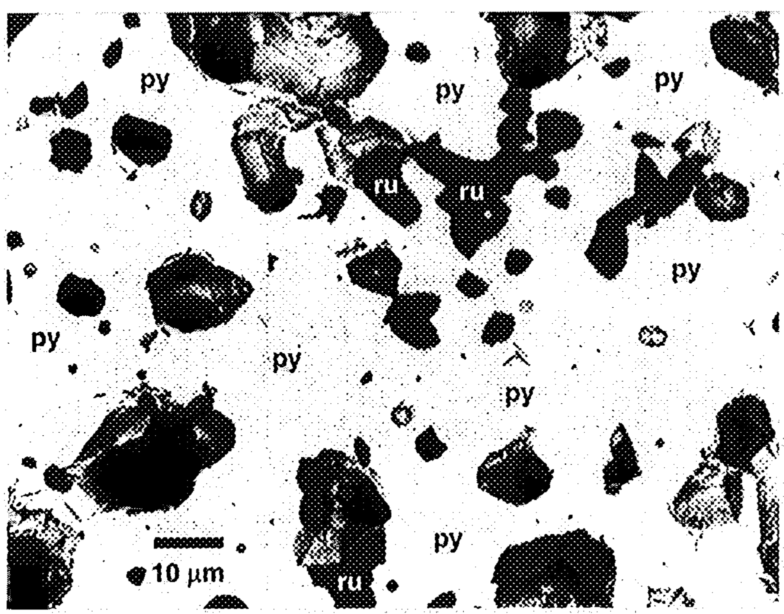

Plate 15. Baseline formulation with 10 wt% Gd_2O_3 added. Sintered at 1350°C in air (14/1). Phase assemblage includes pyrochlore (py) and rutile (ru).

valence is 5.262 (equivalent to UO_x where =2.631). The Ce/Gd molar ratio in this pyrochlore is 0.46, and closely tracks the change in the overall bulk composition. As is the case in the baseline formulation without additives, brannerite displays a preference for the heavier (smaller radius) lanthanides, and has a Ce/Gd molar ratio of 0.67 in the 1350°C experiment. The nominal brannerite formula is $(Ca_{0.07}Ce_{0.17}Gd_{0.24}Hf_{0.09}U_{0.43})(Ti_{1.96}Hf_{0.02})O_{5.718}$ which is oxygen deficient, and the ideal 3/6 stoichiometry is obtained if $Ce^{+4}/\Sigma Ce=0.33$ and the average uranium valence is $UO_{2.59}$.

4.1.20 The baseline assemblage with 10 wt% Ga_2O_3

The addition of 10 wt% Ga_2O_3 to the baseline formulation stabilizes hafnolite and a calcium-gallium titanate with the nominal formula $CaGa_2Ti_3O_{10}$ (Tables 2 and C23, Plate 16). Brannerite and rutile were not observed. The structural formula for pyrochlore is $(Ca_{1.09}Ce_{0.25}Gd_{0.21}Hf_{0.05}U_{0.42})(Ti_{1.85}Ga_{0.10}Hf_{0.05})O_{6.64}$ and it is typically oxygen deficient when based on the lowest potential oxidation states. This composition yields the ideal 4/7 stoichiometry if $Ce^{+4}/\Sigma Ce=0.33$ and the average uranium valence is $UO_{2.77}$. The Ce/Gd molar ratio is ~1.2, and the Ga_2O_3 concentration is 2-2.5 wt%. The pyrochlore in these runs

is similar to that in the additive-free baseline with the exception of an approximately 50% decrease in the HfO_2 concentration presumably due in part to replacement by gallium.

The lower Hf concentration in pyrochlore may also be due to the presence of hafnolite which is relatively enriched in Hf. The structural formula for the hafnolite produced at 1350°C is,

$$(Ca_{0.62}Gd_{0.24}Ce_{0.14})(Ga_{0.59}Ce_{0.05}Hf_{0.29}U_{0.13})(Ti_{1.88}Hf_{0.1})O_{6.89}$$

Hafnolite contains less uranium than the coexisting pyrochlore (Table C23) and the ideal 4/7 stoichiometry requires an average uranium valence of $UO_{2.15}$. Hafnolite is also enriched in gallium relative to pyrochlore containing as much as ~15 wt% Ga_2O_3 at 1300°C, and displays a strong preference for the heavy lanthanides with a Ce/Gd molar ratio of 0.57.

The accessory phase, $CaGa_2Ti_3O_{10}$, contains greater than 30 wt% Ga_2O_3. It also contains ~5 wt% Ce_2O_3 and ~7 wt% UO_2, but only ~5 wt% Gd_2O_3 and HfO_2. However, given the ability of both pyrochlore and hafnolite to accommodate gallium, we do not expect this phase to form under any realistic compositional or processing scenario. For instance, an assemblage with 80 wt% pyrochlore and 20 wt% hafnolite with a Ga_2O_3/PuO_2 ratio of 0.43 would yield no Ga-rich accessory phase. We note, however, that in more complex compositions other Ga-rich phases may form at lower Ga concentrations. For instance Stewart *et al.* (1999) synthesized a baseline formulation containing Al, Cr, Mn, Fe ±V and Ga. When sintered in either Ar or air at 1350°C these materials resulted in the assemblage pyrochlore – hafnolite – perovskite saturated with a Ga-rich accessory titanate phase tentatively identified as loveringite. The concentration of Ga in the coexisting pyrochlore and hafnolite were roughly 50% of what we have observed here, consistent with the lower concentration of Ga in loveringite relative to $CaGa_2Ti_3O_{10}$.

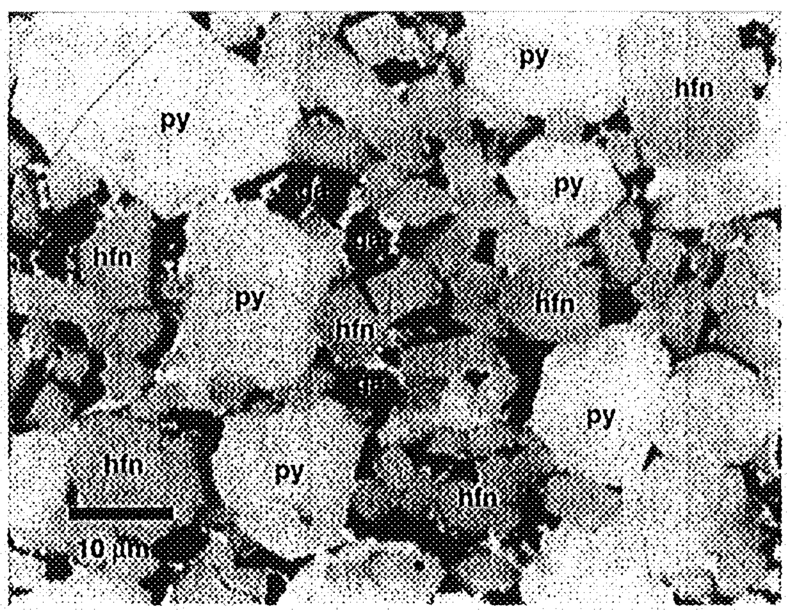

Plate 16. Backscattered electron image of baseline formulation plus 10wt% Ga_2O_3 sintered at 1350°C in air (19/1). Phase assemblage contains pyrochlore (py), hafnolite (hfn) and "galonite" (ga).

4.1.19 The baseline assemblage with 10 wt% Nb_2O_5

The addition of 10 wt% Nb_2O_5 to the baseline formulation yields an assemblage consisting of pyrochlore – brannerite – rutile - $HfTiO_4$ (Tables 2 and C24). The absence of a niobium-rich accessory phase is explained by the ability of pyrochlore to accommodate Nb on the T-site. The pyrochlore observed here at 1350°C has ~13.5 wt% Nb_2O_5 and the structural formula, $(Ca_{1.11}Ce_{0.21}Gd_{0.22}Hf_{0.1}U_{0.37})(Ti_{1.43}Hf_{0.08}Nb_{0.49})O_{6.92}$. The molar Ce/Gd ratio is ~1.

This pyrochlore does not display the pronounced oxygen deficiency observed in most of the other pyrochlores described here. As such, an average uranium valence state of only $UO_{2.11}$ is required to yield the ideal 4/7 stoichiometry (for $Ce^{+4}/\sum Ce=0.33$). This may be related to the excess charge on the T-site associated with incorporation of pentavalent Nb that can be charge-balanced by reducing the charge on the A-site (Table C24). In this connection, brannerite has substantially less niobium, and a lower excess charge on the T-site. The average uranium valence required for 3/6 stoichiometry is $UO_{2.57}$.

Rutile contains only minor niobium, ~2 wt%. Other than the small amount of niobium accommodated in the hafnium-titanate,~2 wt%, no other mechanism provides a means to explain the presence of this phase. As such, it may represent unreacted starting materials.

5.0 Discussion

The pyrochlore compositions presented here can be used to define a set of endmember components that describe its compositional variability and can be used in formulating additives for the potential wastestream compositions. The coordinate transformation is accomplished by writing a series of mass-balance equations expressing the concentrations of the initial components, in this case normalized cations, in terms of the new components. Inversion of this matix then yields a series of equations expressing the new components in terms of the initial components. Once established, the solubility limits observed for the various accessory phases can be expressed in terms of this new component set. This recasting of the solubility limits may help to minimize the effects of coupled substitutions.

The endmember components proposed here (Table 4) were chosen based on the following critieria:

1.) Pyrochlore stoichiometry, $A_2T_2O_7$ in which the 2 A-sites are equivalent and coupled substitutions involving the A and T sites are allowed. This insures that coupled substitutions are realistically simulated.

2.) Multiple oxidation states for cerium and uranium. The compositional trends and results from other work at different oxygen fugacities indicate that both elements are present in more than one oxidation state.

3.) Isolation of each impurity element in a single component. This allows the amount of additive required to accommodate each impurity element in pyrochlore to be easily calculated.

4.) Minimization of negative concentrations for the components chosen. Components that yield negative concentrations when applied to the observed compositions are valid, though of little practical use in determining the amounts of additives required by a particular wastestream composition.

5.) While a particular set of components may yield positive concentrations for some compositions, but result in some negative concentrations for others. We have attempted to maximize the positive concentrations for the components that include the major elements, Al, Ca, Ti, Ce, Gd, Hf, and U.

Table 4. Pyrochlore endmember components

$NaUTi_2O_7$	$Ca_2Nb_2O_7$
$CaUTiMgO_7$	Ca_2TiMoO_7
$Ti_2Al_2O_7$	$Ca_2Ta_2O_7$
$Cr_2Ti_2O_7$	Ca_2TiWO_7
$Mn_2Ti_2O_7$	$Gd_2Ti_2O_7$
$Fe_2Ti_2O_7$	$Ce_2Ti_2O_7$
$CoTi_3O_7$	$CaHfTi_2O_7$
$NiTi_3O_7$	$CaCeTiHfO_7$
$CuTi_3O_7$	$CaUTi_2O_7$
$ZnTi_3O_7$	$Ca_{1.5}U_{0.5}Ti_2O_7$
$Ti_2Ga_2O_7$	

These criteria are actually quite restrictive. For instance, for the baseline composition we have chosen the $Ti_2Al_2O_7$, $Gd_2Ti_2O_7$, $Ce_2Ti_2O_7$, $CaCeTiHfO_7$, $CaHfTi_2O_7$, $CaUTi_2O_7$, and $Ca_{1.5}U_{0.5}Ti_2O_7$ as components. Here $Ce_2Ti_2O_7$ accommodates Ce^{+3} and $CaCeTiHfO_7$ accommodates Ce^{+4}. These components restrict the concentration of Ce^{+4} in pyrochlore to be less than that of Hf that is also present as $CaHfTi_2O_7$. Similarly, uranium is present as U^{+4} in $CaUTi_2O_7$ and U^{+6} in $Ca_{1.5}U_{0.5}Ti_2O_7$. A U^{+5}-bearing component is a linear combination of U^{+4} and U^{+6}-bearing components. When applied to all of the runs containing only the major elements Al, Ca, Ti, Ce, Gd, Hf, and U only 4 negative concentrations out of 144 are obtained (Table 5). The negative concentrations are from the pyrochlores produced from the CaO-doped, Ca-perovskite-saturated experiments that have

Table 5. Pyrochlore component mole fractions for baseline compositions without additives

	Ti_2Al_2O7	$Gd_2Ti_2O_7$	$Ce_2Ti_2O_7$	$CaCeTiHfO_7$	$CaHfTi_2O_7$	$CaUTi_2O_7$	$Ca_{1.5}U_{0.5}Ti_2O_7$
1/1	0.004	0.112	0.056	0.125	0.070	0.135	0.498
1/2	0.000	0.116	0.059	0.127	0.101	0.180	0.417
1/3	0.008	0.116	0.087	0.072	0.149	0.120	0.448
5/1	0.002	0.117	0.057	0.120	0.065	0.182	0.456
5/2	0.003	0.115	0.061	0.106	0.119	0.172	0.423
5/3	0.006	0.116	0.050	0.129	0.094	0.168	0.436
7/1	0.013	0.109	0.084	0.098	0.033	0.099	0.561
7/2	0.015	0.132	0.039	0.145	0.043	0.142	0.479
7/3	0.014	0.106	0.092	0.081	0.068	0.104	0.533
3/1	0.003	0.087	0.012	0.174	0.045	0.086	0.593
3/2	0.005	0.089	0.006	0.173	0.094	0.108	0.525
3/3	0.006	0.086	0.009	0.171	0.091	0.103	0.533
9/1	0.001	0.096	-0.105	0.420	-0.034	0.225	0.396
9/2	0.000	0.055	-0.069	0.345	-0.053	0.214	0.487
13/1	0.013	0.092	0.087	0.048	0.093	0.025	0.639
13/2	0.008	0.093	0.085	0.060	0.057	0.042	0.654
14/1	0.003	0.211	0.050	0.090	0.126	0.130	0.389
14/2	0.003	0.210	0.036	0.122	0.093	0.123	0.413
Avg.	0.007	0.115	0.065	0.111	0.083	0.145	0.472
Std. Dev.	0.006	0.007	0.018	0.024	0.037	0.032	0.050

the highest Ca concentrations, suggesting that another set of components might be a more appropriate choice for such compositions. Aluminum is cast at $Ti_2Al_2O_7$ in which Ti resides on the A-site and Al on the T-site. Structurally, this is probably not the best choice of components for Al as Ti has a small ionic radius compared with other cations found on the A-site. Nevertheless, we feel that is a conservative choice that would tend to result in excess TiO_2 that is easily accommodated in rutile. $Ce_2Al_2O_7$ is another possible choice for an Al-rich component, but yields almost identical results due to the low concentrations of Al in pyrochlore.

We note that our initial choice of components included $Ce_2Ti_2O_7$, $CaCeTi_2O_7$, $CaUTi_2O_7$, $Ca_{1.5}U_{0.5}Ti_2O_7$ which appeared to be less restrictive in terms of fixing the oxidation states of cerium and uranium. Unfortunately, this set of components is not linearly independent and are related by the following equation,

$$CaCeTi_2O_7 + 1/2\ CaUTi_2O_7 = Ca_{1.5}U_{0.5}Ti_2O_7 + 1/2\ Ce_2Ti_2O_7$$

The divalent transition metals, M, have been cast as MTi_3O_7 and include $CoTi_3O_7$, $NiTi_3O_7$, $ZnTi_3O_7$, etc. This requires Ti on the A-site, but again represents a conservative choice as it would result in excess TiO_2. Iron, chromium and manganese are all considered to be trivalent under proposed processing conditions and are cast as $Fe_2Ti_2O_7$, $Cr_2Ti_2O_7$ and $Mn_2Ti_2O_7$. Our analysis of the compositions of pyrochlores in Mg-doped runs suggests that Mg resides on the T-site. The Mg-component used is $CaUTiMgO_7$ in which Mg is charged balanced by U^{+6}. Gallium is treated like aluminum and yields $Ti_2Ga_2O_7$. The high-field strength elements Nb, Ta, Mo and W reside on the T-site and are charge balanced by replacing tri- with divalent cations on the A-site, $Ca_2Nb_5O_7$, $Ca_2Ta_5O_7$, Ca_2TiMoO_7, Ca_2TiWO_7. Sodium is cast as $NaUTi_2O_7$ in which U^{+5} and Na^+ substitute on the A-site. This is based upon our measurements of Na-bearing, but Nb/Ta-free compositions. Coupled substitution involving Na and Nb/Ta for Ca and Ti have been demonstrated elsewhere, and could be used as alternate components for Na. It is our expectation that Na will typically be more abundant on a molar basis than Nb+Ta, and components like $NaCe^{+4}TiNbO_7$ would commonly result in negative concentrations. Conversely, uranium will always be more abundant than sodium resulting in positive concentrations for $NaUTi_2O_7$.

The concentrations of endmember components for impurity-free runs (Al, Ca, Ti, Ce, Gd, Hf, and U only) are given in Table 5, and yield a well-defined average for the perovskite-free samples. The major component is $Ca_{1.5}U_{0.5}Ti_2O_7$ with a mole fraction of 0.47±0.05, followed by roughly equal amounts of Gd_2Ti_2O7, $CaCeTiHfO_7$, $CaUTi_2O_7$ with mole fractions of 0.11-0.15. $Ce_2Ti_2O_7$ and $CaHfTi_2O_7$ have mole fractions of 0.065 and 0.083, respectively, and $Ti_2Al_2O_7$ is negligible. This corresponds to an average baseline pyrochlore composition of $Ca_{1.05}Ce_{0.24}Gd_{0.23}U_{0.39}Hf_{0.09}Ti_{1.89}Al_{0.01}Hf_{0.10}O_7$. The variations in pyrochlore component compositions produced by impurity additions (Table 6) are easily reconciled in terms of pyrochlore crystal-chemistry.

Sodium is associated with hexavalent uranium in the molecule $NaUTi_2O_7$. The major effect of sodium addition is to consume the quadravelent uranium-bearing component, $CaUTi_2O_7$. This is equivalent to oxidation of uranium that was discussed earlier.

The addition of calcium (as either oxide or fluoride) is reflected as an increase in $CaCeTiHfO_7$ and decreases in $Ce_2Ti_2O_7$ and $CaHfTi_2O_7$ that in some cases yield small negative concentrations. By fixing cerium and hafnium in $CaCeTiHfO_7$ the remaining components are relatively depleted, corresponding to a decrease in the concentrations of $Ce_2Ti_2O_7$ and $CaHfTi_2O_7$. We have tried a number of other possible component sets in combination with assumptions regarding the valence states of cerium and uranium, and find no improvement over the components presented here for high-Ca pyrochlores.

The addition of Mg yields $CaUTiMgO_7$ with corresponding decreases in the other uranium-bearing components, $CaUTi_2O_7$ and $Ca_{1.5}U_{0.5}Ti_2O_7$. The fixation of Ca in $CaUTiMgO_7$ may also lead to small negative concentrations of $Ce_2Ti_2O_7$ and $CaHfTi_2O_7$ for reasons outlined for high-Ca samples above.

Table 6. Pyrochlore mole fractions of impurity runs on Ce-Hf-U formulation with and without added impurities

	$NaUTi_2O_7$	$CaUTiMgO_7$	Ti_2Al_2O7	$Cr_2Ti_2O_7$	$Mn_2Ti_2O_7$	$Fe_2Ti_2O_7$	$CoTi_2O_7$	$NiTi_2O_7$	$CuTi_2O_7$	$ZnTi_2O_7$	$Ti_2Ga_2O_7$	$Ca_2Nb_2O_7$	Ca_2TiMoO_7	$Ca_2Ta_2O_7$	Ca_2TiWO_7	$Gd_2Ti_2O_7$	$Ce_2Ti_2O_7$	$CaHfTi_2O_7$	$CaCeTiHfO_7$	$CaUTi_2O_7$	$Ca_{1.5}U_{0.5}Ti_2O_7$
1/1	0.000	0.000	0.004	0.000	0.000	0.000	0.000	-0.000	0.000	-0.000	0.000	0.000	0.000	0.000	0.000	0.112	0.055	0.068	0.127	0.140	0.494
1/2	0.000	0.000	0.000	0.000	0.000	0.000	0.000	-0.000	0.000	-0.000	0.000	0.000	0.000	0.000	0.000	0.116	0.059	0.101	0.127	0.180	0.417
1/3	0.000	0.000	0.008	0.000	0.000	0.000	0.000	-0.000	0.000	-0.000	0.000	0.000	0.000	0.000	0.000	0.116	0.085	0.146	0.075	0.131	0.440
5/1	0.000	0.000	0.002	0.000	0.000	0.000	0.000	-0.000	0.000	-0.000	0.000	0.000	0.000	0.000	0.000	0.117	0.057	0.064	0.121	0.185	0.454
5/2	0.000	0.000	0.003	0.000	0.000	0.000	0.000	-0.000	0.000	-0.000	0.000	0.000	0.000	0.000	0.000	0.115	0.060	0.118	0.108	0.176	0.420
5/3	0.000	0.000	0.006	0.000	0.000	0.000	0.000	-0.000	0.000	-0.000	0.000	0.000	0.000	0.000	0.000	0.116	0.048	0.091	0.132	0.177	0.430
7/1	0.000	0.000	0.013	0.000	0.000	0.000	0.000	-0.000	0.000	-0.000	0.000	0.000	0.000	0.000	0.000	0.109	0.081	0.027	0.104	0.119	0.548
7/2	0.000	0.000	0.015	0.000	0.000	0.000	0.000	-0.000	0.000	-0.000	0.000	0.000	0.000	0.000	0.000	0.132	0.036	0.036	0.153	0.164	0.464
7/3	0.000	0.000	0.014	0.000	0.000	0.000	0.000	-0.000	0.000	-0.000	0.000	0.000	0.000	0.000	0.000	0.106	0.089	0.061	0.088	0.125	0.519
3/1	0.000	0.000	0.003	0.000	0.000	0.000	0.000	-0.000	0.000	-0.000	0.000	0.000	0.000	0.000	0.000	0.087	0.011	0.044	0.175	0.090	0.591
3/2	0.000	0.000	0.005	0.000	0.000	0.000	0.000	-0.000	0.000	-0.000	0.000	0.000	0.000	0.000	0.000	0.089	0.004	0.091	0.175	0.114	0.521
3/3	0.000	0.000	0.006	0.000	0.000	0.000	0.000	-0.000	0.000	-0.000	0.000	0.000	0.000	0.000	0.000	0.086	0.007	0.088	0.174	0.111	0.528
9/1	0.000	0.000	0.001	0.000	0.000	0.000	0.000	-0.000	0.000	-0.000	0.000	0.000	0.000	0.000	0.000	0.096	-0.105	-0.035	0.420	0.228	0.395
9/2	0.000	0.000	0.000	0.000	0.000	0.000	0.000	-0.000	0.000	-0.000	0.000	0.000	0.000	0.000	0.000	0.055	-0.069	-0.053	0.345	0.214	0.487
13/1	0.000	0.000	0.013	0.000	0.000	0.000	0.000	-0.000	0.000	-0.000	0.000	0.000	0.000	0.000	0.000	0.092	0.083	0.087	0.055	0.044	0.626
13/2	0.000	0.000	0.008	0.000	0.000	0.000	0.000	-0.000	0.000	-0.000	0.000	0.000	0.000	0.000	0.000	0.093	0.083	0.052	0.064	0.055	0.645
14/1	0.000	0.000	0.003	0.000	0.000	0.000	0.000	-0.000	0.000	-0.000	0.000	0.000	0.000	0.000	0.000	0.211	0.049	0.124	0.092	0.135	0.386
14/2	0.000	0.000	0.003	0.000	0.000	0.000	0.000	-0.000	0.000	-0.000	0.000	0.000	0.000	0.000	0.000	0.210	0.036	0.092	0.123	0.127	0.410
6/1	0.000	0.153	0.001	0.000	0.000	0.000	0.000	-0.000	0.000	-0.000	0.000	0.000	0.000	0.000	0.000	0.122	-0.037	-0.056	0.346	0.164	0.307
6/2	0.000	0.218	0.000	0.000	0.000	0.000	0.000	-0.000	0.000	-0.000	0.000	0.000	0.000	0.000	0.000	0.118	0.028	0.072	0.197	0.106	0.260
6/3	0.000	0.215	0.001	0.000	0.000	0.000	0.000	-0.000	0.000	-0.000	0.000	0.000	0.000	0.000	0.000	0.118	-0.005	0.032	0.270	0.122	0.246
12/1	0.000	0.091	0.013	0.000	0.000	0.000	0.000	-0.000	0.000	-0.000	0.000	0.000	0.000	0.000	0.000	0.110	0.122	0.150	0.009	0.051	0.454
12/2	0.000	0.081	0.010	0.000	0.000	0.000	0.000	-0.000	0.000	-0.000	0.000	0.000	0.000	0.000	0.000	0.105	0.115	0.111	0.021	0.062	0.495
17/1	0.000	0.000	0.002	0.000	0.000	0.000	0.000	0.127	0.000	-0.000	0.000	0.000	0.000	0.000	0.000	0.114	-0.049	-0.125	0.342	0.185	0.401
17/2	0.000	0.000	0.000	0.000	0.000	0.000	0.000	0.111	0.000	-0.000	0.000	0.000	0.000	0.000	0.000	0.112	-0.009	-0.092	0.274	0.135	0.469
18/1	0.000	0.000	0.003	0.055	0.000	0.000	0.000	-0.000	0.000	-0.000	0.000	0.000	0.000	0.000	0.000	0.128	0.007	-0.060	0.249	0.182	0.436
18/2	0.000	0.000	0.004	0.054	0.000	0.000	0.000	-0.000	0.000	-0.000	0.000	0.000	0.000	0.000	0.000	0.130	0.028	-0.015	0.213	0.055	0.512
19/1	0.000	0.000	0.000	0.000	0.000	0.000	0.000	-0.000	0.000	-0.000	0.049	0.000	0.000	0.000	0.000	0.104	0.047	-0.058	0.154	0.128	0.575
19/2	0.000	0.000	0.002	0.000	0.000	0.000	0.000	-0.000	0.000	-0.000	0.053	0.000	0.000	0.000	0.000	0.080	0.057	-0.093	0.155	0.094	0.652
20/1	0.000	0.000	0.005	0.000	0.230	0.000	0.000	-0.000	0.000	-0.000	0.000	0.000	0.000	0.000	0.000	0.095	0.028	0.092	0.132	0.256	0.162
20/2	0.000	0.000	0.007	0.000	0.233	0.000	0.000	-0.000	0.000	-0.000	0.000	0.000	0.000	0.000	0.000	0.092	0.029	0.081	0.137	0.234	0.188
21/1	0.000	0.000	0.003	0.000	0.000	0.000	0.000	-0.000	0.091	-0.000	0.000	0.000	0.000	0.000	0.000	0.122	-0.002	0.022	0.230	0.191	0.345
21/2	0.000	0.000	0.002	0.000	0.000	0.000	0.000	-0.000	0.063	-0.000	0.000	0.000	0.000	0.000	0.000	0.123	0.008	-0.018	0.225	0.187	0.408
22/1	0.000	0.000	0.004	0.000	0.000	0.000	0.000	-0.000	0.000	0.018	0.000	0.000	0.000	0.000	0.000	0.123	0.056	0.134	0.121	0.181	0.362
22/2	0.000	0.000	0.000	0.000	0.000	0.000	0.000	-0.000	0.000	0.116	0.000	0.000	0.000	0.000	0.000	0.089	0.032	-0.071	0.166	0.083	0.585
P229	0.000	0.000	0.000	0.000	0.000	0.000	0.000	-0.000	0.000	-0.000	0.000	0.000	0.057	0.000	0.000	0.128	0.040	0.115	0.132	0.184	0.345
P232	0.000	0.000	0.000	0.000	0.000	0.000	0.000	-0.000	0.000	-0.000	0.000	0.000	0.000	0.000	0.309	0.111	0.086	0.153	0.015	0.384	-0.058
P243	0.000	0.000	0.000	0.000	0.000	0.000	0.000	-0.000	0.000	-0.000	0.000	0.087	0.000	0.000	0.000	0.105	0.049	-0.175	0.392	0.195	0.348
15/1	0.141	0.000	0.006	0.000	0.000	0.000	0.000	-0.000	0.000	-0.000	0.000	0.000	0.000	0.000	0.000	0.122	0.058	0.085	0.131	0.022	0.433
15/2	0.148	0.000	0.005	0.000	0.000	0.000	0.000	-0.000	0.000	-0.000	0.000	0.000	0.000	0.000	0.000	0.110	0.070	0.045	0.121	0.012	0.490
16/1	0.163	0.000	0.005	0.000	0.000	0.000	0.000	-0.000	0.000	-0.000	0.000	0.000	0.000	0.000	0.000	0.136	0.042	0.066	0.185	0.001	0.400
16/2	0.179	0.000	0.004	0.000	0.000	0.000	0.000	-0.000	0.000	-0.000	0.000	0.000	0.000	0.000	0.000	0.115	0.087	0.067	0.098	-0.048	0.496

Magnesium is the only divalent cation we believe to be incorportated on the T-site. The effect of adding other divalent cations is best illustrated by the Ni-bearing runs. Here nickel is incorporated as $NiTi_3O_7$, which requires 3 Ti/Ni atoms. The relatively high Ti content of this component depletes the amount of Ti available to the other components, and is reflected in negative concentrations for the remaining components with the highest Ti/M ratios, $Ce_2Ti_2O_7$ and $CaHfTi_2O_7$. $Gd_2Ti_2O_7$ is unaffected as it is the only Gd-bearing molecule formulated. Minor improvement, i.e., smaller negative concentrations, can be obtained by casting Ni as $NiCeTi_2O_7$, $NiHfTi_2O_7$ or $NiUTi_2O_7$ where the ratio of Ti to Ni is lower. However, if these components are to be used in formulating additives, $NiTi_3O_7$ is the preferred component as it will result in an excess of Ti that is buffered by rutile. The other divalent cations will yield similar results.

Similar patterns are also produced by the addition of trivalent cations such as Cr, Fe, Mn and Ga where $M_2Ti_2O_7$ components fix Ti and can yield concentrations for $Ce_2Ti_2O_7$ and $CaHfTi_2O_7$. Molecules based on more complicated substitutions, including substitution of trivalent cations on the T-site help to reduce the concentrations of negative components but are not as conservative with respect to the production of excess TiO_2. For instance, casting Fe as $FeCe^{+4}(FeTi)O_7$ virtually eliminates negative concentrations for the Fe-bearing runs presented here.

The high-field strength cations Mo, W and Nb all tie up Ca and to a lesser extent Ti. Since divalent cations are required to charge balance U^{+6} on the A-site, incorporation of these elements should convert $Ca_{1.5}U_{0.5}Ti_2O_7$ to $CaUTi_2O_7$. This is best illustrated by comparing the component concentrations for Mo- and W-bearing runs (Table 6). Tungsten is more compatible than molybdenum in pyrochlore and $Ca_{1.5}U_{0.5}Ti_2O_7$ is completely consumed in the W-bearing materials. $CaCeTiHfO_7$ is also decreased in the W-bearing samples as it is the only Ca-bearing component not specifically tied to a single quadravlent cation other than Ti. $Ca_2Nb_2O_7$ ties up Ca, but no Ti; addition of niobium consumes $CaHfTi_2O_7$ and increases the concentration of $CaCeTiHfO_7$. Another possible substitution for niobium could be as a replacement for Ti in $Ca_{1.5}U_{0.5}Ti_2O_7$, $Ca_{1.5}U_{0.5}TiNbO_7$. in which U^{+6} is reduced to U^{+4}. The consumption of U^{+4} species is also apparent when we apply these components (Table 4) to the impurity-bearing samples made by ANSTO (Vance *et al.*, 1999) (Table 7) in which Nb/Ta-bearing materials have negative concentrations for $Ca_{1.5}U_{0.5}Ti_2O_7$.

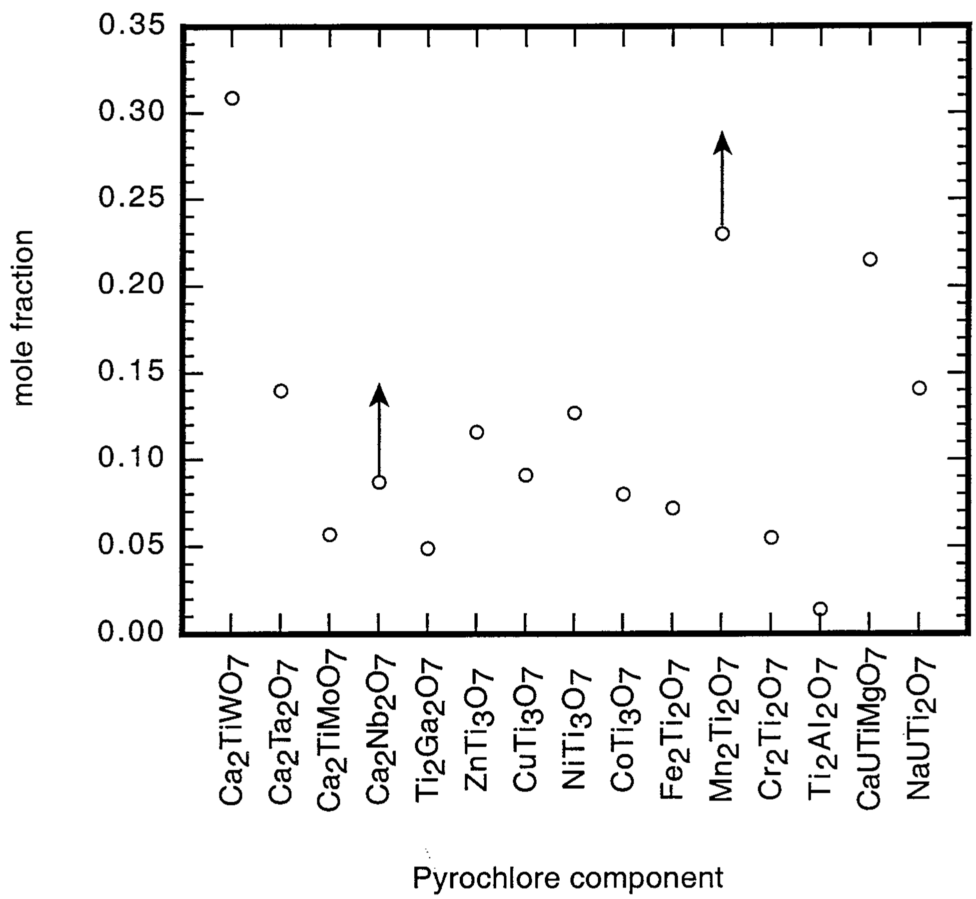

Figure 1. Saturation limits for various pyrochlore components in accessory phase saturated assemblages synthesized at 1350°C in air. The components with "up arrows" are not saturated with an accessory phase, and represent lower bounds.

The components in Table 4 have also been applied to pyrochlores from impurity-bearing Pu-Hf-Ce ceramics synthesized at LLNL (Ebbinghaus *et al*, 2000) (Table 8). We treat plutonium in a fashion identical to cerium, replacing $Ce_2Ti_2O_7$ with $Pu_2Ti_2O_7$, etc. The results of the transformation for these compositions is excellent with few negative concentrations and none on absolute magnitude greater than 0.033. It is also interesting to note that the negative concentrations are observed almost exclusively for $Pu_2Ti_2O_7$. This is consistent with Pu being present in a higher oxidation state than Ce at the same redox conditions.

The saturation limits for the components in Table 4 in the nominal baseline pyrochlore, $Ca_{1.05}Ce/Pu_{0.24}Gd_{0.23}U_{0.39}Hf_{0.09}Ti_{1.89}Al_{0.01}Hf_{0.10}O_7$, are plotted in Figure 1. In cases where the saturation limits were not exceeded a limiting value established from the highest concentration measured is given (denoted by "up" arrows on figure). The composition of additives for a particular wastestream can then be established as follows:

1.) Impurity fraction. Cast each of the impurities in its appropriate component and determine the additives required to convert metals to these components.

2.) Baseline fraction. Determine additives to required to convert Pu to the nominal baseline pyrochlore composition.

3.) Using the masses of the impurity and baseline fractions, determine the mole fraction of each impurity and compare to limits in Figure 1. If a solubility limit is exceeded, dilute mixture with additional baseline fraction additives to comply with limits.

4.) Add rutile component to mixture to obtain desired rutile/pyrochlore ratio.

Table 7. Pyrochlore mole fractions of impurity runs on Ce-Hf-U and Pu-Hf-U formulation with and without added impurities (Vance *et al.*, 1999)

	$NaUTi_2O_7$	$CaUTiMgO_7$	$Ti_2Al_2O_7$	$Cr_2Ti_2O_7$	$Mn_2Ti_2O_7$	$Fe_2Ti_2O_7$	$CoTi_3O_7$	$NiTi_3O_7$	$CuTi_3O_7$	$ZnTi_3O_7$	$Ti_2Ga_2O_7$	Ca_2Nb_2O	Ca_2TiMoO_7	$Ca_2Ta_2O_7$	Ca_2TiWO_7	$Gd_2Ti_2O_7$	$Ce_2Ti_2O_7$	$CaHfTi_2O_7$	$CaCeTiHfO_7$	$CaUTi_2O_7$	$Ca_{1.5}U_{0.5}Ti_2O_7$
F-1	0.000	0.060	0.000	0.000	0.000	0.000	0.080	0.030	0.000	0.000	0.000	0.000	0.000	0.000	0.000	0.125	0.000	-0.020	0.230	0.385	0.130
F-2 Ar bright	0.000	0.060	0.000	0.000	0.030	0.020	0.080	0.030	0.000	0.000	0.000	0.000	0.000	0.000	0.000	0.135	-0.025	-0.080	0.270	0.420	0.080
F-2 Air	0.000	0.050	0.000	0.000	0.025	0.015	0.060	0.000	0.000	0.000	0.000	0.000	0.000	0.000	0.000	0.110	-0.038	0.095	0.205	0.355	0.150
F-3	0.000	0.000	0.015	0.015	0.065	0.040	0.000	0.000	0.000	0.000	0.015	0.000	0.000	0.000	0.000	0.115	0.013	-0.085	0.205	0.400	0.200
F-4 Ar	0.000	0.000	0.015	0.015	0.055	0.045	0.000	0.000	0.000	0.000	0.020	0.000	0.000	0.000	0.000	0.110	0.015	-0.060	0.180	0.485	0.130
F-4 Air	0.000	0.000	0.015	0.015	0.055	0.020	0.000	0.000	0.000	0.000	0.015	0.000	0.000	0.000	0.000	0.105	-0.007	-0.175	0.275	0.365	0.330
F-4 3.7% H2	0.000	0.000	0.015	0.040	0.085	0.000	0.000	0.000	0.000	0.000	0.000	0.000	0.000	0.000	0.000	0.115	0.028	0.195	0.065	0.895	-0.430
F-5 Ar	0.000	0.000	0.000	0.000	0.000	0.000	0.000	0.000	0.000	0.000	0.000	0.000	0.000	0.000	0.000	0.125	0.025	0.080	0.200	0.365	0.190
F-5 Air	0.000	0.000	0.000	0.000	0.000	0.000	0.000	0.000	0.000	0.000	0.000	0.000	0.000	0.000	0.000	0.110	0.015	0.030	0.210	0.295	0.310
F-5 3.7%H2	0.000	0.000	0.000	0.000	0.000	0.000	0.000	0.000	0.000	0.000	0.000	0.000	0.000	0.000	0.000	0.110	0.062	0.295	0.045	0.650	-0.200
F-6 Ar	0.000	0.000	0.000	0.000	0.000	0.000	0.000	0.000	0.000	0.000	0.000	0.110	0.000	0.140	0.000	0.125	0.108	0.105	0.025	0.465	-0.090
F-6 Air	0.000	0.000	0.000	0.000	0.000	0.000	0.000	0.000	0.000	0.000	0.000	0.105	0.000	0.135	0.000	0.115	0.085	0.100	0.060	0.430	-0.020
F-6 3.7% H2	0.000	0.000	0.000	0.000	0.000	0.000	0.000	0.000	0.000	0.000	0.000	0.075	0.000	0.105	0.000	0.095	0.148	0.265	-0.085	0.560	-0.180
F-7 Ar	0.000	0.000	0.000	0.000	0.000	0.000	0.000	0.000	0.000	0.000	0.000	0.000	0.060	0.000	0.140	0.125	0.105	0.220	0.020	0.410	-0.080
F-7 Air	0.000	0.000	0.000	0.000	0.000	0.000	0.000	0.000	0.000	0.000	0.000	0.000	0.040	0.000	0.150	0.105	0.063	0.175	0.075	0.400	0.000
F-7 3.7% H2	0.000	0.000	0.000	0.000	0.000	0.000	0.000	0.000	0.000	0.000	0.000	0.000	0.007	0.000	0.040	0.105	0.149	0.329	-0.109	0.562	-0.104
F-8 Ar*	0.000	0.110	0.000	0.000	0.050	0.035	0.050	0.000	0.000	0.000	0.000	0.000	0.000	0.000	0.000	0.125	0.020	0.050	0.190	0.265	0.130
F-8 Air*	0.000	0.090	0.000	0.000	0.035	0.025	0.050	0.000	0.000	0.000	0.000	0.000	0.000	0.000	0.000	0.125	0.030	-0.020	0.190	0.215	0.290
F-9 Ar*	0.000	0.000	0.000	0.025	0.065	0.040	0.000	0.000	0.000	0.000	0.000	0.000	0.000	0.000	0.000	0.105	0.055	0.000	0.130	0.335	0.250
F-9 Air*	0.000	0.000	0.015	0.025	0.055	0.040	0.000	0.000	0.000	0.000	0.000	0.000	0.000	0.000	0.000	0.105	0.028	-0.065	0.195	0.340	0.280
F-10 Ar**	0.000	0.000	0.000	0.000	0.000	0.000	0.000	0.000	0.000	0.000	0.000	0.000	0.000	0.000	0.000	0.115	-0.005	0.220	0.230	0.395	0.050
F-10 Air**	0.000	0.000	0.000	0.000	0.000	0.000	0.000	0.000	0.000	0.000	0.000	0.000	0.000	0.000	0.000	0.120	-0.023	0.205	0.255	0.345	0.110
F-11 Ar*	0.000	0.000	0.000	0.000	0.000	0.000	0.000	0.000	0.000	0.000	0.000	0.120	0.000	0.130	0.000	0.120	0.103	0.135	-0.005	0.400	-0.020
F-11 Air*	0.000	0.000	0.000	0.000	0.000	0.000	0.000	0.000	0.000	0.000	0.000	0.125	0.000	0.135	0.000	0.115	0.095	0.130	0.000	0.415	-0.030
F-12 Ar*	0.000	0.040	0.000	0.000	0.000	0.020	0.000	0.000	0.000	0.000	0.000	0.000	0.040	0.000	0.160	0.130	0.090	0.180	0.020	0.345	-0.030
F-12 Air*	0.000	0.040	0.000	0.000	0.000	0.010	0.000	0.000	0.000	0.000	0.000	0.000	0.020	0.000	0.150	0.120	0.080	0.160	0.050	0.275	0.090
F-14 1250	0.000	0.000	0.020	0.000	0.000	0.000	0.000	0.000	0.000	0.000	0.000	0.000	0.000	0.000	0.000	0.115	0.080	0.150	0.040	0.315	0.290
F-14 1300	0.000	0.000	0.025	0.000	0.000	0.000	0.000	0.000	0.000	0.000	0.000	0.000	0.000	0.000	0.000	0.115	0.063	0.175	0.045	0.460	0.120
F-14 1350	0.000	0.000	0.015	0.000	0.000	0.000	0.000	0.000	0.000	0.000	0.000	0.000	0.000	0.000	0.000	0.120	0.055	0.170	0.070	0.430	0.160
F-15+Al	0.000	0.000	0.025	0.000	0.000	0.000	0.000	0.000	0.000	0.000	0.000	0.000	0.000	0.000	0.000	0.130	0.050	0.030	0.110	0.390	0.280
F-15+B	0.000	0.000	0.015	0.000	0.000	0.000	0.000	0.000	0.000	0.000	0.000	0.000	0.000	0.000	0.000	0.140	0.023	0.095	0.115	0.415	0.210
F-15+Na&K	0.170	0.000	0.010	0.000	0.000	0.000	0.000	0.000	0.000	0.000	0.000	0.000	0.000	0.000	0.000	0.125	-0.038	0.025	0.245	0.300	0.180

Table 8. Pyrochlore mole fractions of impurity runs on Ce-Hf-U and Pu-Hf-U formulation with and without added impurities (Ebbinghaus *et al.*, 1999)

	$NaUTi_2O_7$	$CaUTiMgO_7$	$Ti_2Al_2O_7$	$Cr_2Ti_2O_7$	$Mn_2Ti_2O_7$	$Fe_2Ti_2O_7$	$CoTi_3O_7$	$NiTi_3O_7$	$CuTi_3O_7$	$ZnTi_3O_7$	$Ti_2Ga_2O_7$	Ca_2Nb_2O	Ca_2TiMoO_7	$Ca_2Ta_2O_7$	Ca_2TiWO_7	$Gd_2Ti_2O_7$	$Ce_2Ti_2O_7$	$CaHfTi_2O_7$	$CaCeTiHfO_7$	$CaUTi_2O_7$	$Ca_{1.5}U_{0.5}Ti_2O_7$
ME3688 Air*	0.000	0.000	0.000	0.000	0.000	0.000	0.000	0.000	0.000	0.000	0.002	0.000	0.000	0.000	0.000	0.091	-0.033	0.007	0.261	0.229	0.444
ME3688 Ar*	0.001	0.000	0.000	0.000	0.000	0.000	0.000	0.000	0.000	0.000	0.002	0.000	0.000	0.000	0.000	0.089	-0.002	0.023	0.223	0.159	0.506
ME3688 CO2*	0.000	0.000	0.000	0.000	0.000	0.000	0.000	0.000	0.000	0.000	0.002	0.000	0.000	0.000	0.000	0.086	-0.010	-0.008	0.247	0.145	0.540
ME3692 Air*	0.000	0.146	0.000	0.000	0.000	0.000	0.000	0.000	0.000	0.000	0.000	0.000	0.000	0.000	0.000	0.121	0.005	0.130	0.132	0.271	0.195
ME3692 Ar*	0.000	0.132	0.000	0.000	0.000	0.000	0.000	0.000	0.000	0.000	0.002	0.000	0.000	0.000	0.000	0.123	0.005	0.129	0.148	0.246	0.217
ME3692 CO2*	0.000	0.135	0.000	0.000	0.000	0.000	0.000	0.000	0.000	0.000	0.001	0.000	0.000	0.000	0.000	0.119	0.040	0.115	0.136	0.175	0.278
ME3707 Air*	0.000	0.000	0.000	0.000	0.234	0.000	0.000	0.000	0.000	0.000	0.001	0.000	0.000	0.000	0.000	0.085	0.079	0.169	0.031	0.252	0.149
ME3707 Ar*	0.001	0.000	0.000	0.000	0.242	0.000	0.000	0.000	0.000	0.000	0.001	0.000	0.000	0.000	0.000	0.085	0.085	0.180	0.027	0.292	0.089
ME3707 CO2r*	0.000	0.000	0.000	0.000	0.245	0.000	0.000	0.000	0.000	0.000	0.000	0.000	0.000	0.000	0.000	0.085	0.078	0.180	0.030	0.297	0.085
ME3717 Airr*	0.000	0.000	0.000	0.063	0.000	0.000	0.000	0.000	0.000	0.000	0.002	0.000	0.000	0.000	0.000	0.119	0.077	0.075	0.095	0.203	0.367
ME3717Ar*	0.000	0.000	0.000	0.055	0.000	0.000	0.000	0.000	0.000	0.000	0.000	0.000	0.000	0.000	0.000	0.105	0.095	0.119	0.047	0.201	0.378
ME3717 CO2*	0.000	0.000	0.000	0.052	0.000	0.000	0.000	0.000	0.000	0.000	0.000	0.000	0.000	0.000	0.000	0.110	0.110	0.135	0.030	0.191	0.372

6. Conclusions

The elements added to the baseline formulation can be divided into two somewhat arbitrary groups – those for which the solubility limits in the baseline phase assemblage are sufficiently low such that expected impurity levels stabilize an accessory mineral, and a second group for which the solubility limits are high enough to allow the element to be accommodated as a solid solution component within the four primary phases. The first group includes Fe_2O_3, MgO, Al_2O_3, $FeAl_2O_4$, $MgAl_2O_4$, $CaAl_2O_4$, NiO, Cr_2O_3, Ga_2O_3, MoO_3, WO_3 which all result in the formation of a crystalline accessory phase at synthesis conditions between 1300-1400°C. In addition, these components can also have significant solubility in one of the baseline phases; divalent and trivalent cations typically stabilizing hafnolite, while penta- and higher valence cations stabilize pyrochlore. Fe_2O_3 may be the most troublesome impurity as it leads to melting at 1350°C at the 10 wt% level. SiO_2, $NaAlSiO_4$ and P_2O_5 result in the formation of a grain boundary melt at synthesis conditions, and P_2O_5 also stabilizes a crystalline, Ca-lanthanide phosphate. CaO, MnO_2 and Nb_2O_5 additions do not result in the formation of new phases. Nb_2O_5 is highly soluble in pyrochlore and no solubility limit was observed for the compositions investigated here. CaO reacts with brannerite to form perovskite. MnO is enriched in pyrochlore, displacing CaO which again reacts with brannerite to form perovskite.

7. References

Armstrong, J.T. CITZAF: a package of correction programs for the quantitative electron microbeam analysis of thick polished materials, thin films and particles. *Microbeam Anal.*, **4**, 177-200, 1995.

Ebbinghaus, B.B., C. Cicero-Herman, L. Gray and H. Shaw, Plutonium immobilizaiton project: Baseline Formulation, Lawrence Livermore National Laboratory, 1999.

Lumpkin, G.R., K.P. Hart, P.J. McGlinn, and T.E. Payne, Retention of actinides in natural pyrochlores and zirconolites, *Radiochimica Acta*, **66/67**, 460-474, 1994.

Morgan PED, Clarke DR, Jantzen CM, Harker AB, High-Alumina Tailored Nuclear Waste Ceramics, Journal of the American Ceramic Society 64: (5) 249-258 1981

Nesbitt HW, Bancroft GM, Fyfe WS, Karkhanis SN, Nishijima, A, Thermodynamic Stability And Kinetics Of Perovskite Dissolution, Nature 289: (5796) 358-362 1981

Ringwood, A.E., S.E. Kesson, N.G. Ware, W. Hibberson, and A. Major, Immobilization of high level nuclear reactor waste in SYNROC, *Nature*, **278**, 219-223, 1979.

Ryerson, F.J., Phase equilibria in nuclear waste ceramics: The effect of oxygen fugacity, *J. Am. Ceram. Soc*, **67**, 75-82, 1984.

Subramanian, M.A., G. Aravamudan, and G.V. Subba Rao, Oxide pyrochlores-A review, *Progress in Solid State Chemistry*, **15**, 55-143, 1983.

Appendix A. Starting Materials

Table 2. Starting materials

Al_2O_3	$Al(OH)_3$
CaO	$CaCO_3$, CaF_2
TiO_2	TiO_2 (rutile)
HfO_2	HfO_2
CeO_2	$(NH_4)_2Ce(NO_3)_6$, CeO_2
Gd_2O_3	$Gd(NO_3)_3.6H_2O$, Gd_2O_3
Fe_2O_3	Fe_2O_3
MnO_2	MnO_2
MgO	MgO
SiO_2	SiO_2
Na_2O	Na_2CO_3
NiO	NiO
Cr_2O_3	Cr_2O_3
Ga_2O_3	Ga_2O_3
CuO	CuO
ZnO	ZnO
P_2O_5	$NH_4H_2PO_4$
UO_2	$UO_2(NO_3)_2$ $6H_2O$, UO_2

Appendix B. Probe standards

MgO	Natural Olivine
Na_2O	Natural Albite
Al_2O_3	Corundum
SiO_2	Natural Diopside
P_2O_5	Natural Apatite
CaO	Natural Wollastonite
TiO_2	Rutile
Cr_2O_3	Natural Chromite
MnO	Natural Spessartine Garnet
NiO	Synthetic Ni-olivine
Ga_2O_3	Gadolinium Gallium Garnet
Nb_2O_5	Nb metal
MoO_3	$CaMoO_4$
HfO_2	Hf metal
Ce_2O_3	CeO_2
Gd_2O_3	Gadolinium Gallium Garne
WO_3	W metal
UO_2	Synthetic UO_2

Table C1. Microprobe analyses (wt%) and structural formulae for the Ce-analog with no additives

Run:	1-1 Pyrochlore	1300 C	1-1 Brannerite	1300 C	1-1 Rutile	1300 C	1-2 Pyrochlore	1400 C	1-2 Brannerite	1400 C	1-2 Rutile	1400 C	1-3 Pyrochlore	1350 C 9	1-3 Rutile	1350 C 3
	wt%	std dev	wt%	std dev	wt%	std dev	wt%	std dev	wt%	std dev	wt%	std dev	wt%	std dev	wt%	std dev
Al_2O_3	0.08	0.01	0.41	0.03	0.55	0.03	0.00	0.00	0.00	0.00	0.61	0.03	0.16	0.01	0.69	0.03
CaO	13.25	0.18	2.19	1.22	0.14	0.04	12.62	0.14	1.34	0.04	0.07	0.03	12.53	1.17	0.01	0.01
TiO_2	32.86	0.22	40.62	1.05	78.12	0.99	32.58	0.40	39.73	0.13	75.93	0.30	33.86	1.27	78.30	0.95
CeO_2	8.53	0.24	10.19	0.38	0.10	0.02	8.75	0.12	9.66	0.02	0.08	0.02	8.87	0.60	0.04	0.02
Gd_2O_3	8.95	0.14	7.57	0.21	0.09	0.04	9.17	0.35	6.75	0.30	0.09	0.06	9.30	0.95	0.00	0.00
HfO_2	8.98	0.32	6.43	0.53	18.34	0.60	10.47	0.20	6.41	0.09	19.41	0.29	10.23	0.47	18.50	0.85
UO_2	22.97	0.59	28.80	0.56	2.21	0.10	22.82	0.31	30.64	0.02	2.68	0.05	20.95	1.91	2.39	0.20
Total	95.62 -		96.20 -		99.54	0.87	96.41 -		94.51 -		98.89 -		95.89 -		99.93 -	
Al	0.008	0.001	0.030	0.002	0.010	0.000	0.000	0.000	0.000	0.000	0.011	0.000	0.015	0.002	0.012	0.001
Ca	1.076	0.012	0.146	0.080	0.002	0.001	1.034	0.008	0.094	0.003	0.001	0.000	1.012	0.041	0.000	0.000
Ti	1.873	0.015	1.915	0.069	0.899	0.003	1.873	0.015	1.960	0.010	0.891	0.002	1.925	0.059	0.898	0.006
Ce	0.237	0.006	0.234	0.010	0.001	0.000	0.245	0.004	0.232	0.000	0.000	0.000	0.245	0.006	0.000	0.000
Gd	0.225	0.003	0.157	0.003	0.000	0.000	0.232	0.008	0.147	0.006	0.000	0.000	0.232	0.012	0.000	0.000
Hf	0.194	0.007	0.115	0.008	0.080	0.003	0.228	0.004	0.120	0.002	0.086	0.001	0.221	0.005	0.081	0.004
U	0.387	0.009	0.402	0.011	0.008	0.000	0.388	0.005	0.447	0.001	0.009	0.000	0.351	0.018	0.008	0.001
Catatoms	4.000	0.000	3.000	0.000	1.000	0.000	4.000 -		3.000 -		1.000 -		4.000	0.000	1.000	0.000
Oxygen	6.690 -		5.643 -		1.992 -		6.728 -		5.717 -		1.993 -		6.743	0.046	1.994	0.000
Ca																
Gd																
Sum																
Charge																
Ca	1.076		0.146		0.002		1.034		0.094		0.001		1.012		0.000	
Ce(+3)	0.158		0.156		0.000		0.163		0.155		0.000		0.163		0.000	
Ce(+4)	0.079		0.078		0.000		0.082		0.077		0.000		0.082		0.000	
Gd	0.225		0.157		0.000		0.232		0.147		0.000		0.232		0.000	
Hf	0.075		0.061		0.000		0.101		0.080		0.000		0.160		0.000	
U	0.387		0.402		0.008		0.388		0.447		0.009		0.351		0.008	
Sum	2.000		1.000		0.011		2.000		1.000		0.011		2.000		0.008	
Charge	6.008		4.031		0.053		5.999		4.002		0.061		6.014		0.050	
Ti	1.873		1.915		0.899		1.873		1.960		0.891		1.925		0.898	
Hf	0.119		0.054		0.080		0.127		0.040		0.086		0.061		0.081	
Al	0.008		0.030		0.010		0.000		0.000		0.011		0.015		0.012	
Sum	2.000		2.000		2.000		2.000		2.000		2.000		2.000		2.000	
Charge	7.992		7.970		3.947		8.000		8.000		3.943		7.985		3.954	
UOx	2.7		2.793		3		2.595		2.55		2.8		2.615		2.8	
Model Oxygens	7.000		6.000		2.000		7.000		6.001		2.000		7.000		2.000	

Table C2. Microprobe analyses of Ce-analog made from oxides with no additives

	5-1	1300	5-1	1300	5-1	1300	5-2	1400	5-2	1400	5-2	1400
	Pyrochlore		Brannerite		Rutile		Pyrochlore		Brannerite		Rutile	
	wt%	std dev	wt%	std dev	wt%	std dev	wt%	std dev	wt%	std dev	wt%	std dev
Al_2O_3	0.05	0.01	0.28	0.06	0.43	0.02	0.06	0.01	0.28	0.01	0.43	0.03
CaO	12.89	0.51	1.42	0.12	0.05	0.02	12.90	0.09	1.34	0.07	0.08	0.05
TiO_2	33.08	1.32	40.28	0.44	77.02	0.39	33.71	0.21	41.49	0.45	78.20	0.36
CeO_2	8.42	0.36	9.83	0.65	0.10	0.02	8.34	0.19	9.34	0.52	0.09	0.04
Gd_2O_3	9.20	0.42	7.34	0.61	0.01	0.01	9.29	0.20	7.21	0.34	0.10	0.06
HfO_2	8.34	0.22	6.40	0.26	19.58	0.24	10.58	0.18	6.39	0.54	19.83	0.29
UO_2	24.47	1.05	30.68	0.32	2.02	0.14	23.27	0.20	31.31	0.43	2.12	0.11
Total	96.44 -		96.23 -		99.21 -		98.16 -		97.37 -		100.85 -	
Al	0.004	0.001	0.021	0.004	0.008	0.000	0.006	0.001	0.021	0.001	0.008	0.001
Ca	1.052	0.036	0.097	0.007	0.001	0.000	1.032	0.007	0.091	0.005	0.001	0.001
Ti	1.879	0.064	1.941	0.006	0.897	0.002	1.892	0.007	1.968	0.008	0.896	0.002
Ce	0.235	0.008	0.231	0.014	0.001	0.000	0.228	0.005	0.216	0.012	0.001	0.000
Gd	0.233	0.009	0.156	0.013	0.000	0.000	0.230	0.005	0.151	0.006	0.000	0.000
Hf	0.186	0.010	0.117	0.005	0.087	0.001	0.226	0.004	0.115	0.010	0.086	0.001
U	0.412	0.016	0.437	0.007	0.007	0.000	0.386	0.004	0.439	0.003	0.007	0.000
Catatoms	4.000	0.000	3.000	0.000	1.000	0.000	4.000 -		3.000 -		1.000 -	
Oxygen	6.712 -		5.699 -		1.995 -		6.736 -		5.716 -		1.994 -	
Ca	1.000						1.000					
Gd	0.000						0.000					
Sum	1.000						1.000					
Charge	2.000						2.000					
Ca	0.052		0.146		0.001		0.032		0.146		0.001	
Ce(+3)	0.235		0.231		0.001		0.228		0.216		0.001	
Gd	0.233		0.157		0.000		0.230		0.157		0.000	
Hf	0.106		0.079		0.007		0.106		0.103		0.006	
U(+4)	0.199		0.187		0.001		0.087		0.220		0.001	
U(+6)	0.213		0.250		0.006		0.299		0.219		0.006	
Sum	1.037		1.042		1.042		0.982		1.042		1.042	
Charge	4.004		4.005		4.005		4.005		4.005		4.005	
Ti	1.879		1.941		0.897		1.892		1.968		0.896	
Hf	0.117		0.038		0.080		0.102		0.012		0.080	
Al	0.004		0.021		0.008		0.006		0.021		0.008	
Sum	2.000		2.000		2.000		2.000		2.000		2.000	
Charge	7.996		7.970		3.947		7.994		7.970		3.947	
Model Oxygen	7.000		6.000		2.001		7.000		6.000		2.000	

Table 8. Microprobe analyses of Ce-analog made from oxides with no additives

	5-3	1350	5-3	1350	5-3	1350
	Pyrochlore		Brannerite		Rutile	
	wt%	std dev	wt%	std dev	wt%	std dev
Al_2O_3	0.14	0.01	0.47	0.02	0.55	0.03
CaO	12.93	0.10	1.47	0.14	0.02	0.01
TiO_2	32.94	0.37	41.50	0.34	77.23	0.22
CeO_2	8.26	0.17	9.10	0.82	0.01	0.01
Gd_2O_3	9.24	0.20	7.30	0.15	0.00	0.00
HfO_2	10.36	0.19	6.72	0.06	19.88	0.15
UO_2	23.36	0.51	31.33	0.35	2.08	0.19
Total	97.23 -		97.89 -		99.75 -	
Al	0.012	0.001	0.035	0.001	0.010	0.000
Ca	1.045	0.004	0.099	0.006	0.000	0.000
Ti	1.868	0.014	1.950	0.008	0.892	0.005
Ce	0.228	0.005	0.207	0.014	0.000	0.000
Gd	0.231	0.006	0.153	0.004	0.000	0.000
Hf	0.223	0.004	0.119	0.001	0.090	0.005
U	0.392	0.009	0.437	0.003	0.007	0.000
Catatoms	4.000	0.000	3.000	0.000	1.000	0.000
Oxygen	6.719 -		5.704 -		1.995 -	
Ca	1.000					
Gd	0.000					
Sum	1.000					
Charge	2.000					
Ca	0.045		0.146		0.000	
Ce(+3)	0.228		0.207		0.000	
Gd	0.231		0.157		0.000	
Hf	0.106		0.105		0.010	
U(+4)	0.116		0.195		0.001	
U(+6)	0.276		0.242		0.006	
Sum	1.002		1.042		1.042	
Charge	4.012		4.005		4.005	
Ti	1.868		1.950		0.892	
Hf	0.120		0.015		0.080	
Al	0.012		0.035		0.010	
Sum	2.000		2.000		2.000	
Charge	7.988		7.970		3.947	
Model Oxygen	7.000		6.000		2.001	

Table C3. Microprobe analyses (wt%) of the Ce-analog with 10% Al_2O_3 added

	7-1 Pyrochlore wt%	1300 std dev	7-1 Hafnolite wt%	1300 std dev	7-1 Brannerite wt%	1300 std dev	7-1 Corundum wt%	1300 std dev	7-1 Rutile wt%	1300 std dev	7-2 Pyrochlore wt%	1400 std dev	7-2 Hafnolite wt%	1400 std dev	7-2 Rutile wt%	1400 std dev
Al_2O_3	0.30	0.15	3.81	0.45	1.13	0.02	100.50	0.27	2.14	1.40	0.34	0.02	3.82	0.58	0.98	0.15
CaO	13.59	0.09	10.01	0.45	1.29	0.02	0.16	0.17	0.17	0.06	13.08	0.09	9.62	0.51	0.56	0.57
TiO_2	34.27	0.42	32.75	0.13	39.87	0.29	0.55	0.42	83.12	0.57	32.84	0.16	31.61	0.54	84.34	0.83
CeO_2	9.84	0.39	3.95	0.79	10.69	0.11	0.10	0.13	0.18	0.01	8.15	0.16	3.68	0.65	0.50	0.35
Gd_2O_3	8.94	0.13	7.58	0.28	6.79	0.13	0.14	0.13	0.10	0.01	10.70	0.27	9.36	0.23	0.24	0.18
HfO_2	6.22	0.82	31.46	2.91	4.30	0.11	0.18	0.04	11.03	0.28	8.81	0.24	31.62	2.49	9.91	0.04
UO_2	23.98	1.27	9.08	2.30	32.38	0.26	0.30	0.34	3.38	0.16	23.85	0.25	9.72	1.79	4.34	0.91
Total	97.14 -		98.64 -		96.44 -		101.93	0.96	100.13	1.03	97.76	0.51	99.43	0.70	100.87	1.36
Al	0.026	0.013	0.328	0.039	0.085	0.001	1.987	0.011	0.036	0.023	0.030	0.002	0.336	0.056	0.017	0.002
Ca	1.072	0.012	0.783	0.035	0.088	0.002	0.003	0.003	0.003	0.001	1.049	0.006	0.754	0.039	0.009	0.009
Ti	1.896	0.013	1.797	0.009	1.902	0.006	0.007	0.005	0.903	0.024	1.847	0.005	1.753	0.026	0.916	0.016
Ce	0.265	0.009	0.106	0.021	0.248	0.003	0.001	0.001	0.001	0.000	0.224	0.004	0.097	0.018	0.003	0.002
Gd	0.218	0.003	0.183	0.006	0.143	0.002	0.001	0.001	0.000	0.000	0.265	0.006	0.229	0.007	0.001	0.001
Hf	0.131	0.016	0.655	0.061	0.078	0.002	0.001	0.000	0.045	0.000	0.189	0.006	0.679	0.049	0.041	0.000
U	0.393	0.024	0.148	0.037	0.457	0.005	0.001	0.001	0.011	0.001	0.396	0.004	0.153	0.028	0.014	0.003
Catatoms	4.000	0.000	4.000	0.000	3.000	0.000	2.000	0.000	1.000	0.000	4.000	0.000	4.000	0.000	1.000	0.000
Oxygen	6.674 -		6.909 -		5.675 -		3.003 -		1.978 -		6.692	0.006	6.916	0.018	1.981	0.011
Ca	1.000		0.783								1.000		0.754			
Gd	0.000		0.183								0.000		0.229			
Sum	1.000		0.966								1.000		0.982			
Charge	2.000		2.116								2.000		2.194			
Ca	0.072		0.000		0.146						0.049		0.000			
Ce(+3)	0.265		0.106		0.248						0.224		0.097			
Gd	0.218		0.000		0.157						0.265		0.000			
Hf	0.106		0.655		0.065						0.106		0.679			
U(+4)	0.174		0.057		0.212						0.168		0.069			
U(+6)	0.219		0.091		0.245						0.228		0.084			
Sum	1.053		0.908		1.073						1.040		0.929			
Charge	4.026		3.710		4.085						4.029		3.786			
Ti	1.896		1.797		1.902		0.007		0.903		1.847		1.753		0.916	
Hf	0.078		0.000		0.013		0.001		0.045		0.123		0.000		0.080	
Al	0.026		0.328		0.085		1.987		0.036		0.030		0.336		0.017	
Sum	2.000		2.125		2.000		1.995		2.000		2.000		2.089		2.000	
Charge	7.974		8.174		7.915		5.991		3.904		7.970		8.020		4.034	
Model Oxygen	7.000		7.000		6.000		2.996		1.952		7.000		7.000		2.017	

Table C3. Microprobe analyses (wt%) of the Ce-analog with 10% Al_2O_3 added

	7-2	1400	7-3	1350	7-3	1350	7-3	1350	7-3	1350
	Brannerite?		Pyrochlore	4	Brannerite	3	Hafnolite	3	Psuedobrookite	2
	wt%	std dev	wt%	std dev	wt%	std dev	wt%	std dev	wt%	std dev
Al_2O_3	0.00	0.00	0.32	0.01	1.44	0.05	4.35	0.18	56.74	1.75
CaO	3.22	0.93	13.41	0.11	1.25	0.05	10.13	0.54	0.02	0.02
TiO_2	20.55	2.28	34.77	0.35	40.27	0.09	33.43	0.11	42.09	2.11
CeO_2	19.50	1.65	9.89	0.35	10.28	0.18	4.25	0.56	0.00	0.00
Gd_2O_3	3.23	0.74	8.72	0.22	6.30	0.24	7.40	0.40	0.00	0.00
HfO_2	5.60	0.53	7.10	0.07	5.08	0.13	30.43	2.36	0.00	0.00
UO_2	43.21	1.99	23.62	0.72	32.68	0.26	9.55	1.41	0.00	0.00
Total	95.29	3.56	97.83 -		97.30 -		99.52 -		98.85	0.33
Al	0.000	0.000	0.028	0.001	0.107	0.004	0.368	0.013	2.036	0.053
Ca	0.269	0.072	1.051	0.005	0.084	0.003	0.775	0.025	0.001	0.001
Ti	1.211	0.157	1.912	0.013	1.897	0.002	1.799	0.006	0.964	0.053
Ce	0.559	0.037	0.265	0.008	0.236	0.003	0.112	0.010	0.000	0.000
Gd	0.084	0.018	0.211	0.004	0.131	0.005	0.175	0.006	0.000	0.000
Hf	0.125	0.009	0.148	0.002	0.091	0.002	0.616	0.039	0.000	0.000
U	0.753	0.020	0.384	0.013	0.456	0.004	0.155	0.016	0.000	0.000
Catatoms	3.000 -		4.000	0.000	3.000	0.000	4.000	0.000	3.000	0.000
Oxygen	5.410 -		6.697 -		5.680 -		6.897 -		4.982 -	
Ca			1.000				0.775			
Gd			0.000				0.175			
Sum			1.000				0.950			
Charge			2.000				2.075			
Ca	0.269		0.051		0.084		0.000			
Ce(+3)	0.559		0.265		0.236		0.112			
Gd	0.084		0.211		0.131		0.000			
Hf	0.000		0.106		0.091		0.616			
U(+4)	0.163		0.116		0.136		0.052			
U(+6)	0.590		0.268		0.320		0.103			
Sum	3.792		2.914		2.658		3.111			
Charge	4.005		4.027		4.005		3.625			
Ti	1.211		1.912		1.897		1.799		0.964	
Hf	0.125		0.060		0.000		0.000		0.000	
Al	0.000		0.028		0.107		0.368		2.036	
Sum	1.336		2.000		2.004		2.167		2.999	
Charge	5.345		7.972		7.908		8.301		9.962	
Model Oxygen	6.000		7.000		6.000		7.000		4.981	

Table C4. Microprobe analyses (wt%) and structural formulae for the Ce-analog with 10 wt% Fe_2O_3 added

	4-1	1300	4-1	1300	4-1	1300	4-1	1300
	Pyrochlore		Hafnolite		Brannerite		Ilmenite	
	wt%	std dev	wt%	std dev	wt%	std dev	wt%	std dev
Al_2O_3	0.05	0.00	0.37	0.01	0.16	0.01	1.97	0.04
CaO	13.87	0.12	8.40	0.14	1.56	0.34	0.14	0.04
TiO_2	33.92	0.26	36.66	0.33	38.18	0.25	39.04	0.51
FeO	2.35	0.10	10.98	0.13	3.07	0.09	51.81	0.29
CeO_2	9.44	0.34	6.57	0.18	10.30	0.23	0.09	0.04
Gd_2O_3	6.18	0.10	7.39	0.40	4.74	0.14	0.06	0.03
HfO_2	3.51	0.08	16.41	0.53	2.33	0.11	1.43	0.08
UO_2	27.61	0.44	10.82	0.39	34.38	0.33	0.12	0.05
Total	96.92 -		97.58 -		94.72 -		94.66	0.48
Al	0.004	0.000	0.030	0.001	0.012	0.000	0.061	0.001
Ca	1.080	0.004	0.619	0.009	0.107	0.023	0.004	0.001
Ti	1.854	0.012	1.897	0.014	1.841	0.014	0.776	0.007
Fe	0.143	0.006	0.632	0.005	0.165	0.005	1.146	0.006
Ce	0.251	0.009	0.165	0.005	0.242	0.005	0.001	0.000
Gd	0.149	0.002	0.169	0.009	0.101	0.003	0.001	0.000
Hf	0.073	0.001	0.322	0.012	0.043	0.002	0.011	0.001
U	0.446	0.007	0.166	0.006	0.491	0.005	0.001	0.000
Catatoms	4.000	0.000	4.000	0.000	3.000	0.000	2.000	0.000
Oxygen	6.432 -		5.935 -		5.386 -		1.673 -	
Ca	1.000		0.619					
Ce	0.000		0.165					
Fe	0.000		0.000					
Gd	0.000		0.169					
Hf	0.000		0.000					
U	0.000		0.047					
Sum	1.000		1.000					
Charge	2.000		2.427					
Al	0.000		0.000		0.000		0.000	
Ca	0.000		0.000		0.107		0.000	
Fe(+2)	0.074		0.558		0.000		0.961	
Ce(+3)	0.251		0.000		0.242		0.000	
Gd	0.149		0.000		0.101		0.000	
Hf	0.000		0.322		0.000		0.000	
U(+4)	0.000		0.000		0.013		0.000	
U(+6)	0.446		0.119		0.478		0.000	
Sum	0.920		1.000		0.000		0.000	
Charge	3.998		3.680		0.000		0.000	
Ti	1.854		1.897		1.841		0.776	
Hf	0.073		0.000		0.000		0.011	
Al	0.004		0.030		0.012		0.061	
Fe(+3)	0.069		0.073		0.147		0.185	
Sum	2.000		2.000		2.000		0.848	
Charge	7.927		7.897		7.841		3.768	
Model Oxygen	6.976		6.723		6.000		1.994	

Table C5. Microprobe compositions (wt%) and structural formulae for a Ce-analog with 10 wt% MgO added

	6-1	1300	6-1	1300	6-1	1300	6-1	1300	6-2	1400	6-2	1400	6-2	1400
	Pyrochlore		Perovskite		Hafnolite		MgTiO3		Pyrochlore		Mg2TiO4		MgTiO3	
	wt%	std dev	wt%	std dev	wt%	std dev	wt%	std dev	wt%	std dev	wt%	std dev	wt%	std dev
MgO	1.29	0.06	1.76	0.07	3.91	0.09	33.88	0.17	1.89	0.02	47.50	0.22	32.04	0.22
Al2O3	0.02	0.01	0.24	0.02	0.05	0.00	0.14	0.00	0.00	0.00	0.82	0.02	0.00	0.00
CaO	12.51	0.07	30.98	0.35	6.79	0.15	0.30	0.05	11.86	0.07	0.02	0.04	0.11	0.04
TiO2	25.06	0.78	49.40	0.38	19.97	0.38	64.79	0.38	27.24	0.19	48.36	0.21	64.29	0.33
CeO2	9.35	0.40	6.11	0.62	5.69	0.25	0.10	0.05	8.98	0.18	0.00	0.00	0.00	0.00
Gd2O3	9.25	0.65	10.00	1.20	8.73	0.75	0.14	0.03	9.23	0.13	0.00	0.00	0.00	0.00
HfO2	12.73	1.85	1.51	0.15	30.17	2.42	4.06	0.11	12.18	0.24	0.97	0.06	2.88	0.07
UO2	26.55	0.33	0.28	0.08	22.71	1.72	0.09	0.05	26.36	0.26	0.00	0.00	0.00	0.00
Total	96.74 -		100.28	0.31	98.03 -		103.50 -		97.74	0.35	97.66	0.32	99.32	0.45
Mg	0.153	0.007	0.066	0.003	0.498	0.008	1.000	0.001	0.218	0.002	1.959	0.003	0.984	0.003
Al	0.001	0.000	0.007	0.001	0.005	0.001	0.003	0.000	0.000	0.000	0.027	0.001	0.000	0.000
Ca	1.068	0.009	0.837	0.006	0.621	0.010	0.006	0.001	0.983	0.004	0.000	0.001	0.003	0.001
Ti	1.501	0.036	0.937	0.004	1.283	0.014	0.965	0.003	1.585	0.010	1.006	0.003	0.996	0.003
Ce	0.273	0.010	0.056	0.006	0.178	0.009	0.001	0.000	0.254	0.005	0.000	0.000	0.000	0.000
Gd	0.244	0.016	0.084	0.010	0.247	0.019	0.001	0.000	0.237	0.004	0.000	0.000	0.000	0.000
Hf	0.290	0.044	0.011	0.001	0.736	0.065	0.023	0.001	0.269	0.005	0.008	0.000	0.017	0.000
U	0.471	0.008	0.002	0.000	0.432	0.030	0.000	0.000	0.454	0.005	0.000	0.000	0.000	0.000
Catatoms	4.000	0.000	2.000	0.000	4.000	0.000	2.000	0.000	4.000 -		3.000 -		2.000 -	
Oxygen	6.520 -		3.023 -		6.666 -		2.991 -		6.553 -		4.027 -		3.013 -	
Ca	1.000				0.621				0.983					
Gd	0.000				0.247				0.017					
Ce(+3)	0.000				0.132				0.000					
U(+4)	0.000				0.000				0.000					
Sum	1.000				1.000				1.000					
Charge	2.000				2.379				2.017					
Mg	0.000		0.066		0.000		1.000		0.000					
Ca	0.068		0.837		0.000				0.000					
Ce(+3)	0.273		0.056		0.046				0.254					
Gd	0.244		0.084		0.000				0.237					
Hf	0.000		0.000		0.522				0.000					
U(+4)	0.000		0.002		0.098				0.031					
U(+6)	0.471		0.000		0.334				0.423					
Sum	1.055		1.045		1.000		1.000		0.945					
Charge	4.509		2.231		4.622		2.000		4.133					
Ti	1.501		0.937		1.283		0.965		1.585					
Hf	0.290		0.011		0.214		0.023		0.269					
Mg	0.153		0.000		0.498				0.218					
Al	0.001		0.007		0.005		0.003		0.000					
Sum	1.945		0.955		2.000		0.991		2.072					
Charge	7.472		3.813		6.999		3.962		7.851					
Model Oxygen	6.990		3.022		7.000				7.000					

Table C5. Microprobe compositions (wt%) and structural formulae for a Ce-analog with 10 wt% MgO added

	6-3	1350	6-3	1350	6-3	1350	6-3	1350
	Pyrochlore		Perovskite		Mg2TiO4		MgTiO3	
	wt%	std dev	wt%	std dev	wt%	std dev	wt%	std dev
MgO	1.85	0.11	1.73	0.04	49.68	0.14	33.59	0.27
Al2O3	0.03	0.01	0.18	0.05	1.44	0.03	0.06	0.00
CaO	12.04	0.12	30.45	0.25	0.06	0.08	0.15	0.02
TiO2	25.75	0.52	49.97	0.15	47.58	0.32	64.25	0.51
CeO2	9.07	0.31	7.36	0.10	0.00	0.00	0.00	0.00
Gd2O3	9.08	0.20	8.29	0.44	0.00	0.00	0.00	0.00
HfO2	13.56	1.14	0.88	0.17	1.29	0.09	3.06	0.13
UO2	26.47	0.51	0.18	0.06	0.01	0.01	0.00	0.00
Total	97.84 -		99.04 -		100.06 -		101.13 -	
Mg	0.215	0.011	0.066	0.001	1.984	0.007	1.006	0.007
Al	0.003	0.001	0.005	0.001	0.045	0.001	0.001	0.000
Ca	1.009	0.011	0.830	0.003	0.002	0.002	0.003	0.000
Ti	1.514	0.025	0.954	0.005	0.959	0.006	0.971	0.007
Ce	0.260	0.007	0.069	0.001	0.000	0.000	0.000	0.000
Gd	0.235	0.005	0.069	0.003	0.000	0.000	0.000	0.000
Hf	0.303	0.027	0.007	0.001	0.010	0.001	0.018	0.001
U	0.461	0.010	0.001	0.000	0.000	0.000	0.000	0.000
Catatoms	4.000	0.000	2.000	0.000	3.000	0.000	2.000	0.000
Oxygen	6.527 -		3.033 -		3.991 -		2.990 -	
Ca	1.000							
Gd	0.000							
Ce(+3)	0.000							
U(+4)	0.000							
Sum	1.000							
Charge	2.000							
Mg	0.000		0.066		1.984		1.006	
Ca	0.009		0.830					
Ce(+3)	0.260		0.069					
Gd	0.235		0.069					
Hf	0.000		0.000					
U(+4)	0.000		0.001					
U(+6)	0.461		0.000					
Sum	0.964		1.034		1.984		1.006	
Charge	4.266		2.206		3.968		2.013	
Ti	1.514		0.954		0.959		0.971	
Hf	0.303		0.007		0.010		0.018	
Mg	0.215		0.000					
Al	0.003		0.005		0.045		0.001	
Sum	2.035		0.966		1.014		0.990	
Charge	7.707		3.859		4.011		3.960	
Model Oxygen	6.987		3.032					

Table C6. Microprobe analyses of Ce-analog with 10 wt% NiO

	17-1	1350	17-1	1350	17-1	1350	13-2	1300	13-2	1300	13-2	1300
	Pyrochlore		Ni-titanate		Hafnolite		Pyrochlore		Hafnolite		Ni-Titanate	
	wt%	std dev	wt%	std dev	wt%	std dev	wt%	std dev	wt%	std dev	wt%	std dev
Al_2O_3	0.05	0.01	0.88	0.03	0.24	0.05	0.00	0.00	0.33	0.02	0.89	0.88
CaO	12.50	0.14	0.00	0.00	6.76	0.17	12.82	0.14	6.70	0.07	0.00	0.00
TiO_2	31.74	0.27	49.16	0.42	28.60	0.84	32.88	0.84	27.82	0.74	49.48	49.84
NiO	2.11	0.08	44.79	0.48	6.22	0.22	1.85	0.08	6.51	0.21	44.95	45.56
Ce_2O_3	8.89	0.25	0.08	0.03	5.72	0.18	9.43	0.60	5.73	0.08	0.12	0.14
Gd_2O_3	9.20	0.28	0.07	0.06	9.06	0.13	9.13	0.60	8.99	0.19	0.01	0.00
HfO_2	10.15	0.21	4.47	0.13	29.70	0.55	8.61	0.19	28.46	1.27	3.96	3.65
UO_2	23.12	0.51	0.20	0.04	12.27	1.47	22.33	1.73	14.09	1.43	0.24	0.23
Total	97.74	0.78	99.66	0.70	98.57	0.59	97.04 -		98.62 -		99.65	100.30
Al	0.004	0.001	0.028	0.001	0.023	0.004	0.000	0.000	0.031	0.002	0.027	0.001
Ca	1.004	0.008	0.000	0.000	0.575	0.011	1.020	0.017	0.574	0.005	0.004	0.010
Ti	1.789	0.015	0.981	0.005	1.709	0.035	1.836	0.029	1.672	0.028	0.984	0.004
Ni	0.127	0.004	0.955	0.005	0.397	0.018	0.111	0.005	0.418	0.017	0.951	0.024
Ce	0.244	0.007	0.001	0.000	0.167	0.007	0.256	0.014	0.168	0.004	0.001	0.001
Gd	0.228	0.006	0.001	0.001	0.239	0.003	0.225	0.012	0.238	0.006	0.001	0.002
Hf	0.217	0.004	0.034	0.001	0.674	0.007	0.182	0.005	0.649	0.023	0.029	0.003
U	0.386	0.008	0.001	0.000	0.217	0.028	0.369	0.032	0.251	0.028	0.003	0.006
Catatoms	4.000 -		2.000 -		4.000 -		4.000 -		4.000 -		2.000 -	
Oxygens	6.631 -		3.030 -		6.814 -		6.629 -		6.790 -		3.031 -	
Ca	1.004				0.575		1.020		0.574			
Gd	0.000				0.239		0.000		0.238			
Ce(+3)	0.000				0.167		0.000		0.168			
U(+4)	0.000				0.000		0.000		0.000			
Sum	1.004				0.980		1.020		0.979			
Charge	2.007				2.366		2.041		2.365			
Ca	0.000		0.000		0.000		0.000		0.000		0.000	
Ni	0.127		0.955		0.397		0.111		0.418		0.951	
Ce(+3)	0.244		0.001		0.000		0.256		0.000		0.001	
Gd	0.228		0.001		0.000		0.225		0.000		0.001	
Hf	0.011		0.034		0.405		0.019		0.352		0.029	
U(+4)	0.016		0.001		0.031		0.000		0.041		0.003	
U(+6)	0.370		0.000		0.186		0.369		0.210		0.000	
Sum	0.996		0.992		1.020		0.980		1.021		0.985	
Charge	2.888		2.055		3.098		2.847		3.036		2.037	
Ti	1.789		0.981		1.709		1.836		1.672		0.984	
Hf	0.206		0.000		0.269		0.164		0.297		0.000	
Al	0.004		0.028		0.023		0.000		0.031		0.027	
Sum	2.000		1.008		2.000		2.000		2.000		1.011	
Charge	7.996		4.005		7.977		8.000		7.969		4.016	
Model Oxygen	7.000		3.030		7.000		6.997		7.000		3.027	

Table C7. Microprobe analyses of Ce-analog with 10 wt% CuO

	21-1	1350	21-1	1350	21-2	1300	21-2	1300
	Pyrochlore wt%	std dev	Rutile wt%	std dev	Pyrochlore wt%	std dev	Rutile wt%	std dev
Al_2O_3	0.06	0.02	0.37	0.02	0.05	0.01	0.36	0.07
CaO	12.23	0.10	0.02	0.03	12.74	0.09	0.02	0.03
TiO_2	33.77	0.28	77.53	0.32	33.11	0.32	79.99	0.99
CuO	1.64	0.08	0.12	0.01	1.14	0.04	0.10	0.02
Ce_2O_3	8.39	0.34	0.04	0.02	8.93	0.21	0.04	0.03
Gd_2O_3	10.02	0.18	0.00	0.00	10.04	0.32	0.00	0.00
HfO_2	12.03	0.76	19.03	0.41	9.83	0.28	16.78	0.63
UO_2	22.30	0.42	1.26	0.12	24.35	0.38	1.57	0.39
Total	100.44 -		98.37 -		100.18 -		98.87 -	
Al	0.005	0.002	0.007	0.000	0.004	0.000	0.006	0.001
Ca	0.960	0.009	0.000	0.000	1.006	0.005	0.000	0.001
Ti	1.861	0.008	0.903	0.003	1.835	0.014	0.914	0.006
Cu	0.091	0.005	0.001	0.000	0.063	0.002	0.001	0.000
Ce	0.225	0.008	0.000	0.000	0.241	0.005	0.000	0.000
Gd	0.243	0.004	0.000	0.000	0.245	0.007	0.000	0.000
Hf	0.252	0.015	0.084	0.002	0.207	0.006	0.073	0.003
U	0.364	0.007	0.004	0.000	0.399	0.007	0.005	0.001
Catatoms	4.000 -		1.000 -		4.000 -		1.000 -	
Oxygen	6.713 -		1.995 -		6.686 -		1.995 -	
Ca	0.960				1.006			
Gd	0.040				0.000			
Ce(+3)	0.000				0.000			
U(+4)	0.000				0.000			
Sum	1.000				1.006			
Charge	2.040				2.011			
Ca	0.000				0.000			
Cu	0.091				0.063			
Ce(+3)	0.225				0.241			
Gd	0.204				0.245			
Hf	0.117				0.046			
U(+4)	0.077				0.112			
U(+6)	0.287				0.287			
Sum	1.000				0.994			
Charge	3.103				3.078			
Ti	1.861		0.903		1.835		0.914	
Hf	0.134		0.084		0.161		0.073	
Al	0.005		0.007		0.004		0.006	
Sum	2.000		0.994		2.000		0.993	
Charge	7.995		3.968		7.996		3.965	
Model Oxygen	7.000		1.984		6.973		1.983	

Table C8. Microprobe analyses of Ce-analog with 10 wt% ZnO

	22-1	1350	22-1	1350	22-2	1300	22-2	1300
	Pyrochlore		Rutile		Pyrochlore		Hafnolite	
	wt%	std dev	wt%	std dev	wt%	std dev	wt%	std dev
Al_2O_3	0.10	0.04	0.48	0.05	0.00	0.00	0.34	0.05
CaO	12.39	0.32	0.06	0.06	14.16	0.15	7.95	0.22
TiO_2	34.21	0.21	78.79	0.67	37.26	0.22	40.00	1.19
ZnO	0.34	0.02	0.00	0.00	2.25	0.11	7.63	0.39
Ce_2O_3	8.66	0.26	0.06	0.05	9.00	0.16	6.53	0.21
Gd_2O_3	10.06	0.37	0.00	0.00	7.73	0.08	8.60	0.45
HfO_2	12.10	1.03	19.00	0.34	4.78	0.32	18.89	0.58
UO_2	22.07	0.64	1.69	0.28	24.24	0.22	11.94	0.82
Total	99.92	0.37	100.08	0.49	99.41 -		101.90 -	
Al	0.008	0.003	0.009	0.001	0.000	0.000	0.028	0.004
Ca	0.979	0.022	0.001	0.001	1.056	0.008	0.588	0.010
Ti	1.898	0.012	0.902	0.004	1.950	0.003	2.077	0.045
Zn	0.018	0.001	0.000	0.000	0.116	0.006	0.389	0.019
Ce	0.234	0.006	0.000	0.000	0.229	0.004	0.165	0.005
Gd	0.246	0.010	0.000	0.000	0.178	0.002	0.197	0.011
Hf	0.255	0.022	0.083	0.002	0.095	0.006	0.372	0.011
U	0.362	0.010	0.006	0.001	0.375	0.004	0.184	0.013
Catatoms	4.000 -		1.000 -		4.000 -		4.000 -	
Oxygen	6.759 -		1.995 -		6.625 -		6.828 -	
Ca	0.979				1.056		0.588	
Gd	0.021				0.000		0.197	
Ce(+3)	0.000				0.000		0.165	
U(+4)	0.000				0.000		0.000	
Sum	1.000				1.056		0.950	
Charge	2.021				2.111		2.263	
Al	0.000				0.000		0.028	
Ca	0.000				0.000		0.000	
Cu	0.018				0.116		0.389	
Ce(+3)	0.234				0.229		0.000	
Gd	0.225				0.178		0.000	
Hf	0.161				0.046		0.372	
U(+4)	0.121				0.000		0.012	
U(+6)	0.241				0.375		0.172	
Sum	1.000				0.944		0.945	
Charge	3.264				2.763		2.829	
Ti	1.898		0.902		1.950		2.077	
Hf	0.094		0.083		0.049		0.000	
Al	0.008		0.009		0.000		0.000	
Sum	2.000		0.993		2.000		2.077	
Charge	7.992		3.964		8.000		8.308	
Model Oxygen	7.000		1.982		7.000		7.000	

Table C9. Microprobe analyses of Ce-analog with 10 wt% Cr_2O_3

	18-1	1350	18-1	1350	18-1	1350	18-2	1300	18-2	1300	18-2	1300
	Pyrochlore		Hafnolite		rutile		Pyrochlore		Hafnolite		Rutile	
	wt%	std dev	wt%	std dev	wt%	std dev	wt%	std dev	wt%	std dev	wt%	std dev
Al_2O_3	0.07	0.01	0.57	0.02	0.10	0.03	0.09	0.04	0.56	0.02	0.07	0.04
CaO	12.99	0.12	9.52	0.13	0.25	0.43	12.91	0.35	9.58	0.16	0.19	0.12
TiO_2	31.60	0.18	29.79	0.41	62.75	2.79	31.48	0.50	29.93	0.57	62.44	1.07
Cr_2O_3	1.88	0.10	5.76	0.33	8.51	0.87	1.84	0.31	5.84	0.24	8.49	0.09
Ce_2O_3	9.78	0.20	3.59	0.11	0.23	0.26	9.93	0.34	3.54	0.09	0.16	0.07
Gd,O3	10.48	0.15	7.42	0.47	0.18	0.35	10.61	0.45	7.63	0.63	0.07	0.12
HfO_2	8.98	0.35	34.46	1.60	14.20	0.92	9.39	3.09	34.57	2.24	13.23	0.63
UO_2	24.41	0.29	9.29	0.50	11.97	1.39	23.96	1.17	9.19	0.67	12.97	0.57
Total	100.18 -		100.41 -		98.20 -		100.21 -		100.84 -		97.61 -	
Al	0.006	0.001	0.050	0.002	0.002	0.001	0.008	0.003	0.049	0.002	0.001	0.001
Ca	1.025	0.008	0.763	0.011	0.004	0.007	1.020	0.029	0.763	0.009	0.003	0.002
Ti	1.751	0.009	1.672	0.017	0.771	0.019	1.746	0.028	1.674	0.022	0.774	0.009
Cr	0.109	0.006	0.341	0.019	0.110	0.013	0.107	0.018	0.343	0.014	0.111	0.002
Ce	0.264	0.005	0.098	0.003	0.001	0.001	0.268	0.010	0.096	0.002	0.001	0.000
Gd	0.256	0.004	0.183	0.011	0.001	0.002	0.259	0.011	0.188	0.015	0.000	0.001
Hf	0.189	0.007	0.739	0.039	0.066	0.005	0.198	0.064	0.734	0.052	0.062	0.003
U	0.400	0.005	0.155	0.008	0.044	0.006	0.393	0.021	0.152	0.010	0.048	0.002
Catatoms	4.000 -		4.000 -		1.000 -		4.000 -		4.000 -		1.000 -	
Oxygen	6.657 -		6.902 -		1.938 -		6.658 -		6.898 -		1.940 -	
Ca	1.025		0.763				1.020		0.763			
Gd	0.000		0.183				0.000		0.188			
Ce(+3)	0.000		0.055				0.000		0.049			
U(+4)	0.000		0.000				0.000		0.000			
Sum	1.025		1.000				1.020		1.000			
Charge	2.050		2.237				2.041		2.237			
Ca	0.000		0.000				0.000		0.000			
Cr	0.055		0.341				0.058		0.343			
Ce(+3)	0.264		0.043				0.268		0.048			
Gd	0.256		0.000				0.259		0.000			
Hf	0.000		0.461				0.000		0.457			
U(+4)	0.058		0.057				0.051		0.050			
U(+6)	0.342		0.098				0.342		0.102			
Sum	0.975		1.000				0.980		1.000			
Charge	2.984		3.518				2.990		3.507			
Ti	1.751		1.672		0.771		1.746		1.674		0.774	
Hf	0.189		0.278		0.066		0.198		0.277		0.062	
Al	0.006		0.050		0.002		0.008		0.049		0.001	
Cr	0.054		0.000		0.110		0.049		0.000		0.111	
Sum	1.946		2.000		0.840		1.951		2.000		0.837	
Charge	7.777		7.950		3.356		7.798		7.951		3.347	
Model Oxygen	7.000		7.000		1.843		7.000		7.000		1.840	

Table C10. Microprobe analyses of Ce-analog with 10wt% $FeAl_2O_4$

	11-1	1350	11-1	1350	11-1	1350	11-2	1300	11-2	1300	11-2	1300
	Pyrochlore		Hafnolite		Psuedobrookite		Pyrochlore		Hafnolite		Psuedobrookite	
	wt%	std dev	wt%	std dev	wt%	std dev	wt%	std dev	wt%	std dev	wt%	std dev
Al_2O_3	0.35	0.21	3.51	0.09	42.15	0.92	0.24	0.05	3.27	0.04	39.96	0.54
CaO	12.94	0.32	7.95	0.09	0.12	0.03	13.77	0.18	8.19	0.11	0.09	0.03
TiO_2	33.36	0.58	34.81	0.30	42.27	0.24	35.00	0.79	36.56	0.98	41.95	0.27
FeO	1.47	0.34	5.20	0.11	12.83	0.27	1.13	0.06	5.39	0.14	14.80	0.35
Ce_2O_3	9.22	0.85	5.37	0.17	0.07	0.04	10.79	0.88	5.57	0.30	0.11	0.05
Gd_2O_3	9.66	0.24	10.48	0.32	0.09	0.08	8.37	0.29	9.68	0.40	0.06	0.06
HfO_2	6.44	1.54	23.32	0.41	1.39	0.08	4.42	0.23	21.85	0.65	1.16	0.03
UO_2	23.42	0.93	7.88	0.29	0.12	0.07	23.33	1.68	6.89	0.65	0.04	0.03
Total	96.86 -		98.51 -		99.04 -		97.04 -		97.40 -		98.18 -	
Al	0.031	0.019	0.290	0.008	1.606	0.023	0.020	0.004	0.267	0.001	1.544	0.013
Ca	1.023	0.019	0.597	0.006	0.004	0.001	1.064	0.018	0.609	0.010	0.003	0.001
Ti	1.850	0.021	1.836	0.012	1.028	0.013	1.898	0.030	1.908	0.028	1.034	0.003
Fe	0.091	0.021	0.305	0.007	0.347	0.009	0.068	0.004	0.313	0.008	0.406	0.011
Ce	0.249	0.022	0.138	0.004	0.001	0.000	0.285	0.021	0.141	0.006	0.001	0.001
Gd	0.236	0.005	0.244	0.008	0.001	0.001	0.200	0.006	0.223	0.008	0.001	0.001
Hf	0.136	0.033	0.467	0.007	0.013	0.001	0.091	0.005	0.433	0.018	0.011	0.000
U	0.384	0.014	0.123	0.005	0.001	0.000	0.375	0.030	0.106	0.011	0.000	0.000
Catatoms	4.000	0.000	4.000	0.000	3.000	0.000	4.000 -		4.000 -		3.000 -	
Oxygen	6.628 -		6.762 -		4.845 -		6.616	0.000	6.763	0.000	4.818	0.000
Ca	1.023		0.597				1.064		0.609			
Gd	0.000		0.244				0.000		0.223			
Ce(+3)	0.000		0.138						0.141			
Sum	1.023		0.979				1.064		0.973			
Charge	2.045		2.339				2.128		2.310			
Ca	0.000		0.000		0.000		0.000		0.000		0.000	
Al	0.000		0.127		0.000						0.000	
Fe(+3)	0.091		0.305		1.606		0.068		0.313		1.544	
Ce(+3)	0.249		0.000		0.347		0.285		0.141		0.406	
Gd	0.236		0.000		0.000		0.200		0.000		0.000	
Hf	0.017		0.467		0.000		0.009		0.433		0.000	
U(+4)	0.058		0.037		0.000		0.025		0.025		0.000	
U(+6)	0.326		0.086		0.000		0.350		0.081		0.000	
Sum	0.977		1.021		1.953		0.936		0.994		1.950	
Charge	3.894		3.826		5.858		3.824		3.370		5.849	
Ti	1.850		1.836		1.028		1.898		1.908		1.034	
Hf	0.119		0.000		0.013		0.082		0.000		0.011	
Al	0.031		0.164		0.000		0.020		0.267		0.000	
Sum	2.000		2.000		1.041		2.000		2.175		1.045	
Charge	7.969		7.836		4.163		7.980		8.432		4.180	
Model Oxygen	7.000		7.000		5.010		7.000		7.000		5.014	

Table C11. Microprobe analyses of Ce-analog with 10wt% $MgAl_2O_4$

	12-1	1350	12-1	1350	12-2	1300	12-2	1300	12-2	1300
	Pyrochlore		Psuedobrookite		Pyrochlore		Psuedobrookite		Hafnolite	
	wt%	std dev	wt%	std dev	wt%	std dev	wt%	std dev		
MgO	0.83	0.07	9.67	0.38	0.74	0.09	10.13	0.19	1.48	0.06
Al_2O_3	0.31	0.03	28.50	4.20	0.24	0.01	26.50	1.33	2.49	0.43
CaO	12.47	0.19	0.36	0.47	12.98	0.36	0.21	0.08	8.80	0.42
TiO_2	34.39	0.64	58.24	4.06	34.50	0.76	60.39	0.71	31.54	0.63
Ce_2O_3	9.37	0.39	0.27	0.33	9.37	0.45	0.08	0.07	4.71	0.34
Gd_2O_3	9.04	0.44	0.00	0.00	8.65	0.28	0.08	0.03	8.79	0.94
HfO_2	7.56	0.15	3.28	0.26	6.32	0.22	3.04	0.13	30.59	1.53
UO_2	22.57	1.36	0.11	0.04	23.95	1.54	0.12	0.08	12.46	1.15
Total	96.53 -		100.44 -		96.74 -		100.55 -		100.86 -	
Mg	0.091	0.008	0.464	0.025	0.081	0.010	0.488	0.013	0.162	0.005
Al	0.027	0.002	1.078	0.131	0.020	0.001	1.008	0.040	0.216	0.042
Ca	0.982	0.013	0.012	0.015	1.017	0.020	0.007	0.003	0.693	0.024
Ti	1.901	0.031	1.411	0.124	1.899	0.020	1.467	0.029	1.743	0.007
Ce	0.252	0.010	0.003	0.004	0.251	0.009	0.001	0.001	0.127	0.008
Gd	0.220	0.010	0.000	0.000	0.210	0.007	0.001	0.000	0.214	0.020
Hf	0.159	0.003	0.030	0.003	0.132	0.004	0.028	0.001	0.642	0.036
U	0.369	0.023	0.001	0.000	0.390	0.030	0.001	0.001	0.204	0.016
Catatoms	4.000 -		3.000 -		6.662 -		5.000 -		6.867 -	
Oxygen	6.678 -		4.983 -		4.000 -		3.000 -		4.000 -	
Ca	0.982				1.017				0.693	
Gd	0.018				0.000				0.214	
Ce(+3)	0.000				0.000				0.093	
Sum	1.000				1.017				0.907	
Charge	2.018				2.035				2.027	
Ca	0.000				0.000				0.000	
Al	0.000		1.078		0.000		1.008		0.000	
Mg	0.091		0.464		0.081		0.488		0.162	
Ce(+3)	0.252		0.000		0.251		0.000		0.033	
Gd	0.202		0.000		0.210		0.000		0.000	
Hf	0.086		0.000		0.051		0.000		0.601	
U(+4)	0.047		0.000		0.052		0.000		0.204	
U(+6)	0.322		0.000		0.338		0.000		0.000	
Sum	1.000		1.543		0.983		1.495		1.000	
Charge	4.009		0.928		3.985		0.975		3.643	
Ti	1.901		1.411		1.899		1.467		1.743	
Hf	0.073		0.030		0.081		0.028		0.041	
Al	0.027		0.000		0.020		0.000		0.216	
Sum	2.000		1.442		2.000		1.495		2.000	
Charge	7.973		5.766		7.980		5.978		7.784	
Model Oxygen	7.000		4.965		7.000		4.989		6.867	

Table C12. Microprobe analyses of Ce-analog with 10wt% $CaAl_2O_4$

	13-1	1350	13-1	1350	13-1	1350	13-2	1300	13-2	1300	13-2	1300	13-2	1300	13-2	1300
	Pyrochlore		Hafnolite		CTA		Pyrochlore		Hafnolite		CTA		Rutile		Corundum	
	wt%	std dev	wt%	std dev	wt%	std dev	wt%	std dev	wt%	std dev	wt%	std dev	wt%	std dev	wt%	std dev
Al_2O_3	0.32	0.09	3.47	0.74	57.64	0.37	0.20	0.01	3.73	0.17	57.64	0.37	1.10	0.01	99.08	1.31
CaO	14.78	0.17	11.37	0.94	5.86	0.08	14.84	0.09	11.04	0.15	5.86	0.08	0.22	0.01	0.08	0.05
TiO_2	36.41	0.39	37.01	0.63	30.36	0.10	35.93	0.19	36.74	0.29	30.36	0.10	87.43	0.45	0.30	0.11
Ce_2O_3	8.50	0.17	3.62	1.23	5.33	0.13	8.75	0.23	2.98	0.31	5.33	0.13	0.08	0.04	0.06	0.01
Gd_2O_3	7.79	0.19	6.54	0.53	0.87	0.06	7.81	0.21	6.52	0.24	0.87	0.06	0.06	0.04	0.02	0.03
HfO_2	6.97	0.77	28.23	4.92	1.31	0.14	5.70	0.16	31.37	1.20	1.31	0.14	8.93	0.26	0.16	0.02
UO_2	22.62	0.59	8.79	3.34	0.15	0.09	23.66	0.27	7.18	1.03	0.15	0.09	2.37	0.04	0.06	0.02
Total	97.38 -		99.04 -		101.52 -		96.88 -		99.55	0.52	101.52 -		100.19 -		99.76 -	
Al	0.027	0.007	0.284	0.062	8.178	0.030	0.017	0.001	0.305	0.013	8.184	0.020	0.018	0.000	1.993	0.002
Ca	1.125	0.015	0.846	0.067	0.755	0.011	1.139	0.006	0.821	0.013	0.755	0.010	0.003	0.000	0.001	0.001
Ti	1.945	0.012	1.932	0.015	2.748	0.015	1.936	0.008	1.917	0.013	2.757	0.017	0.934	0.001	0.004	0.001
Ce	0.221	0.005	0.092	0.031	0.235	0.005	0.229	0.006	0.076	0.008	0.233	0.002	0.000	0.000	0.000	0.000
Gd	0.183	0.005	0.151	0.012	0.035	0.002	0.185	0.005	0.150	0.006	0.034	0.002	0.000	0.000	0.000	0.000
Hf	0.141	0.015	0.560	0.100	0.045	0.005	0.116	0.003	0.621	0.022	0.035	0.002	0.036	0.001	0.001	0.000
U	0.358	0.011	0.136	0.051	0.004	0.002	0.377	0.003	0.111	0.016	0.004	0.001	0.007	0.000	0.000	0.000
Catatoms	4.000	0.000	4.000	0.000	12.000	0.000	4.000	0.000	4.000	0.000	12.000	0.000	1.000	0.000	2.000	0.000
oxygen	6.660	0.014	6.891	0.058	19.021	0.008	6.645 -		6.914 -		-		1.987 -		3.002 -	
Ca	1.000		0.846				1.000		0.821							
Gd	0.000		0.151				0.000		0.150							
Sum	1.000		0.996				1.000		0.971							
Charge	2.000		2.143				2.000		2.091							
Ca	0.125		0.000		0.755		0.139		0.000		0.755					
Ce(+3)	0.221		0.092		0.235		0.229		0.076		0.233					
Gd	0.183		0.000		0.035		0.185		0.000		0.034					
Hf	0.113		0.560		0.000		0.106		0.621		0.000					
U(+4)	0.018		0.027		0.004		0.096		0.025		0.004					
U(+6)	0.340		0.109		0.000		0.281		0.086		0.000					
Sum	1.000		0.788		1.029		1.037		0.808		1.025					
Charge	4.026		3.276		2.335		4.016		3.327		2.323					
Ti	1.945		1.932		2.748		1.936		1.917		2.757		0.934			
Hf	0.028		0.000		0.045		0.047		0.000		0.035		0.080			
Al	0.027		0.284		8.178		0.017		0.305		8.184		0.018		1.993	
Sum	2.000		2.216		10.972		2.000		2.222		10.975		2.000		2.000	
Charge	7.973		8.581		35.708		7.983		8.582		35.718		3.947		3.947	
Model Oxygen	7.000		7.000		19.022		7.000		7.000		19.021		2.055		2.990	

Table C!3. Mircoprobe compostions for Ce-analog with MoO_3

	P229	1350	P229	1350	P229	1350
	Pyrochlore		Brannerite		Ca-Mo	
	wt%	std dev	wt%	std dev	wt%	std dev
Al_2O_3	0.00	0.00	0.00	0.00	0.00	0.00
CaO	12.62	0.09	1.25	0.06	26.60	0.11
TiO_2	30.70	0.21	39.73	0.47	0.12	0.05
MoO_3	1.73	0.13	0.08	0.04	70.21	0.39
Ce_2O_3	7.38	0.10	9.02	0.33	0.92	0.03
Gd_2O_3	9.85	0.38	8.17	0.16	0.81	0.04
HfO_2	11.02	0.17	7.44	0.43	0.19	0.06
UO_2	20.39	0.37	27.84	0.34	0.07	0.02
Total	93.70 -		93.53 -		98.91 -	
Al	0.000	0.000	0.000	0.000	0.000	0.000
Ca	1.061	0.006	0.088	0.004	0.973	0.001
Ti	1.812	0.010	1.966	0.011	0.003	0.001
Mo	0.057	0.004	0.002	0.001	1.001	0.002
Ce	0.212	0.003	0.217	0.008	0.011	0.000
Gd	0.256	0.010	0.178	0.002	0.009	0.000
Hf	0.247	0.003	0.140	0.009	0.002	0.001
U	0.356	0.006	0.408	0.003	0.001	0.000
Catatoms	4.000 -		3.000 -		2.000 -	
Oxygen	6.762 -		5.716 -		4.017 -	
Ca	1.000					
Mo(+6)	0.000					
Gd	0.000					
Ce(+3)	0.000					
U(+4)	0.000					
Sum	1.000					
Charge	2.000					
Ca	0.061		0.088		0.973	
Mo(+6)	0.000		0		0	
Ce(+3)	0.212		0.217		0.011	
Gd	0.256		0.178		0.009	
Hf	0.115		0.108		0.002	
U(+4)	0.118		0.124		0	
U(+6)	0.238		0.284		0.001	
Sum	1.000		1.000		0.996	
Charge	3.173		3.144		2.017	
Ti	1.812		1.966		0.003	
Hf	0.132		0.031		0	
Al	0.000		0.000		0.000	
Mo(+6)	0.057		0.002		1.001	
Sum	2.000		2.000		1.004	
Charge	7.774		7.991		0.013	
Model Oxygen	7.000		6.000		4.018	

Table C14. Microprobe analyses of Ce-analog with WO_3

	P232	1350	P232	1350	P232	1350	P232	1350
	Pyrochlore		Brannerite		Ca-W		Rutile	
	wt%	std dev	wt%	std dev	wt%	std dev	wt%	std dev
Al_2O_3	0.00	0.00	0.00	0.00	0.00	0.00	0.05	0.01
CaO	12.19	0.08	1.14	0.03	18.55	0.07	0.07	0.03
TiO_2	26.90	0.29	39.01	0.36	0.27	0.05	67.53	0.64
Ce_2O_3	6.15	0.17	9.32	0.32	0.86	0.03	0.16	0.15
Gd_2O_3	8.09	0.19	8.64	0.14	0.84	0.03	0.14	0.06
HfO_2	7.12	0.18	7.76	0.63	0.33	0.02	26.52	0.54
WO_3	14.37	0.09	1.50	0.17	73.99	0.24	0.83	0.15
UO_2	19.28	0.33	26.69	0.26	0.17	0.05	1.27	0.33
Total	94.09 -		94.05 -		95.01 -		96.56 -	
Al	0.000	0.000	0.000	0.000	0.000	0.000	0.001	0.000
Ca	1.083	0.008	0.081	0.002	0.994	0.003	0.001	0.000
Ti	1.676	0.015	1.940	0.009	0.010	0.002	0.859	0.004
Ce	0.187	0.005	0.226	0.007	0.016	0.001	0.001	0.001
Gd	0.222	0.006	0.189	0.003	0.014	0.000	0.001	0.000
Hf	0.168	0.004	0.146	0.013	0.005	0.000	0.128	0.002
W	0.309	0.002	0.026	0.003	0.959	0.004	0.004	0.001
U	0.355	0.005	0.393	0.001	0.002	0.001	0.005	0.001
Catatoms	4.000 -		3.000 -		2.000 -		1.000 -	
Oxygen	7.021 -		5.737 -		3.950 -		2.001 -	
Ca	1.000							
W(+6)	0.000							
Gd	0.000							
Ce(+3)	0.000							
U(+4)	0.000							
Sum	1.000							
Charge	2.000							
Ca	0.083		0.081		0.994			
W(+6)	0.000		0		0			
Ce(+3)	0.187		0.226		0.016			
Gd	0.222		0.189		0.014			
Hf	0.153		0.112		0			
U(+4)	0.355		0.130		0			
U(+6)	0.000		0.263		0.002			
Sum	1.000		1.000					
Charge	3.426		3.161					
Ti	1.676		1.940		0.010		0.859	
Hf	0.015		0.035		0.005		0.128	
Al	0.000		0.000		0.000		0.001	
W(+6)	0.309		0.026		0.959		0.004	
Sum	2.000		2.000		0.974		0.992	
Charge	8.558		7.974		2.937		3.964	
Model Oxygen	7.021		6.000		3.952		1.987	

Table C15. Microprobe analyses (wt%) and structural formulae for the Ce-analog with 10 wt% P_2O_5 added

	2-1	1300 C	2-1	1300 C	2-1	1300 C	2-1	1300 C	2-2	1400 C	2-2	1400 C	2-2	1400 C
	Brannerite		Rutile		Whitlockite		P-Glass		Brannerite		Rutile		P-Glass	
	wt%	std dev	wt%	std dev	wt%	std dev	wt%	std dev	wt%	std dev	wt%	std dev	wt%	std dev
Al_2O_3	0.02	0.01	0.07	0.01	0.00	0.00	0.00	0.00	0.00	0.00	0.00	0.00	0.01	0.02
P_2O_5	0.46	0.43	0.08	0.03	40.26	0.94	36.77	2.30	0.00	0.00	0.00	0.00	37.96	0.81
CaO	2.39	0.70	0.29	0.07	41.26	1.56	29.99	0.38	1.39	0.03	0.05	0.04	30.42	0.30
TiO_2	40.63	2.00	72.82	1.49	1.60	2.17	0.74	0.19	40.72	0.58	69.52	0.65	0.21	0.06
CeO_2	7.61	0.57	0.10	0.03	7.75	0.33	17.78	0.21	6.80	0.17	0.08	0.02	16.96	0.32
Gd_2O_3	7.19	0.53	0.08	0.06	7.80	0.52	13.75	0.37	8.16	0.20	0.14	0.06	14.15	0.31
HfO_2	7.79	0.39	26.09	1.58	0.30	0.31	0.31	0.12	8.77	0.36	29.15	0.61	0.32	0.13
UO_2	31.65	1.66	1.33	0.25	1.10	1.22	0.36	0.18	31.42	0.64	1.41	0.07	0.24	0.16
Total	97.74 -		100.85 -		100.06 -		99.70	-	97.27 -		100.36 -		100.26 -	
Al	0.001	0.001	0.001	0.000	0.000	0.000	0.000	0.000	0.000	0.000	0.000	0.000	0.001	0.003
P	0.024	0.023	0.001	0.000	4.805	0.084	4.162	0.164	0.000	0.000	0.000	0.000	4.248	0.047
Ca	0.161	0.050	0.005	0.001	6.233	0.217	4.301	0.136	0.096	0.003	0.001	0.001	4.308	0.029
Ti	1.916	0.073	0.869	0.009	0.170	0.231	0.074	0.018	1.968	0.008	0.856	0.004	0.021	0.006
Ce	0.167	0.014	0.001	0.000	0.381	0.018	0.831	0.020	0.152	0.003	0.000	0.000	0.783	0.017
Gd	0.150	0.012	0.000	0.000	0.365	0.023	0.610	0.026	0.174	0.004	0.001	0.000	0.620	0.015
Hf	0.139	0.008	0.118	0.008	0.012	0.012	0.012	0.005	0.161	0.005	0.136	0.003	0.012	0.005
U	0.442	0.021	0.005	0.001	0.034	0.038	0.011	0.006	0.449	0.004	0.005	0.000	0.007	0.005
Catatoms	3.000 -		1.000 -		12.000	-	10.000	-	3.000 -		1.000 -		10.000 -	
Oxygen	5.776 -		1.995 -		19.987	-	17.475	-	5.817 -		1.999 -		17.505 -	
Ca														
Gd														
Sum														
Charge														
Ca	0.161		0.005		6.233		4.301		0.096		0.001			
Ce(+3)	0.167		0.001		0.381		0.831		0.152		0.000			
Gd	0.150		0.000		0.365		0.610		0.174		0.001			
Hf	0.081		0.000		0.000		0.000		0.128		0.000			
U(+4)	0.134		0.000		0.025		0.002		0.190		0.000			
U(+6)	0.308		0.005		0.009		0.009		0.259		0.005			
Sum	1.000		0.011		7.013		5.753		1.000		0.007			
Charge	2.706		0.029		0.156		0.061		2.829		0.031			
Ti	1.916		0.869		0.170		0.074		1.968		0.856			
Hf	0.058		0.118		0.012		0.012		0.032		0.136			
P	0.024		0.001		4.805		4.162		0.000		0.000			
Al	0.001		0.001		0.000		0.000		0.000		0.000			
Sum	2.000		0.989		4.987		4.247		2.000		0.993			
Model Oxygen	6.000		1.996		15.001		12.907		6.000		2.003			

Table C15. Microprobe analyses (wt%) and structural formulae for the Ce-analog with 10 wt% P_2O_5 added

	2-3	1350 C	2-3	1350 C	2-3	1350 C	2-3	1350 C
	Brannerite		Rutile		whitlockite		P-glass	
	wt%	std dev	wt%	std dev	wt%	std dev	wt%	std dev
Al_2O_3	0.01	0.01	0.00	0.00	0.00	0.00	0.00	0.00
P_2O_5	0.24	0.59	0.12	0.11	40.95	1.02	37.40	2.05
CaO	1.97	0.42	0.45	0.10	42.32	0.26	29.78	0.33
TiO_2	40.99	0.69	69.34	1.50	0.28	0.22	0.83	0.40
CeO_2	6.53	0.58	0.27	0.15	7.15	0.46	17.23	0.90
Gd_2O_3	7.52	0.18	0.19	0.03	7.10	0.34	13.78	0.31
HfO_2	8.08	0.53	28.70	0.65	0.06	0.10	0.47	0.04
UO_2	32.41	1.24	1.77	0.83	0.27	0.24	0.20	0.19
Total	97.75 -		100.84 -		98.14 -		99.69 -	
Al	0.000	0.001	0.000	0.000	0.00	0.00	0.000	0.000
P	0.013	0.031	0.002	0.001	4.89	0.08	4.223	0.141
Ca	0.133	0.028	0.008	0.002	6.39	0.07	4.258	0.094
Ti	1.950	0.044	0.848	0.006	0.03	0.02	0.083	0.039
Ce	0.144	0.012	0.002	0.001	0.35	0.02	0.803	0.050
Gd	0.158	0.004	0.001	0.000	0.33	0.01	0.610	0.024
Hf	0.146	0.010	0.133	0.004	0.00	0.00	0.018	0.002
U	0.456	0.020	0.006	0.003	0.01	0.01	0.006	0.006
Catatoms	3.000 -		1.000 -		12.00	-	10.000 -	
Oxygen	5.794 -		1.992 -		19.89	-	17.548 -	
Ca								
Gd								
Sum								
Charge								
Ca	0.133		0.008		6.390			
Ce(+3)	0.144		0.002		0.352			
Gd	0.158		0.001		0.332			
Hf	0.109		0.000		0.000			
U(+4)	0.178		0.001		0.000			
U(+6)	0.278		0.005		0.008			
Sum	1.000		0.017		7.082			
Charge	2.816		0.036		0.050			
Ti	1.950		0.848		0.030			
Hf	0.037		0.133		0.002			
P	0.013		0.002		4.886			
Al	0.000		0.000		0.000			
Sum	2.000		0.983		4.918			
Model Oxygen	6.000		1.995		19.89			

Table C16. Microprobe analyses of Ce-analog with 10wt% SiO_2

	10-1	1350	10-1	1350	10-1	1350	10-2	1300	10-2	1300	10-2	1300
	Brannerite		Rutile		Glass		Brannerite		Glass		Hafnon	
	wt%	std dev	wt%	std dev	wt%	std dev	wt%	std dev	wt%	std dev	wt%	std dev
Al_2O_3	0.00	0.00	0.05	0.00	0.23	0.01	0.01	0.01	0.46	0.02	0.00	0.00
SiO_2	0.00	0.00	0.00	0.00	15.21	0.07	0.00	0.00	24.88	0.50	16.57	1.75
CaO	1.09	0.05	0.03	0.01	10.83	0.19	1.22	0.27	23.80	0.14	0.22	0.16
TiO_2	40.55	0.27	73.18	0.65	32.40	0.20	40.64	0.32	32.95	0.34	1.75	1.49
Ce_2O_3	8.46	0.19	0.03	0.03	7.96	0.09	10.38	0.32	0.84	0.09	1.09	0.56
Gd_2O_3	9.22	0.23	0.00	0.00	5.98	0.18	9.12	0.16	2.16	0.10	1.13	0.71
HfO_2	9.25	0.27	25.27	0.45	8.99	0.15	6.66	0.59	12.21	0.75	73.28	3.99
UO_2	29.53	0.38	0.98	0.07	15.07	0.39	28.14	0.80	0.19	0.02	1.99	1.57
Total	98.11 -		99.54 -		96.65 -		96.17 -		97.50 -		96.03 -	
Al	0.000	0.000	0.001	0.000	0.043	0.001	0.001	0.000	0.068	0.003	0.000	0.000
Si	0.000	0.000	0.000	0.000	2.443	0.013	0.000	0.000	3.100	0.044	0.411	0.035
Ca	0.074	0.003	0.000	0.000	1.864	0.032	0.084	0.019	3.178	0.028	0.006	0.004
Ti	1.945	0.009	0.880	0.002	3.914	0.022	1.956	0.012	3.088	0.028	0.033	0.029
Ce	0.198	0.005	0.000	0.000	0.468	0.005	0.243	0.007	0.038	0.004	0.010	0.005
Gd	0.195	0.005	0.000	0.000	0.318	0.009	0.194	0.004	0.089	0.004	0.009	0.006
Hf	0.169	0.006	0.115	0.002	0.412	0.008	0.122	0.011	0.435	0.028	0.519	0.019
U	0.419	0.004	0.003	0.000	0.539	0.013	0.401	0.010	0.005	0.001	0.011	0.009
Catatoms	3.000 -		1.000	0.000	10.000	0.000	3.000	0.000	10.000	0.000	1.000	0.000
Oxygen	5.729 -		1.999 -		17.722 -		5.697 -		16.725 -		1.984 -	
Ca												
Gd												
Sum												
Charge												
Ca	0.074				1.864		0.084		3.178			
Ce(+3)	0.198				0.468		0.243		0.038			
Gd	0.195				0.318		0.194		0.089			
Hf	0.114				0.412		0.079		0.435			
U(+4)	0.170				0.539		0.152		0.005			
U(+6)	0.249				0.000		0.249		0.000			
Sum	1.000				3.600		1.000		3.745			
Charge	4.000				4.000		4.000		4.000			
Ti	1.945		0.880		3.914		1.956		3.088		0.033	
Hf	0.055		1.119		0.000		0.043		0.000		1.967	
Al	0.000		0.001		0.043		0.001		0.068		0.000	
Si	0.000		0.000		2.443		0.000		3.100		0.411	
Sum	2.000		2.000		2.000		2.000		2.000		2.000	
Charge	7.992		7.992		7.992		7.992		7.992		7.992	
Model Oxygens	5.978		4.000				5.946				4.000	

Table C17. Microprobe analyses of Ce-analog with 10 wt% $NaAlSiO_4$

	15-1	1350	15-1	1350	15-1	1350	15-2	1300	15-2	1300	15-2	1300	15-2	1300
	Pyrochlore		Hafnolite		Glass		Pyrochlore		Hafnolite		Rutile		glass	
	wt%	std dev	wt%	std dev	wt%	std dev	wt%	std dev	wt%	std dev	wt%	std dev	wt%	std dev
Na_2O	0.99	0.07	0.56	0.04	4.01	0.39	1.04	0.07	0.71	0.07	0.02	0.03	4.77	0.76
Al_2O_3	0.15	0.04	2.59	0.19	8.79	1.53	0.11	0.01	2.66	0.42	0.69	0.02	19.24	0.85
SiO_2	0.05	0.01	0.57	0.06	15.43	2.60	0.01	0.02	0.72	0.27	0.22	0.03	35.25	1.42
CaO	11.24	0.13	8.85	0.19	6.39	1.19	11.61	0.09	9.39	0.36	0.09	0.02	6.32	0.29
TiO_2	33.70	0.20	33.57	0.26	42.94	3.72	34.08	0.22	34.91	0.40	80.66	0.40	22.98	1.97
Ce_2O_3	9.16	0.11	3.52	0.34	4.00	1.16	9.69	0.16	3.84	0.87	0.06	0.01	1.08	0.33
Gd_2O_3	9.99	0.22	7.73	0.07	1.77	1.23	9.07	0.22	7.21	0.26	0.12	0.06	0.41	0.28
HfO_2	10.26	0.42	34.23	1.75	5.94	0.88	7.90	0.21	32.97	3.92	14.84	0.14	3.09	0.24
UO_3	23.17	0.33	7.57	1.16	9.99	2.90	24.81	0.21	8.27	2.39	2.04	0.09	5.55	1.00
Total	98.71 -		99.19 -		99.27 -		98.32 -		100.67 -		98.72 -		98.69 -	
Na	0.141	0.010	0.080	0.006	0.987	0.051	0.148	0.009	0.098	0.009	0.000	0.001	0.982	0.133
Al	0.013	0.004	0.223	0.016	1.309	0.158	0.010	0.001	0.222	0.033	0.012	0.000	2.416	0.087
Si	0.004	0.001	0.041	0.004	1.950	0.226	0.001	0.001	0.050	0.019	0.003	0.000	3.756	0.116
Ca	0.888	0.007	0.693	0.015	0.881	0.219	0.912	0.005	0.711	0.034	0.001	0.000	0.722	0.043
Ti	1.868	0.011	1.844	0.018	4.100	0.197	1.879	0.010	1.856	0.019	0.911	0.001	1.842	0.165
Ce	0.247	0.003	0.094	0.009	0.190	0.067	0.260	0.004	0.100	0.024	0.000	0.000	0.042	0.014
Gd	0.244	0.005	0.187	0.002	0.078	0.059	0.220	0.005	0.169	0.008	0.001	0.000	0.015	0.010
Hf	0.216	0.009	0.714	0.033	0.218	0.046	0.165	0.004	0.665	0.074	0.064	0.000	0.094	0.009
U	0.380	0.005	0.123	0.019	0.288	0.102	0.405	0.003	0.130	0.039	0.007	0.000	0.132	0.026
Catatoms	4.000 -		4.000 -		10.000 -		4.000 -		4.000 -		1.000 -		10.000 -	
oxygen	6.648 -		6.935 -		16.851 -		6.621 -		6.897 -		1.991 -		16.569 -	
Na	0.141		0.080				0.148		0.098					
Ca	0.888		0.693				0.912		0.711					
Gd	0.000		0.187				0.000		0.169					
Sum	1.029		0.960				1.060		0.978					
Charge	1.917		2.028				1.972		2.027					
Ca	0.000		0.000				0.000		0.000					
Al	0.000		0.068						0.077					
Ce(+3)	0.247		0.094				0.260		0.100					
Gd	0.244		0.000				0.220		0.000					
Hf	0.096		0.714				0.054		0.665					
U(+4)	0.021		0.000				0.025		0.000					
U(+6)	0.359		0.123				0.380		0.130					
Sum	0.967		0.999				0.939		0.972					
Charge	3.020		3.507				2.897		3.349					
Ti	1.868		1.844				1.879		1.856		0.911			
Hf	0.120		0.000				0.111		0.000		0.064			
Al	0.013		0.156				0.010		0.145		0.012			
Sum	2.000		2.000				2.000		2.000		0.987			
Charge	7.987		7.844				7.990		7.856		3.936			
Model Oxygen	7.000		6.976				7.000		6.927		1.968			

Table C18. Microprobe analyses of Ce-analog with 20 wt% $NaAlSiO_4$

	16-1	1350	16-1	1350	16-1	1350	16-2	1300	16-2	1300	16-2	1300
	Pyrochlore		Glass		Hafnolite		Pyrochlore		Hafnolite		Glass	
	wt%	std dev	wt%	std dev	wt%	std dev	wt%	std dev	wt%	std dev	wt%	std dev
Na_2O	1.12	0.08	4.67	0.44	0.66	0.10	1.26	0.07	0.95	0.11	6.36	0.89
Al_2O_3	0.11	0.01	9.72	0.30	2.49	0.17	0.10	0.01	2.91	0.80	15.27	0.49
SiO_2	0.08	0.01	17.18	0.31	0.58	0.07	0.09	0.07	2.09	1.81	27.93	0.80
CaO	10.55	0.11	7.41	0.24	8.61	0.24	10.98	0.11	8.81	0.16	4.80	0.67
TiO_2	31.97	0.24	33.01	0.50	31.71	0.18	34.47	0.21	35.82	0.60	29.80	0.74
Ce_2O_3	9.77	0.21	4.32	0.23	3.56	0.56	10.11	0.20	3.08	0.21	1.60	0.38
Gd_2O_3	10.90	0.22	2.52	0.31	8.13	0.42	9.43	0.22	6.81	0.38	1.00	0.27
HfO_2	11.67	0.31	6.46	0.16	35.50	2.18	7.88	0.20	34.16	1.84	3.63	0.27
UO_3	21.71	2.06	12.54	0.44	7.27	1.48	23.31	0.25	6.05	0.40	7.88	0.80
Total	97.88	1.90	97.83	0.65	98.50	0.96	97.64 -		100.69 -		98.26 -	
Na	0.163	0.013	1.167	0.098	0.096	0.015	0.179	0.009	0.127	0.015	1.374	0.155
Al	0.010	0.001	1.479	0.037	0.219	0.015	0.009	0.001	0.234	0.057	2.010	0.042
Si	0.006	0.001	2.217	0.029	0.043	0.005	0.006	0.005	0.141	0.117	3.121	0.055
Ca	0.852	0.005	1.024	0.037	0.688	0.014	0.862	0.008	0.649	0.026	0.574	0.075
Ti	1.812	0.013	3.203	0.056	1.780	0.005	1.899	0.010	1.853	0.079	2.506	0.103
Ce	0.270	0.006	0.204	0.012	0.097	0.015	0.271	0.005	0.078	0.007	0.066	0.016
Gd	0.272	0.006	0.108	0.014	0.201	0.010	0.229	0.005	0.155	0.013	0.037	0.010
Hf	0.251	0.008	0.238	0.008	0.756	0.046	0.165	0.004	0.671	0.053	0.116	0.011
U	0.364	0.033	0.360	0.016	0.121	0.024	0.380	0.005	0.093	0.007	0.196	0.023
Catatoms	4.000 -		10.000 -		4.000 -		4.000 -		4.000 -		10.000 -	
oxygen	6.628 -		16.330 -		6.910 -		6.615 -		6.928 -		16.308 -	
Na	0.163				0.096		0.179		0.127			
Ca	0.852				0.688		0.862		0.649			
Gd	0.000				0.201		0.000		0.155			
Sum	1.015				0.985		1.041		0.931			
Charge	1.867				2.075		1.903		1.890			
Ca	0.000				0.000		0.000		0.000			
Al	0.000				0.000		0.000		0.000			
Ce(+3)	0.270				0.097		0.271		0.078			
Gd	0.272				0.000		0.229		0.000			
Hf	0.073				0.756		0.072		0.671			
U(+4)	0.000				0.000		0.000		0.000			
U(+6)	0.364				0.121		0.380		0.093			
Sum	0.979				0.974		0.952		0.841			
Charge	3.010				3.678		2.929		3.195			
Ti	1.812				1.780		1.899		1.853			
Hf	0.178				0.000		0.093		0.000			
Al	0.010				0.219		0.009		0.234			
Sum	2.000				1.998		2.000		2.087			
Charge	7.990				7.774		7.991		8.113			
Model Oxygen	6.979				6.945		6.982		6.738			

Table C19. Microprobe analyses of Ce-analog with 10wt% CaO

	9-1 Pyrochlore wt%	1300 std dev	9-1 Perovskite wt%	1300 std dev	9-2 Pyrochlore wt%	1400 Std dev	9-2 Perovskite wt%	1400 Std dev	9-3 Pyrochlore wt%	1350 std dev	9-3 Perovskite wt%	1350 std dev
Al_2O_3	0.03	0.01	0.53	0.14	0.00	0.00	0.00	0.00	0.03	0.01	0.46	0.07
CaO	14.51	0.31	33.26	0.51	15.05	0.14	32.17	0.20	14.44	0.46	32.38	0.51
TiO_2	26.93	1.01	53.85	0.63	27.99	0.36	54.49	0.24	26.88	1.07	53.66	0.32
CeO_2	7.70	0.22	5.07	0.68	7.38	0.10	6.37	0.55	7.28	0.41	6.07	0.44
Gd_2O_3	7.27	0.22	6.75	0.79	7.61	0.13	5.62	0.93	7.34	0.20	5.76	0.55
HfO_2	15.65	2.43	1.27	0.30	13.33	0.81	0.69	0.41	17.08	2.71	1.66	0.75
UO_2	25.51	0.95	0.25	0.06	26.84	0.29	0.02	0.04	24.60	1.88	0.09	0.10
Total	97.61 -		100.98 -		98.19 -		99.36 -		97.64 -		100.09 -	
Al	0.003	0.001	0.016	0.004	0.000	0.000	0.000	0.000	0.003	0.001	0.014	0.002
Ca	1.205	0.009	0.876	0.009	1.236	0.006	0.863	0.004	1.205	0.024	0.865	0.009
Ti	1.580	0.038	0.997	0.007	1.614	0.015	1.026	0.004	1.580	0.037	1.006	0.010
Ce	0.210	0.004	0.046	0.006	0.207	0.003	0.058	0.005	0.210	0.014	0.055	0.004
Gd	0.192	0.004	0.054	0.006	0.194	0.004	0.047	0.008	0.192	0.008	0.048	0.004
Hf	0.385	0.059	0.009	0.002	0.292	0.018	0.005	0.003	0.385	0.063	0.012	0.005
U	0.425	0.011	0.001	0.000	0.458	0.005	0.000	0.000	0.425	0.027	0.001	0.001
Catatoms	4.000	0.000	2.000	0.000	4.000 -		2.000 -		4.000	0.000	2.000	0.000
Oxygen	6.593 -		3.066 -		6.564 -		3.084 -		6.593 -		3.077 -	
Ca	1.000				1.000				1.000			
Gd	0.000				0.000				0.000			
Sum	1.000				1.000				1.000			
Charge	2.000				2.000				2.000			
Ca	0.205		0.876		0.236		0.863		0.205		0.865	
Ce(+3)	0.210		0.046		0.207		0.058		0.210		0.055	
Gd	0.192		0.054		0.194		0.047		0.192		0.048	
Hf	0.106		0.009		0.106		0.005		0.106		0.012	
U(+4)	0.294		0.001		0.422		0.000		0.294		0.001	
U(+6)	0.131		0.000		0.036		0.000		0.131		0.000	
Sum	1.031		0.987		1.031		0.974		1.031		0.980	
Charge	4.000		2.097		4.000		2.062		4.000		2.088	
Ti	1.580		0.997		1.614		1.026		1.580		1.006	
Hf	0.417		0.000		0.386		0.000		0.418		0.000	
Al	0.003		0.016		0.000		0.000		0.003		0.014	
Sum	2.000		1.013		2.000		1.026		2.000		1.020	
Charge	7.992		4.035		7.992		4.106		7.992		4.065	
Model Oxygen	7.000		3.066		7.000		3.084		7.000		3.077	

Table C20 Microprobe analyses (wt%) and structural formulae for the Ce-analog with 10wt% CaF_2

	3-1	1300	3-1	1300	3-1	1300	3-2	1400	3-2	1400	3-3	1350	3-3	1350
	Pyrochlore		Hafnolite		Perovskite		Pyrochlore		Perovskite		Pyrochlore		Perovskite	
	wt%	std dev	wt%	std dev	wt%	std dev	wt%	std dev	wt%	std dev	wt%	std dev	wt%	std dev
Al_2O_3	0.06	0.03	1.90	0.17	0.80	0.11	0.11	0.01	0.91	0.02	0.13	0.07	0.92	0.06
CaO	15.13	0.14	12.09	0.50	32.04	0.22	14.62	0.26	30.61	0.58	14.88	0.39	30.76	0.70
TiO_2	32.93	0.31	33.70	0.28	52.86	0.42	32.55	0.49	51.96	0.53	33.25	0.12	52.73	0.38
CeO_2	7.31	0.13	2.69	0.49	7.23	0.19	6.81	0.19	9.02	0.04	7.04	0.16	8.48	0.26
Gd_2O_3	7.13	0.05	5.00	0.27	6.46	0.11	7.18	0.11	6.54	0.48	7.12	0.21	6.58	0.32
HfO_2	10.39	0.31	37.02	1.76	1.20	0.20	12.47	0.61	1.57	0.07	12.57	1.44	1.42	0.17
UO_2	23.50	0.34	7.90	2.14	0.22	0.04	22.78	0.47	0.30	0.08	23.08	1.27	0.28	0.04
Total	96.47 -		100.30	1.20	100.82	0.25	96.52 -		100.92 -		98.06 -		101.16 -	
Al	0.005	0.003	0.162	0.016	0.024	0.003	0.009	0.001	0.028	0.001	0.011	0.006	0.028	0.002
Ca	1.194	0.012	0.933	0.033	0.854	0.007	1.162	0.017	0.830	0.012	1.165	0.024	0.831	0.009
Ti	1.825	0.016	1.826	0.026	0.991	0.005	1.825	0.014	0.990	0.009	1.826	0.015	0.997	0.009
Ce	0.197	0.003	0.071	0.013	0.067	0.002	0.184	0.005	0.084	0.001	0.188	0.005	0.079	0.003
Gd	0.174	0.001	0.119	0.006	0.054	0.002	0.178	0.003	0.055	0.003	0.172	0.006	0.054	0.003
Hf	0.219	0.006	0.762	0.041	0.009	0.001	0.267	0.016	0.011	0.000	0.262	0.031	0.010	0.001
U	0.385	0.006	0.127	0.034	0.001	0.000	0.375	0.007	0.002	0.000	0.375	0.018	0.002	0.000
Catatoms	4.000	0.000	4.000	0.000	2.000	0.000	4.000	0.000	2.000	0.000	4.000	0.000	2.000	0.000
Oxygen	6.617	0.011	6.891	0.033	3.074	0.005	6.652 -		3.087 -		6.649 -		3.089 -	
Ca	1.000		0.933				1.000				1.000			
Gd	0.000		0.067				0.000				0.000			
Sum	1.000		1.000				1.000				1.000			
Charge	2.000		2.067				2.000				2.000			
Ca	0.194		0.000		0.854		0.162		0.830		0.165		0.831	
Ce(+3)	0.197		0.071		0.067		0.184		0.084		0.188		0.079	
Gd	0.174		0.053		0.054		0.178		0.055		0.172		0.054	
Hf	0.106		0.750		0.009		0.106		0.011		0.106		0.010	
U(+4)	0.117		0.018		0.001		0.038		0.002		0.037		0.002	
U(+6)	0.268		0.109		0.000		0.337		0.000		0.338		0.000	
Sum	1.057		1.000		0.985		1.005		0.982		1.031		0.976	
Charge	4.004		4.094		2.110		4.009		2.129		4.011		2.108	
Ti	1.825		1.826		0.991		1.825		0.990		1.826		0.997	
Hf	0.170		0.012		0.000		0.166		0.000		0.163		0.000	
Al	0.005		0.162		0.024		0.009		0.028		0.011		0.028	
Sum	2.000		2.000		1.015		2.000		1.018		2.000		1.024	
Charge	7.995		7.838		4.038		7.991		4.044		7.989		4.070	
Model Oxygen	7.000		7.000		3.074		7.000		3.087		7.000		3.089	

Table C21. Microprobe analyses of Ce-analog with 10 wt% MnO_2

	20-1	1350	20-1	1350	20-2	1300	20-2	1300
	Pyrochlore		Perovskite		Pyrochlore		Perovskite	
	wt%	std dev	wt%	std dev	wt%	std dev	wt%	std dev
Al_2O_3	0.12	0.01	0.79	0.05	0.16	0.00	0.89	0.05
CaO	9.16	0.06	29.39	0.24	9.35	0.08	29.62	0.25
TiO_2	33.66	0.10	51.15	0.43	33.85	0.13	51.13	0.23
MnO	7.36	0.21	4.74	0.08	7.52	0.16	5.33	0.10
Ce_2O_3	6.93	0.11	5.12	0.16	7.25	0.22	4.33	0.14
Gd_2O_3	7.75	0.18	7.73	0.30	7.58	0.17	7.82	0.17
HfO_2	10.64	0.30	1.26	0.07	10.40	0.19	1.06	0.10
UO_2	20.54	0.27	0.15	0.04	20.14	0.29	0.20	0.04
Total	96.14 -		100.32 -		96.24 -		100.37 -	
Al	0.010	0.001	0.023	0.002	0.014	0.000	0.026	0.001
Ca	0.724	0.006	0.790	0.004	0.733	0.007	0.791	0.004
Ti	1.868	0.008	0.965	0.004	1.863	0.006	0.958	0.004
Mn	0.460	0.011	0.101	0.002	0.466	0.008	0.113	0.002
Ce	0.187	0.003	0.047	0.002	0.194	0.005	0.040	0.001
Gd	0.189	0.004	0.064	0.003	0.184	0.004	0.065	0.001
Hf	0.224	0.006	0.009	0.000	0.217	0.004	0.008	0.001
U	0.337	0.005	0.001	0.000	0.328	0.005	0.001	0.000
Catatoms	4.000 -		2.000 -		4.000 -		2.000 -	
Oxygen	6.623 -		3.042 -		6.605 -		3.032 -	
Ca	0.724				0.733			
Gd	0.189				0.184			
Ce(+3)	0.087				0.083			
U(+4)	0.000				0.000			
Sum	1.000				1.000			
Charge	2.276				2.267			
Ca	0.000		0.790		0.000		0.791	
Mn	0.460		0.101		0.466		0.113	
Ce(+3)	0.100		0.047		0.111		0.040	
Gd	0.000		0.064		0.000		0.065	
Hf	0.102		0.000		0.094		0.000	
U(+4)	0.000		0		0.000		0	
U(+6)	0.337		0.001		0.328		0.001	
Sum	1.000		1.003		1.000		1.008	
Charge	2.643		2.118		2.628		2.120	
Ti	1.868		0.965		1.863		0.958	
Hf	0.122		0.009		0.123		0.008	
Al	0.010		0.023		0.014		0.026	
Sum	2.000		0.997		2.000		0.992	
Charge	7.990		3.966		7.986		3.942	
Model Oxygen	6.960		3.043		6.933		3.033	

Table C22. Microprobe Analyses of Ce-analog with 10 wt% Gd_2O_3

	14-1	1350	14-1	1350	14-1	1350	14-2	1300	14-2	1300	14-2	1300
	Pyrochlore		Brannerite		Rutile		Pyrochlore		Brannerite		Rutile	
	wt%	std dev	wt%	std dev	wt%	std dev	wt%	std dev	wt%	std dev	wt%	std dev
Al_2O_3	0.07	0.01	0.27	0.02	0.39	0.04	0.06	0.01	0.28	0.09	0.33	0.04
CaO	11.35	0.05	0.98	0.05	0.09	0.04	12.00	0.11	1.09	0.20	0.11	0.05
TiO_2	33.21	0.28	40.94	0.25	80.75	2.51	33.54	0.65	41.02	0.60	79.19	1.35
Ce_2O_3	6.81	0.21	7.32	0.31	0.11	0.01	7.13	0.36	7.28	0.97	0.09	0.02
Gd_2O_3	16.62	0.47	11.31	0.31	0.26	0.09	17.01	0.28	11.87	0.29	0.11	0.10
HfO_2	9.88	0.34	6.15	0.53	17.37	1.85	10.13	0.76	5.40	0.61	18.83	1.39
UO_2	19.29	0.26	30.19	0.42	1.93	0.40	20.02	0.67	30.11	0.42	1.62	0.13
Total	97.23 -		97.15 -		100.88 -		99.89 -		97.05 -		100.28 -	
Al	0.007	0.001	0.020	0.002	0.007	0.001	0.005	0.001	0.021	0.007	0.006	0.001
Ca	0.930	0.004	0.067	0.003	0.001	0.001	0.957	0.012	0.074	0.014	0.002	0.001
Ti	1.908	0.012	1.963	0.005	0.909	0.012	1.877	0.023	1.961	0.014	0.904	0.008
Ce	0.191	0.006	0.171	0.007	0.001	0.000	0.194	0.010	0.169	0.021	0.000	0.000
Gd	0.421	0.011	0.239	0.007	0.001	0.000	0.420	0.006	0.250	0.007	0.001	0.001
Hf	0.216	0.008	0.112	0.009	0.074	0.009	0.215	0.015	0.098	0.012	0.082	0.007
U	0.328	0.004	0.428	0.007	0.006	0.001	0.332	0.013	0.426	0.008	0.005	0.000
Catatoms	4.000	0.000	3.000	0.000	1.000	0.000	4.000	0.000	3.000	0.000	1.000	0.000
oxygen	6.761 -		5.718 -		1.994 -		6.733 -		5.706 -		1.995 -	
Ca	0.930						0.957					
Gd	0.070						0.043					
Sum	1.000						1.000					
Charge	2.070						2.043					
Ca	0.000		0.146		0.001		0.000		0.146			
Ce(+3)	0.191		0.171		0.001		0.194		0.169			
Gd	0.351		0.157		0.001		0.377		0.157			
Hf	0.106		0.095		-0.006		0.106		0.080			
U(+4)	0.039		0.103		0.000		0.083		0.065			
U(+6)	0.289		0.325		0.006		0.249		0.361			
Sum	0.975		1.042		1.042		1.009		1.042			
Charge	3.937		4.005		4.005		3.961		4.005			
Ti	1.908		1.963		0.909		1.877		1.961		0.904	
Hf	0.085		0.017		0.080		0.118		0.018		0.080	
Al	0.007		0.020		0.007		0.005		0.021		0.006	
Sum	2.000		2.000		2.000		2.000		2.000		2.000	
Charge	7.993		7.970		3.947		7.995		7.970		3.947	
Total Oxygen	7.000		6.000		2.000		7.000		6.000		1.977	

Table C23. Microprobe analyses of Ce-analog with 10 wt% Ga_2O_3

	19-1	1350	19-1	1350	19-1	1350	19-2	1300	19-2	1300	19-2	1300
	Pyrochlore		Hafnolite		Galonite		Pyrochlore		Hafnolite		"Galonite"	
	wt%	std dev	wt%	std dev	wt%	std dev	wt%	std dev	wt%	std dev	wt%	std dev
Al_2O_3	0.01	0.01	0.24	0.01	1.16	0.02	0.04	0.01	0.30	0.01	1.62	0.04
CaO	14.25	0.11	8.18	0.09	7.21	0.20	15.04	0.13	8.40	0.15	7.67	0.11
TiO_2	34.45	0.18	35.54	0.99	40.81	0.35	34.88	0.50	34.71	0.61	33.72	0.31
Ga_2O_3	2.14	0.13	12.96	0.24	34.89	0.68	2.36	0.12	14.68	0.19	41.28	0.37
Ce_2O_3	9.51	0.37	5.30	0.25	5.82	0.29	10.44	0.84	5.90	0.19	4.76	0.17
Gd_2O_3	8.84	0.26	10.31	0.34	0.95	0.09	6.90	0.21	9.17	0.55	2.34	0.08
HfO_2	4.76	0.13	19.14	0.67	0.70	0.10	3.10	0.17	17.26	0.46	3.53	0.09
UO_2	26.25	0.18	8.29	0.58	7.24	0.53	26.80	0.98	10.67	0.58	3.88	0.11
Total	100.20 -		99.95 -		98.78 -		99.56 -		101.09 -		98.80 -	
Al	0.001	0.001	0.020	0.001	0.082	0.001	0.003	0.001	0.025	0.001	0.115	0.002
Ca	1.087	0.009	0.618	0.007	0.465	0.012	1.134	0.010	0.627	0.009	0.496	0.007
Ti	1.845	0.004	1.883	0.030	1.849	0.016	1.845	0.014	1.820	0.024	1.529	0.011
Ga	0.097	0.006	0.586	0.007	1.347	0.024	0.106	0.006	0.656	0.010	1.596	0.015
Ce	0.248	0.009	0.137	0.005	0.128	0.007	0.269	0.020	0.151	0.004	0.105	0.003
Gd	0.209	0.006	0.241	0.008	0.019	0.002	0.161	0.005	0.212	0.012	0.047	0.002
Hf	0.097	0.003	0.385	0.018	0.012	0.002	0.062	0.004	0.344	0.010	0.061	0.002
U	0.416	0.003	0.130	0.010	0.097	0.007	0.420	0.018	0.166	0.010	0.052	0.002
Catatoms	4.000 -		4.000 -		4.000 -		4.000 -		4.000 -		4.000 -	
Oxygen	6.635 -		6.890 -		6.746 -		6.597 -		6.851 -		6.573 -	
Ca	1.000		0.618		0.465		1.000		0.627		0.496	
Ga	0.000		0.000		0.290		0.000		0.000		0.252	
Gd	0.000		0.241		0.019		0.000		0.212		0.047	
Ce(+3)	0.000		0.137		0.128		0.000		0.151		0.105	
U(+4)	0.000		0.000		0.097		0.000		0.000		0.052	
Sum	1.000		0.996		1.000		1.000		0.990		0.951	
Charge	2.000		2.369		1.761		2.000		2.343		1.655	
Ca	0.087		0.000		0.000		0.134		0.000		0.000	
Ga	0.040		0.586		1.000		0.017		0.656		1.000	
Ce(+3)	0.248		0.000		0.000		0.269		0.000		0.000	
Gd	0.209		0.000		0.000		0.161		0.000		0.000	
Hf	0.000		0.289		0.000		0.000		0.188		0.000	
U(+4)	0.051		0.020		0.000		0.017		0.017		0.000	
U(+6)	0.365		0.110		0.000		0.403		0.149		0.000	
Sum	1.000		1.004		1.000		1.000		1.010		1.000	
Charge	2.964		3.322		3.000		2.883		3.235		3.000	
Ti	1.845		1.883		1.849		1.845		1.820		1.529	
Hf	0.097		0.097		0.012		0.062		0.155		0.012	
Al	0.001		0.020		0.082		0.003		0.025		0.115	
Ga	0.057		0.000		0.057		0.089		0.000		0.344	
Sum	2.000		2.000		2.000		2.000		2.000		2.000	
Charge	7.770		7.980		7.690		7.639		7.975		6.510	
Model Oxygen	7.000		7.000		6.746		7.000		7.000		6.476	

Table C24. Mircoprobe analyses of Ce-Analog with Nb_2O_5

	P243	1350	P243	1350	P243	1350	P243	1350
	Pyrochlore		Brannerite		Rutile		Hf-Ti	
	wt%	std dev	wt%	std dev	wt%	std dev	wt%	std dev
Al_2O_3	0.00	0.00	0.00	0.00	0.10	0.02	0.07	0.00
CaO	12.79	0.08	1.56	0.04	0.09	0.04	0.38	0.06
TiO_2	23.60	0.48	36.73	0.40	70.77	2.25	30.44	0.22
Nb_2O_5	13.41	0.20	4.02	0.21	2.09	0.14	2.01	0.05
Ce_2O_3	7.09	0.30	9.10	0.53	0.06	0.03	0.55	0.02
Gd_2O_3	8.11	0.13	8.23	0.27	0.04	0.05	1.52	0.15
HfO_2	7.54	0.22	8.00	0.35	22.02	2.11	60.66	0.02
UO_2	20.49	0.23	25.58	0.23	0.42	0.11	1.91	0.04
Total	93.04	-	93.21	-	95.59	-	97.515	-
Al	0.000	0.000	0.000	0.000	0.002	0.000	0.004	0.000
Ca	1.107	0.012	0.111	0.003	0.002	0.001	0.019	0.003
Ti	1.434	0.020	1.836	0.009	0.875	0.012	1.071	0.007
Nb	0.490	0.008	0.121	0.006	0.016	0.001	0.042	0.001
Ce	0.210	0.008	0.221	0.012	0.000	0.000	0.009	0.000
Gd	0.217	0.002	0.181	0.006	0.000	0.000	0.024	0.002
Hf	0.174	0.005	0.152	0.006	0.104	0.011	0.811	0.000
U	0.368	0.005	0.378	0.004	0.002	0.000	0.020	0.000
Catatoms	4.000	-	3.000	-	1.000	-	2.000	-
Oxygen	6.924	-	5.748	-	2.005	-	3.984	-
Ca	1.000							
Gd	0.000							
Sum	1.000							
Charge	2.000							
Ca	0.107		0.111				0.019	
Ti	0.000		0.000				0.071	
Nb	0.000		0.000				0.042	
Ce(+3)	0.210		0.221				0.009	
Gd	0.217		0.181				0.024	
Hf	0.097		0.108				0.811	
U(+4)	0.349		0.315				0.015	
U(+6)	0.019		0.063				0.005	
Sum	1.000		1.000				0.995	
Charge	3.397		3.502				3.468	
Ti	1.434		1.836		0.875		1.000	
Hf	0.076		0.044		1.107		0.000	
Nb	0.490		0.121		0.016		0.000	
Al	0.000		0.000		0.002		0.004	
Sum	2.000		2.000		2.000		1.004	
Charge	8.490		8.121		8.014		4.011	
Model Oxygens	7.000		6.000		4.007		4.002	